COMPUTATIONAL STUDY OF ANTICODON LOOPS OF tRNAs HAVING MODIFIED NUCLEOSIDES

THESIS

submitted to the

UNIVERSITY OF PUNE

for the degree of

DOCTOR OF PHILOSOPHY

in

PHYSICS

By

UDDHAVESH BHASKAR SONAVANE

PHYSICAL CHEMISTRY DIVISION

NATIONAL CHEMICAL LABORATORY

PUNE - 411 008, INDIA

JULY 2002

Dedicated to…

My parents and those selfless people who helped in my development

CERTIFICATE

This is to certify that the work incorporated in the thesis entitled, "**Computational study of anticodon loop of tRNAs having modified nucleosides**" submitted by **Mr. Uddhavesh Bhaskar Sonavane**, for the Degree of **Doctor of Philosophy**, was carried out by the candidate under my supervision in the Physical Chemistry Division, National Chemical Laboratory, Pune, INDIA. Such material as has been obtained from other sources has been duly acknowledged in the thesis.

Dr. R. Tewari
Research Guide

ACKNOWLEDGEMENTS

It is pleasure to acknowledge with respect the valuable guidance and support given by Dr. R. Tewari, Scientist -F, NCL, Pune during the course of this work. His critical analysis always helped me to improve myself. I am expressing my sincere regards for him forever.

I am grateful to Dr S. K. Date, Head, Physical Chemistry Division for his encouragement.

I am also deeply indebted to Dr. Suresh and his students (Biochemistry Division) for their timely help. I wish to express my thanks to all other scientific and nonscientific staff in the Physical Division, NCL, for their help and cooperation given to me in completing my research work successfully.

I take this opportunity to express my thanks to Kailas for his encouragement, timely help and valuable discussions. I would like to thank all labmates (Dr. Pal and group) for their good discussions and keeping healthy environment for any scientific activity. Mrs. Phalgune (Scientist-C) was also very helpful, as per as NMR knowledge is concern. I would like to thank my friends Shivanand Pai, Suresh, Mahesh, Bennur, Milind, Balkrisna, Musale, Sandeep, Prakash, Nandu, Chaini, Rameshwar and my innumerous friends for their wholehearted help and discussion.

It gives me great pleasure to express gratitude towards my parents and all family for their love, unfailing support, tremendous patience, trust and encouragement that they have shown to me.

Finally, my thanks are due to the Council of Scientific & Industrial Research, New Delhi, for my fellowship award and to Dr. P. Ratnasamy, Director, National Chemical Laboratory, for permitting me to carry out my research work at NCL.

Uddhavesh Bhaskar Sonavane

CONTENTS

Abstract of Ph.D. thesis

Computational study of anticodon loops of tRNAs having modified nucleosides

Introduction: Transfer RNA (t-RNA) has the largest number of chemically modified nucleosides. Out of nearly 100 different known modifications about 80 occur in tRNA. Higher organized life domains - multicellular eukaryotes (1-5) are modified to a larger extent and upto 25% of all nucleosides in tRNA gets modified. Many modifications involve simple alkylation, hydrogenation, thiolation or isomerisation of four common ribonucleosides (A, G, C, U) in the base and/or the 2'-hydroxyl group of the ribose, however, some nucleosides have quite extensive chemical modifications (3-8).

Anticodon loop is specially rich in such extensive (hyper) modifications. In view of the strategic locations of such modifications in the anticodon loop, it is of interest to inquire into the chemical modulation of tRNA structure and function through post transcriptional enzymatic modifications. Specially role of tRNA anticodon loop modifications for accuracy and efficiency of protein biosynthesis can be very important and needs to be fully explored.

Computational approaches can supplement experimental probing. Increased availability of high speed /large memory computers and the needed computational - visualization software enables modeling of complex biomolecular systems. In this way it is possible to gain clear atomic and electronic level understanding of large biomolecules. Preparation - availability of suitable samples continues to hamper experimental investigations of nucleic acids and limits the available information.

Present research work was done to study conformational preferences of the modified components present at the first position of anticodon specially 5-methoxy carbonyl methyl –2-thio uridine ($mcm^5s^2U_{34}$) and queuosine (Q). Conformational preferences of modification threonyl carbonyl adenine (tc^6Ade) and its derivatives occurring at anticodon 3'-adjacent position have also been investigated. Further, anticodon loop with these modified components present, has been investigated for understanding the role of these modified components to the loop structure and stability.

Various computational methods like semi-empirical molecular orbital PCILO, MNDO, AM1, PM3 as well as ab-initio HF, Density Functional Theory DFT methods and molecular mechanics force field MMFF, molecular dynamics MD approaches have been utilized in these investigations. The thesis is divided into following chapters.

Chapter I : Introduction

The chapter gives an introduction to nucleic acid constituents, tRNA modifications, perspective on notable developments including tRNA two dimensional cloverleaf sequence scheme and 'L' shaped three dimensional structure. Available data is included on structural studies of modified nucleosides, examples of modified/hypermodified nucleosides which form the subject of the thesis are also given. Brief information about the experimental techniques like x-ray crystallography, NMR etc is included for providing scarce but very valuable structural data. Role of computational approaches for closely simulating interesting biomolecular systems and usefulness of simulation – modelling to our studies is also mentioned. The chapter describes the objectives and scope of the thesis.

Chapter –II Computational methods

The chapter describes various computational methods utilized for structural investigations of tRNA anticodon loop modifications. Information about various softwares utilized for mimicking real biological problems is included. The chapter is mainly divided into two sections.

Section A: Classical/ Statistical mechanics methods

The basic framework and procedure adopted for molecular mechanics (MM) and molecular dynamics (MD) methods is described. These methods have been used mainly for probing structural consequences of including modified nucleosides in anticodon loop of some interesting tRNAs.

Section B : Quantum mechanics methods

Brief theoretical background about various quantum chemical methods. Semi-empirical molecular orbital Perturbative Configuration Interaction with Localized Orbitals (PCILO), Modified Neglect of Differential Overlap (MNDO), Austin Model (AM1), Parametrized Model (PM3) methods, ab-initio self consistent field Hartree Fock (HF), Density Functional Theory (DFT) methods are also included. The chapter also describes the logical procedure adopted for exploring conformational preferences of modified tRNA components in multidimensional conformational space.

Chapter –III(A) Conformational preferences of wobble nucleoside 5-methoxy carbonyl methyl –2- thiouridine (mcm^5s^2U)

Structural investigations on mcm^5s^2U are presented . This modification is present at 34^{th} (1^{st} anticodon or wobble) position of human $tRNA^{lys}$. The preferred conformation of the substituent in $mcm^5s^2U_{34}$ is of special interest and is theoretically explored. The results on accessible alternative stable conformations are also described.

Chapter –III(B) Conformational preferences of another wobble nucleoside queuosine (Q) and its analogs

Structural investigations of protonated Q(PO4 and $NH2^+$) , neutral Q (PO4 and NH) and zwitterionic queuosine ($PO4^-$ and $NH2^+$) molecules are presented. The predicted preferred conformation of protonated Q is such that the substituent imino group linking cyclopentane diol hydrogen bonds with O(6) of 7-deazaguanine. This is in agreement with the observed crystal structure of queuosine. The reported investigations show that this feature is not maintained in neutral Q and Q zwitterion. The interdependence of torsion angles is depicted through two dimensional isoenergy contour maps.

Chapter IV : Effect of protonation on the conformational preferences of threonyl carbonyl adenine (tc^6Ade) system

Conformational transitions induced due to protonation at N(7), N(3) or N(1) sites of tc^6Ade / ms^2tc^6Ade are predicted. The N(3) and N(1) protonation keep unaltered the distal conformation of threonyl carbonyl substituent in tc^6Ade/ ms^2tc^6Ade similar to that for neutral base. However, N(7)-protonation results in proximal conformation becoming preferred, allowing usual canonical base pairing for the modified nucleoside. This may allow extended codon-anticodon interactions also involving the 3'-adjacent nucleoside to anticodon.

Chapter V: Structural consequences of anticodon loop having modified nucleosides.

The consequences of the presence of two hypermodified nucleosides at 34^{th} as well as at the 37^{th} positions in anticodon loop of human $tRNA^{lys}$ ($mcm^5s^2U_{34}$ and $ms^2tc^6A_{37}$) and $tRNA^{asn}$ (Q_{34} and tc^6A_{37}) are studied. Probable significance of modified components for providing an open anticodon loop framework or allowing alternative perturbed framework with new across the loop hydrogen bonding or disallowing otherwise plausible alternative possibilities is discussed.

Conclusions :

Although different conformations are preferred for wobble nucleoside Q and its protonated and zwitterionic forms, nevertheless in each case prospective sites for usual codon - anticodon base pairing remain unobstructed.

Investigations on 37^{th} modification tc^6Ade (and its analogs) shows that the threonyl carbonyl substituent restricts codon – anticodon interactions to occurr, except for the N(7) – protonated molecule which allows such interaction. Extended codon – anticodon interactions permitted due to N(7)- protonation of tc^6Ade may however be prevented by further modification (methylation at N(6)) m^6tc^6Ade.

The open loop framework is preferred for anticodon loop of human $tRNA^{Lys}$(having modification $mcm^5s^2U_{34}$ and $ms^2tc^6A_{37}$) ; however, unconventional or distorted

anticodon loop may preferred by $tRNA^{Asn}$ (Q_{34} and tc^6A_{37}) due to possible hydrogen bonding interactions between hypermodified bases Q_{34} and tc^6A_{37}.

References :

1) P.F.Crain, in Modifications and Editing in tRNA , ASM Press, Washington , 47 (1998).
2) H. Kersten , Prog. Nucleic Acid Res. Mol. Biol. 31 ,59 (1984)
3) R. W. Adamiak and P. Gornicki, Prog. Nucleic Acid Res. Mol. Biol. 32, 27 (1985)
4) G.R.Bjork, J. U. Ericson, C.E.D. Gustafsson, T.G. Hagervall, Y.H. Jomsson and P.M. Wikstrom ,Ann. Rev. Biochem. 56,263 (1987)
5) S.Yokoyama and Susumu Nishimura,Structure, Biosynthesis and Function, American Society for Microbiology, Washington, 207 (1995)
6) W.H.Mcclain, tRNA: Structure, Biosynthesis, and Function, American Society for Microbiology, Washington, 335 (1995)
7) B.C. Persson, Molecular Microbiology 8(6), 1011 (1993)
8) D.R.Davis, in Modifications and Editing in tRNA , ASM Press, Washington , 85 (1998).

Chapter 1: Introduction

1.1 General Introduction: Nucleic acids are molecules having sugar – phosphate chains (backbone) with each sugar linked through glycosyl bond to one of the purine or pyrimidine heterocyclic bases (in side chain). The sequence of the purine and pyrimidine bases carries the genetic information. Two types of nucleic acids DNA and RNA basically differ due to different kinds of pentose sugar (deoxyribose in DNA or ribose in RNA) in the backbone. The deoxyribo - nucleic acid (DNA) usually holds genetic information while the ribonucleic acid (RNA), helps in decoding this genetic information [1-4]. Both DNA and RNA are constructed from four main nucleotide building blocks. Each nucleotide contains a phosphate group linked to sugar group, which, in turn, is joined to purine and pyrimidine bases (Fig.1), however, deleting phosphate group from nucleotide results nucleoside. DNA contains sugar deoxyribose (i.e. absence of oxygen at 2'position of pentose sugar), while in RNA, sugar is ribose (fig.1). Another difference between DNA and RNA is the presence of 5-methyl uracil (thymine) in DNA instead of usual unmodified base uracil in RNA. In DNA and RNA, the nucleotides are joined together by covalent bonds (phosphodiester bond) linking the phosphate group of one nucleotide to a hydroxyl group on the sugar of the adjacent nucleotide [1,2]. If, C2' atom is displaced out of plane of pentose ring toward C5' atom (fig.1), the ring puckering becomes C2'endo. Similarly, displacing C3' atom out of plane of ring toward C5' atom results C3'-endo ring puckering. The labeling of various atom positions in nucleotide is shown in fig.1 along with definitions of backbone torsion angles according to Holbrook model [59].

DNA structure usually consists of anti parallel double helical strands. The two DNA chains are held together by hydrogen bonding between pairs of bases on the strands running in opposite (anti parallel) directions. This specific base pairing takes place between adenine-thymine and guanine-cytosine. Different double stranded forms of DNA are A, B and Z-DNA. A-DNA is wide and short with bases tilted to helix axis, a large and hollow major groove, and a shallow minor groove. B-DNA is slimmer and more elongated, with base planes essentially perpendicular to the helix axis, and with a narrow minor groove and wide major groove of comparable depth. Z-DNA is even

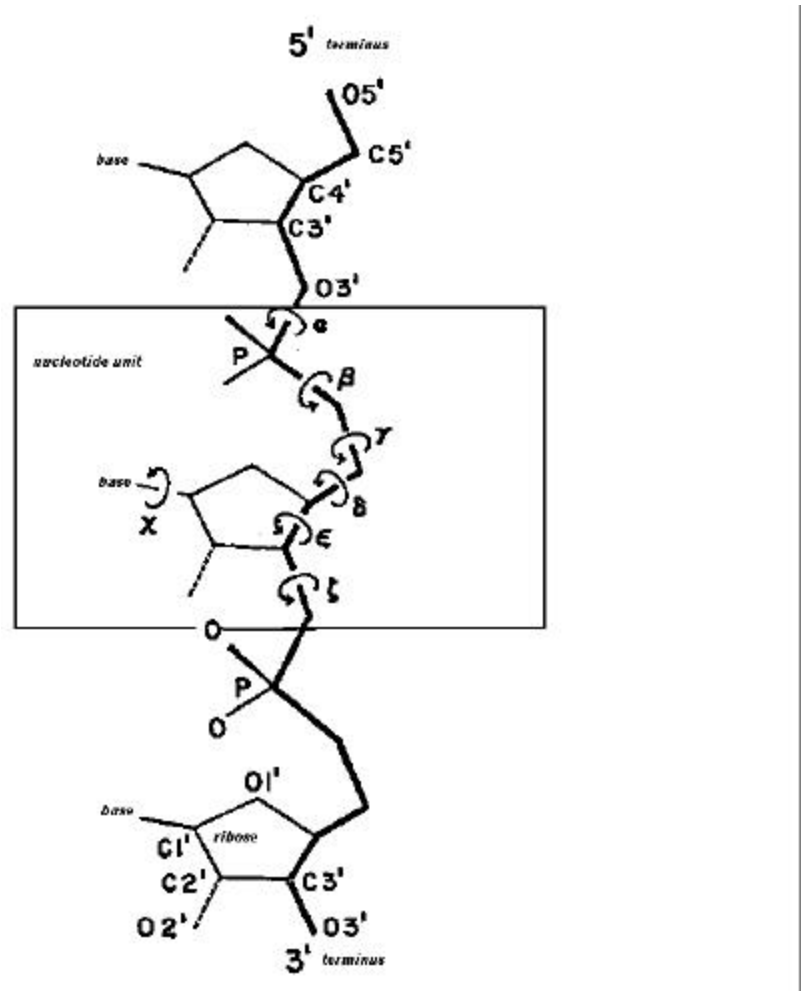

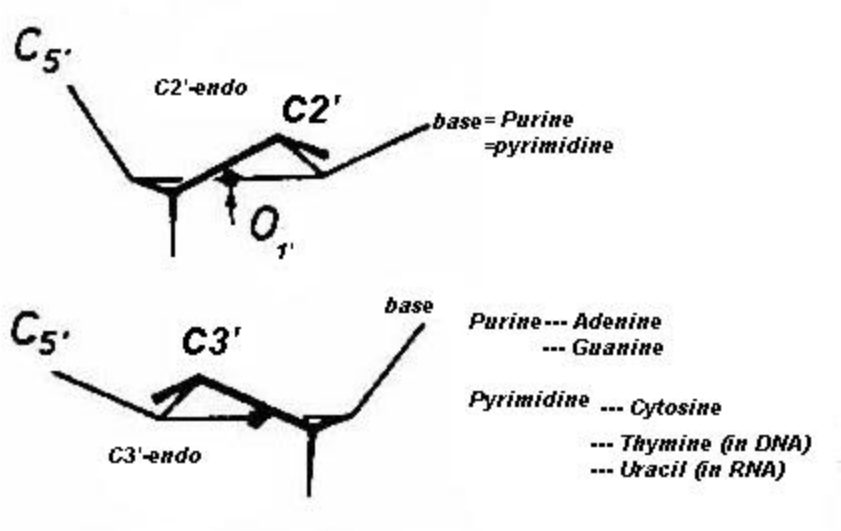

Fig 1. Nucleic acid substituents , Labeling for various atomic positions, backbone torsion angles, ribose puckeing and purine, pyrimidine bases.

thinner and more elongated. In Z-DNA, minor groove is large, hollow and deep, while the major groove is completely flattened out on the surface of the molecule. Z-DNA helix is left handed, while the other two are right handed.

Ribonucleic acid (RNA), a nucleic acid structurally and functionally distinguished by its multiple roles in the intracellular transmission of genetic information from the site of transcription (from DNA) to the site of translation (into protein). RNA has four different bases; adenine, guanine, cytosine and uracil. RNA structure is mainly single stranded A-type helix. There are three main varieties of RNA found in all living cells. a) mRNA b) rRNA c) tRNA [1-4].

The mRNA (messenger RNA) is transcribed directly from a DNA gene and is used to encode proteins. The transcribed mRNA from the gene sequence initially also contains some intervening unexpressed regions called 'introns'. RNA is also shown to have the capability of catalyzing the removal of the intervening 'intron' sequences and joining together of the expressed sequence regions 'exons'.

The rRNA (ribosomal RNA) is a primary constituent of ribosomes. Ribosomes are the protein manufacturing organelles of living cells. The assembly of mRNA, tRNA and rRNA is involved in protein synthesis.

The tRNA (transfer RNA) molecules are short RNA strands used for transporting individual amino acids to ribosomes and match them up with the corresponding three-base codon triplet in mRNA [1-4]. Further information about this molecule is given below.

1.2 History and Introduction to tRNA: In 1965, Holley along with his colleagues [5] determined, for the first time, primary sequence of tRNA molecule. The sequenced tRNA molecule was yeast $tRNA^{Ala}$. Earlier years of tRNA research focused on elucidation of the role of tRNA as an adaptor in protein biosynthesis, determination of the primary sequences of several tRNAs, and in solving the three dimensional structure of tRNA [6,7,8]. Progress has been made on a broad front in the last two decades and tRNA has remained an attractive and active area of research.

The tRNA is a relatively small (70-80 nucleotides) and well characterized RNA of known three dimensional structure [9]. The tRNA plays a crucial

role in protein biosynthesis; however, it also interacts with various proteins including RNA processing enzymes, tRNA-modifying enzymes, aminoacyl-tRNA synthetase, protein synthesis elongation factors, initiation factors, and the ribosome [3]. Also, tRNA participates in a variety of other functions in cellular metabolism such as cell wall biosynthesis, chlorophyll and heme biosynthesis [10]. Its role as primer for reverse transcription of retroviruses is also interesting. The desire to understand mechanism for various functions on structural basis has led to several structural studies of tRNA. The structure of tRNA must fulfil two-fold requirement a) All tRNA should be able to sit in the P and A sites of the ribosome and for this process the entire set must conform to a similar structure. b) Enzymes (in particular, aminoacyl synthetases) that bind to tRNAs, recognize their overall structure and some specific identity elements rather than the entire tRNA nucleotide sequence [11].

1.2.1 There are three hierarchical levels of tRNA structure.

i) Primary Structure: The nucleotide sequence nearly 80 nucleotides long, of tRNA molecule is referred as primary structure. The primary structure is useful for preparing databases and analysis of databases provides valuable information. More than 2000 tRNAs sequences [12] have been known; but x-ray structural information is known for only few tRNA molecule. Therefore, primary structure is the only valuable information for these tRNAs, which may also determine the secondary and tertiary structure for these molecules.

ii) Secondary structure: The sequence of several hundred tRNAs from a variety of species have been determined. All tRNAs sequences may be arranged in similar stem loop arrangement, resembling a cloverleaf pattern when drawn in two dimensions. The short double helical four stems are stabilized by Watson-Crick base pairing fig. (2) [1-4].

The acceptor arm consists of a stem part followed by unpaired sequence of CCA on 3'-end of tRNA. The 2' or 3'OH groups from 3' end CCA are amino-acylated. The other arms consist of base paired stem and loop part. The TψC arm is named for the presence of this triplet sequence in its loop. The T stands for thymine, ψ stands for pseudouridine, and C stands for cytosine in the TψC triplet. The loop part contains 7 nucleosides. This region is involved in binding to ribosomal surface.

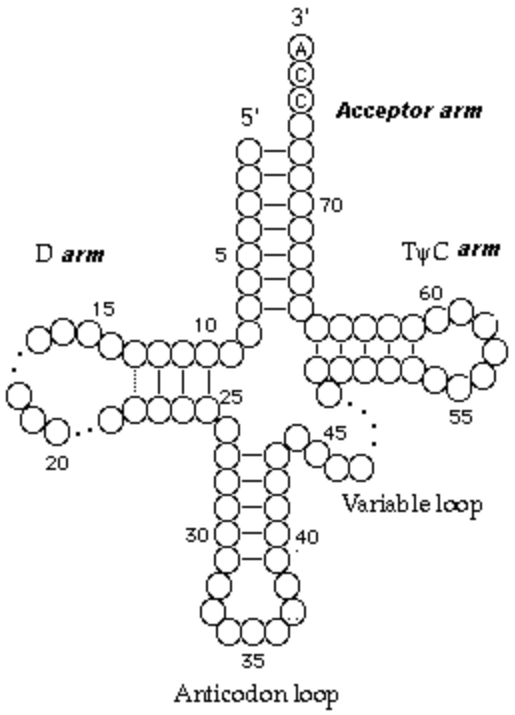

Fig.2 Clover leaf model of tRNA

As we move along the backbone away from the 3'-end, we encounter variable loop after TψC arm. Its size is variable, and is also called the extra loop.

The anticodon arm as well contains stem and loop part. The loop consists of 7 bases including the anticodon triplet. The U-turning between 33rd and 34th nucleotide is seen. In the loop, 2 bases are stacked on one side (5'-side) and 5 bases are partially stacked on the other side (3'-side). Similar U-turning is also seen in the TψC loop.

The next stem loop is Dihydrouridine arm, it contains 8 to 12 unpaired bases and characteristically contains the modified base dihydrouracil and hence the name of the loop is D-loop.

iii) Tertiary structure: The tertiary or three dimensional structure can give information about spatial arrangement of all stem-loops and their interaction pattern. The X-ray diffraction studies of tRNA crystals have provided valuable information about tertiary structures [13,14,15,16,17]. Some good crystals of yeast phenylalanine tRNA (tRNA^{Phe}) obtained [18,19] in several laboratories have allowed elucidation of its three dimensional

(tertiary) structure to atomic resolution. These studies actually revealed A-type helix character, and single stranded loop conformations.

Fig. 3. Three dimensional structure of tRNA

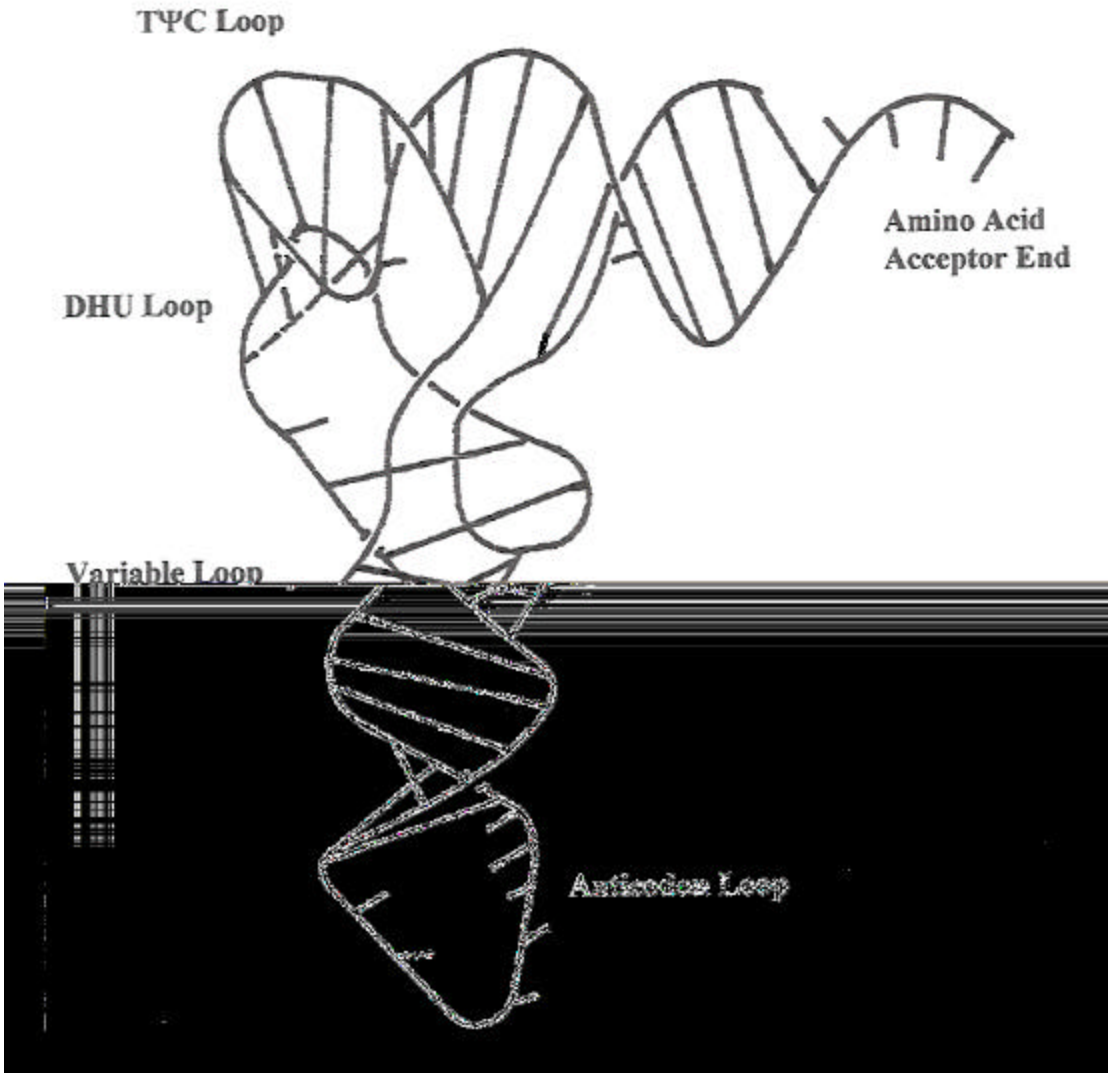

The hydrogen bonding interaction between D-loop and TψC loop, along with base pairing interactions present in all stems, and interactions stabilizing the overall L-shaped three dimensional structure are also revealed by the crystal structure data.

Some of the features of this L-shaped molecule are 1) The amino acid acceptor CCA group is located at one end of the L, around 70A° away from anticodon, which occurs at the other end. 2) The tertiary interactions of D-loop and TψC loop stabilize the

L corner in tRNA. 3) Many tertiary hydrogen bonding interactions involve base pairs different from conventional AU and GC. 4) Stacking is equally important factor in stabilizing the tRNA configuration as much as the tertiary hydrogen bonds. 5) Presence of various modifications (modified nucleosides) at specific sites in several tRNAs is a most fascinating feature.

1.3 tRNA modifications :

Transfer RNA has the largest number of chemically modified nucleosides. Out of nearly 100 different known modifications about 80 occur in tRNA. Higher organized life domains multicellular eukaryotes [20-24] are modified to a larger extent and upto 25% of all nucleosides in eukaryotic tRNA have been found modified. Many modifications involve simple alkylation, hydrogenation, thiolation or isomerisation of four common ribonucleosides (A, G, C, U) in the base and /or the 2'-hydroxyl group of the ribose, however, some nucleosides have quite extensive chemical modifications [22-27]. Table 1 gives list of some modifications and their abbreviations.

The tRNAs from three kingdoms of archaebacteria, eubacteria and eukaryotes contain modified nucleosides [28]. A subset of these modifications (D, ψ, Um, ac^4C, Cm, m^1G, m^7G, Gm, m^1A, t^6A, mt^6A and I) is present in tRNA from all three phylogenetic domains [29]; some modifications occur at specific tRNA site, (ψ_{13}, Cm_{32}, m^1G_{37} , t^6A_{37} , ψ_{38} , ψ_{39}, ψ_{55},and m^1A_{58}) in all three kingdoms [30].

1.3.1 Conversion to modified nucleosides:

The conversion to modified nucleosides is carried out post transcriptionally by tRNA modifying enzymes. Several different tRNA modifying enzymes are present in cell to carryout various modifications. However, specific tRNA modifying enzymes have various specific requirements on sequence structure of their substrate tRNA.

Table 1 List of some modifications with its short form notations

Name	Short form
A. Simple Nucleosides :	
1. Adenosine	A
2. Guanine	G
3. Cytosine	C
4. Uracil	U
B. Modified Nucleosides :	
1. N^4 - acetyl cytidine	ac^4 C
2. 5-carbamoyl methyl uridine	ncm^5 U
3. psuedouridine	psu
4. 5-hydroxymethyl cytidine	hm^5 C
5. 5-methyl aminomethyl uridine	mnm^5 U
6. N^4 –acetyl-2'-omethyl cytidine	ac^4 Cm
C. Hypermodified Nucleosides :	
1. N^6 isopentenyl adenosine	i^6 A
2. 2-methylthio-N^6 –(isopentenyl) adenosine	ms^2 i^6 A
3. N^6 –(cis-hydroxy isopentenyl) adenosine	io^6 A
4. 2-methylthio-N^6 – (hydroxy isopentenyl) adenosine	ms^2 io^6 A
5. N^6 –methylthio –N^6 –threonyl carbamoyl adenosine	m^6 ms^2 t^6 A
6. N^6 –methyl-N^6 –threonyl carbamoyl adenosine	m^6 t^6 A
7. 2-methylthio-N^6 –threonyl carbamoyl adenosine	ms^2 t^6 A
8. Queuosine	Q
9. N^6 –threonyl carbamoyl adenosine	t^6 A
10. wyosine	w
11. inosine	I
12. 5-methoxy carbonyl methyl-2 thiouridine	mcm^5 s^2 U
13. N^6 –glycinyl carbamoyl adenosine	g^6 A
14 7- cyano-7-deazaguanosine	preQo
15. 2 – thiouridine	s^2 U

Different enzymes catalyze the synthesis of the same modified nucleosides in rRNA and in tRNA [31,32]. But, the tRNA (m^5C) methyl transferase shows activity towards rRNA and synthetic polymers [33]. Furthermore, different enzymes produce ψ in the anticodon arm. Thus, these are different enzymes catalyzing the synthesis of same modified nucleoside not only in different nucleic acids but also in different positions of the tRNA. Also, some specific tRNA enzymes have different requirement for target identifications.

1.3.2 Functions of modified nucleosides:

Presence of modified nucleosides increases the surface area by 20% [34], suggesting that the modified nucleosides are present to be recognized by various proteins/ nucleic acids. Also, many modified nucleosides participate in unusual hydrogen bonding [34] and thereby contribute to tRNA structure. However, physicochemical contribution of modified nucleosides can be in many ways, like introduction of transient charges dependent on protonation, alteration and restriction of nucleoside conformation, inhibition of non canonical base pair or disruption of canonical base pair and enhancement of base stacking interactions [35]. But, most dynamic and influential role must be from the extensive (hyper) modifications present at first anticodon (34^{th}, wobble) position and 3'-adjacent to anticodon position (37^{th}) position.

1.3.3 Modification at 34^{th} position and its functional importance:

Various modified nucleosides occur at wobble position of tRNA. The modifications Q, mcm^5s^2U, mnm^5s^2U, n^4aC, s^2U, I, Um etc occur at wobble site. This first position anticodon along with its modification is highly important and interesting, because of its direct involvement in codon - anticodon interactions for protein biosynthesis. Cell utilizes 10 times more energy in protein synthesis than in DNA synthesis [36]. Clearly, translational accuracy and efficiency are important to cellular physiology. Modified nucleosides contribute to genetic translation in several ways. Base modification at the wobble position of tRNA can change the pattern of hydrogen bond donors and acceptors, and thus directly change base pairing specificity. The adenosine to inosine (I) modification allows base pairing of C, U and A bases and extends wobbling. Some of the modifications increase wobbling, while others restrict it [36]. The

modifications of interest for present study at wobble position are mcm^5s^2U and Q.

a) mcm^5s^2U: A large variety of modified uridines occur at the wobble position of tRNA. Various 5-position substituents with and without thio group at 2nd position of uridine are the general pattern for modified uridines. The examples are mcm^5U, mnm^5U, cm^5U, mcm^5s^2U, mnm^5s^2U, $cmnm^5U$ etc. The unmodified uridine at wobble can indeed read codons ending with all four bases [37, 38]. Thus, unmodified U_{34} seems to allow extended wobbling. However, modifications of uridine are associated with restricted wobble. The thio group (s^2) of modified uridine gives preference to A over G [39]. However, all 5-methyl substitutions inhibit reading of pyrimidines [40]. The 5-position substituent may help in stabilizing 3'-endo conformation at the expense of 2'-endo conformation, through interactions with 5'-phosphate. The amino group of mnm^5 of modified uridine (mnm^5s^2U) helps in stabilizing 'U-turn' through interacting with the 2'-OH of 33rd residue [40, 24].

The mnm^5s^2U, which is present in various tRNAs e.g. human $tRNA^{Lys}$ [41], $tRNA^{Arg}$ from bovine liver [42] etc, may restrict wobbling and stabilize U- turn and C3'-endo sugar puckering. The conformational preferences for the individual nucleotide is presented in the chapter 3(A). And, interaction of mcm^5s^2U in presence of hypermodified nucleoside at 37th position, ms^2tc^6Ade, in human $tRNA^{Lys}$ is reported in the chapter 5.

b) Queuosine (Q): Another highly complex modified nucleoside queuosine (Q) is present at the 1st position of anticodon in some tRNAs ($tRNA^{Asn,\ Asp,\ his}$ and $tRNA^{Tyr}$). Q is further modified to galQ and manQ in $tRNA^{Tyr}$ and $tRNA^{Asp}$, respectively, from higher eukaryotes. In Q, the cyclopentenediol moiety is linked to 7-deazaguanine base through – CH2-NH^+2 linker [43]. Formation of the complex hypermodified queuosine at position 34 in eukaryotic tRNAs requires only one enzyme, the tRNA: guanine transglycosylase, which exchanges the guanosine 34 with the free precursor queuine. However, in prokaryotes, at least three enzymes are required to accomplish the stepwise formation of the same queuosine containing tRNAs [44].

The role of this modification in changing or retaining the Watson – Crick base pairing edge of wobble nucleotide is of interest to us. The role of C(7)-substituent of Q may help in stabilizing anticodon loop conformation through interaction

with 33rd residue of anticodon loop. We have explored various possible conformations of this modified nucleotide for understanding its functional significance.

1.3.4 Modification at 37th position and its functional importance:

The modification at 37th position of anticodon is highly correlated with the base at position 36 [45]. The position 37 is virtually always a purine, and is usually modified. Modifications often occur at more than one position on the base. These generalizations hold for all three kingdoms and subcellular organelle systems [46].

A common theme of these modifications may be to help in stabilizing cognate anticodon: codon interactions through increased base stacking. Translational efficiency or reading frame maintenance may be associated with increased stability of anticodon loop. Modification at 37th position may also prevent extended base pairing with the mRNA and can stop frameshift errors.

In the present study the focus is on the conformational preferences and role of tc^6Ade and its derivative ms^2tc^6Ade in the anticodon loop.

a) tc^6Ade and derivative (ms^2tc^6Ade) : Virtually all organisms use tRNAs that have a t^6A derivative 3' to the anticodon to read ANN codons [46,47]. In the synthesis of t^6A, threonine is used along with bicarbonate in, in vitro, ATP dependent reaction [48,49]. Interestingly, same enzyme may also incorporate glysine instead of threonine. A mutation of C_{36} to U_{36} in $tRNA^{Gly}$ results in the synthesis of t^6A [50], which strongly supports the suggestion that the sequence U_{36}-A_{37}-A_{38} is one determinant for the tRNA (t^6A_{37}) synthetase [51].

The presence of t^6A strengthens the binding of tRNA to programmed ribosomes [52], and also the interaction with complementary tRNAs in anticodon – anticodon association experiments [53]. The highly functionalized threonine side chain has the potential to interact in unique ways with other functional groups in the tRNA anticodon. The proposed role of t^6A is for stabilizing the codon - anticodon interaction. Also, a direct interaction between t^6A_{37} and the $mnm^5s^2U_{34}$ nucleoside in tRNA lysine [54] is proposed to explain a unique characteristic about the structure and chemistry in this special tRNA. Similarly, interaction between highly modified base $mcm^5s^2U_{34}$ and $ms^2tc^6Ade_{37}$ present in human tRNA lysine is invoked in Agris [54] model of

unconventional anticodon loop structure for $tRNA^{Lys}$. We have tried to examine this possibility of unconventional structure in case of human $tRNA^{Lys}$ and $tRNA^{Asn}$ (which contains Q_{34} and tc^6Ade_{37} as modified bases).

1.4 Methods useful for structural studies:

a) X-ray crystallography :

In x-ray crystallography [55,56], diffracted waves from periodically arranged atoms in crystals can add up in phase according to Bragg's law (i.e interplanar or interatomic distance should be comparable to wavelength of incident light to have interference) to give diffraction pattern. X-ray crystallography is very useful technique, but growing a useful crystal can be the most serious job. Getting the required high resolution, to get accurate structural information, also poses problems.

b) NMR :

Nuclear Magnetic Resonance [57,58] (NMR) is based on the quantum mechanical property -spin of nuclei. It determines information about atoms from the fact that their local environment influences their response to applied magnetic field. The kind of information obtained from NMR includes the measurement of interatomic distances, and coupling constants that can be interpreted in terms of torsion angles. Increasingly larger molecular systems are becoming amenable to sophisticated multidimensional NMR techniques.

c) Computational methods:

Computational methods like molecular mechanics, semi-empirical and ab-initio molecular orbital approaches have been used for all these structural investigations. Computational techniques are used for molecular modelling and simulation (i.e numerical experiments based on theoretical models of real molecular systems). Advances in fast, efficient computing hardware and software has enhanced the scope for computational techniques. Vast information databases of new sequences, new compounds have also become available, however, accurate structural information remains scarce. Although experimental techniques like X-ray crystallography and NMR give valuable information about various compounds; the preparation - availability of suitable samples continues to hamper experimental investigations of biomolecules and limits the available information. On the other hand, high speed / large memory computers and ability of various softwares

programs to handle realistic biological/chemical problems has opened new possibilities for computational probing. The detailed information about computational methods is provided in next chapter.

1.5 References:

1) Gesteland, R.. F. and Atkins T. F (ed.), The RNA world, Cold Spring Harbor Laboratory Press, Cold Spring Harbor, N.Y. 1993

2) Spencer, J. H., The Physics and Chemistry of DNA and RNA; by W. B. Saunders Company U.S.A and Toppan Company Ltd., Japan, 1972

3) Soll, D and RajBhandary, U. tRNA: Structure, Biosynthesis, and Function, American Society for Microbiology, Washington, DC.20005, 1995

4) Watson, J. D.; Hopkins, N. H.; Roberts, J.W.; Steitz, J. A.; Weiner, A. M. Molecular biology of gene, by The Benjamin/Cummings publishing company. Fourth edition,1987

5) Holley, R. W.; Apgar, T.; Everett, G. A.; Madison, J. T.; Marquisee, M.; Merrill, S.H.; Penswick, J. R.; and Zamir, A. Science ,1965,147,1462-1465

6) Zachau, H.G. Introduction: transfer RNA coming of age. In S. Altman (ed.), Transfer RNA. MIT Press, Cambridge , Mass. 1978.

7) Schimmel, P. R.; Soll, D. and Abelson, J. N. (ed.) Transfer RNA: Structure, properties and recognition.. Cold Spring Harbor Laboratory Press, Cold Spring Harbor, N.Y. 1979.

8) Soll, D.; Schimmel, P. R, and Abelson, J. N. (ed.) Transfer RNA: Biological Aspects. Cold Spring Harbor Laboratory Press, Cold Spring Harbor, N.Y. 1980.

9) Dirheimer, G.; Keith, G.; Dumas, P. and Westhof, E. tRNA: Structure, Biosynthesis and Function, American Society for Microbiology,Washington,1995, 79-92

10) RajBhandary, U. L. and Soll, D. tRNA: Structure, Biosynthesis and Function, Chapter-1, American Society for Microbiology,Washington,1995, 1

11) Schimmel, P.; Ann. Rev. of Biochemistry 1987, 56, 125-158

12) RajBhandary, U. L. Fed. Proc. 1980, 39, 2815-2821

13) Clark, B. F. C.; Doctor, B. P.; Cholmes, K.; Klug, A.; Marcker, K.A.; Morris, S. J. and H.H. Paradies, Nature(London), 1968, 219,1222-1224

14) Cramer, F.; VanderHaar, F.; Saenger, W. and Schlime, E. Angew. Chem.1968, 80,969-970

15) Fresco, J. R.; Blake, R. D. and Langridge, R.; Nature 1968,220,1285-1287

16) Hampel A.; Labanauskas, M.; Connors, P.G.; Kirkegard, L.; RajBhandary, U. L.; Sigler, P. B. and Bock, R. M. Science 1968, 162,1384-1387

17) Kim, S. H and Rich, A. Science 1968,162,1381-1384

18) Ichikawa, T. and Sundaralingam, M. Nature New Biol. 1972, 236,174-175.

19) Kim S.H; Quigley, G.; Suddath, F. L.; Rich, A. Proc. Natl. Acad. Sci (USA) 1971, 68,841-845

20) Crain, P. F. in Modifications and Editing in tRNA, ASM Press, Washington, 1998, 47 - 57

21) Kersten, H. Prog. Nucleic Acid Res. Mol. Biol. 1984, 31, 59-107

22) Adamiak, R. W. and Gornicki, P. Prog. Nucleic Acid Res. Mol. Biol 1985, 32, 27-67

23) Bjork, G. R.; Ericson, J. U.; Gustafsson, C. E. D.; Hagervali, T. G.; Tomsson, Y. H. and Wikstrom, P. M. Ann. Rev. Biochem. 1987, 56, 263-287

24) Yokoyama, S. and Nishimura, S. tRNA: Structure, Biosynthesis and Function, American Society for Microbiology, Washington, 1995, 207-233

25) Mcclain, W. H. tRNA: Structure, Biosynthesis and Function, American Society for Microbiology, Washington, 1995, 335-347

26) Persson, B. C. Molecular Microbiology 1993, 8(6), 1011-1016

27) Davis, D. R. in Modifications and Editing in tRNA, ASM Press,Washington, 1998, 85-102

28)Steinberg, S.; Misch, A. and Sprinzl, M. Nucleic Acids Res. 1993, 21, 3011-3015

29) Edmonds, C. G.; Crain, P. F. Gupta, R.; Hashizume, T.; Hocart, C. H.; Kowalak, J. A.; Pomerantz, S. C.; Stetter, K. O. and McCloskey, J. A. J. Bacteriol. 1991, 173, 3138-3148

30) Bjork, G. R. Chemica Scripta 1984, 26B, 91-95

31) Bjork, G. R.; Isaksson, L. A. J. Mol. Biol. 1970, 51, 83-100

32) Bjork, G.R.; Kjellin-straby, K. J.Bacteriol. 1978, 133, 508-517

33) Keith, J. M.; Winters E. M. Moss, B. J. Biol. Chem. 1980, 255, 4636-44

34) Kim, S. H. In Transfer RNA: Structure, Properties and Recognition. ed. Schimmel, P.

R.; Soll, D. and Abelson, J.N. New York; Cold Spring Harbor Laboratory press. 1979,83-100

35) Agris, P. F. Prog. Nucleic Acid .Res. Mol. Biol. 1996, 53, 79-129

36) Curran, J. F. in Modifications and Editing in tRNA, ASM Press,Washington,1998, 493 –516

37) Andachi, T. F.; Yamao, A.; Muto and Osawa, S. J. Mol. Biol, 1989, 209, 37-54

38) Heckman, T. E.; Sarnoff, J.; Alzner-Deweerd, B.; Yin, S. and RajBhandary, U. L. Proc. Natl. Acad. Sci. USA, 1980, 77, 3159-3163

39) Houssier, C.; Degree, P.; Nicoghosian, K. and Grosjean, H. J. Biomol. Struct. Dyn. 1988, 5, 1259-1266

40) Lim. V. I. J. Mol. Biol. 1994, 240, 8-19

41) Benas P.; Bec, G.; Keith, G.; Marquet, R.; Ehresmann, C.;Ehresmann,B.and Dumas, P. RNA, 2000, 6, 1347-1355

42) Keith, G. Nucleic.Acid Res 1984, 12, 2553-2547

43) Nishimura , S. Prog. Nucleic Acid .Res. Mol. biol. 1983, 28, 49-73

44) Slany, R.K and Kersten, H. Biochimie, 1994, 76, 1178 - 1182

45) Yarus, M. Science 1982, 218, 646-652

46) Grosjean, H.; Sprinzl, M and Steinberg, S. Biochimie 1995, 77, 139-141

47) Sprinzl, M.; Steegborn, C.; Hubel, F. and Steinberg, S. Nucleic Acid. Res 1996, 24, 68-72

48) Elkins, B. N. and Keller, E. B. Biochemistry 1974,13, 4622-4628

49) Korner, A and Soll D. FEBS Lett. 1974, 39, 301-306

50) Roberts, J. W. and Carbon, J. Nature 1974, 250, 412-414

51) Morin, A.; Auxilien, S.; Senger, B.; Tewari, R. and Grosjean, H. RNA, 1998, 4, 24 - 37

52) Miller, J. P.; Hussain, Z. and Schweizer, M. P. Nucleic Acid Res. 1976, 3, 1185-1201

53) Grosjean, H.; deHenau, J. S. and Crothers, D. M. J. Mol. Biol. 1976, 103, 499-519

54) Agris, P. F.; Guenther, R.; Ingram, P.C.; Basti, M.M.; Stuart, J.W.; Sochacka, E.; Malkiewicz, A. RNA 1997, 3, 420-428

55) Drenth, J., Principles of Protein X-ray Crystallography, Springer Verlag 1994.

56) Giaccovazzo, C.; Monaco, H. L.; Viterbo, D.; Scordari, F.; Gilli, G.; Zanotti, G. and

Catti, M., Fundamentals of Crystallography, 2nd edition, Oxford University Press 1992.

57) Abraham, R. J.; Fisher, J. and Loftus, P., Introduction to NMR Spectroscopy, John Wiley & Sons, New York, 1988.

58) Macomber, R. S. NMR Spectroscopy: Essential Theory and Practice, Harcourt Brace Jovanovich, San Diego, CA, 1988.

59) Holbrook, S. R.; Sussman, J. L.; Warrant, R. W.; Kim, S. H. J. Mol. Biol. 1978, 123, 631-660

Chapter 2: Computational Methods

Various computational methods are presently available for studies of molecular structure and simulation [numerical modelling] of bio-molecular properties. The computation methods are broadly divided in the following two sections. Section A) Classical / Statistical mechanics methods, B) Quantum mechanics methods.

2.1 Section A: Classical / Statistical mechanics methods:

2.1.1 Molecular Mechanics: In this method, atoms are considered to be point mass particles connected with spring like bonds and both the atoms perform simple harmonic motion about the equilibrium bond length values. Likewise, various bond angles may also oscillate around their equilibrium values. The energy of the system is given by force field consisting of various bonded and non-bonded interaction terms. The general form of force field is given below.

$$E_{total} = E_{stretch} + E_{bend} + E_{torsion} + E_{non\text{-}bonded\ interaction}$$

or

$$E_{total} = \underset{bonds}{\Sigma} k_r (r-r_{eq})^2 + \underset{angles}{\Sigma} k_\theta (\theta-\theta_{eq})^2 + \underset{dihedrals}{\Sigma}(En/2)\,[1+\cos(n\phi \bullet \gamma)] + \underset{i>j}{\Sigma}\{[(Aij/Rij^{12}) - (Bij/Rij^{6})] + (q_i q_j / \varepsilon\, Rij)\} \ldots (a)$$

E_{total} is the potential energy of the system; k_r and r_{eq} are the bond stretching constant and the equilibrium bond distance; k_θ and θ_{eq} are the bond angle stretching constant and the equilibrium bond angle; En, n and γ are the torsional force constant, the periodicity of the torsional term, and the phase angle; Aij and Bij are the non-bonded (Lennard-Jones) repulsion and attraction coefficients; Rij is the interatomic distances between atom i and j; q_i, q_j are the atomic partial charges on atom i and j; and ε is the effective dielectric constant. The general equation (a) gets modified mainly in the treatment of non-bonded interaction term and various parameter sets adopted by different investigators. This has resulted in various force fields like AMBER (Assisted Model Building with Energy Refinement) [1,2]; CFF (Consistent Force Field) [3,4]; CHARMM (Chemistry at Harvard Macromolecular Mechanics Force Field) [5]; MMFF (Molecular Mechanics Force Field)

[6]; MM3 / MM4 (Molecular Mechanics) [7] etc. Molecular mechanics is easy and powerful method applicable to complex biomolecular system.

2.1.2 Molecular Dynamics (MD) and Monte Carlo:

MD method gives time dependent evaluation of molecular system. MD requires two entities: a force field and a way of integration of the equation of motions [8,9,10]

Sybyl dynamics module is utilized for molecular dynamics simulation. Kollman (All Atom, hybrid and United atom) and tripos type of force field are available in Sybyl software and Verlet or Leapfrog algorithm is utilized for the integration of the equation of motion [8,9,10].

Sybyl dynamics methodology:

Operationally, and at the simplest possible level, two entities are required in an MD programs a force field and a way of integrating the equations of motion.

$$m_i \frac{\partial^2 \underline{x}_i(t)}{\partial t^2} = m_i \underline{a}_i(t) = \underline{F}_i = -\underline{\nabla}_i E \quad \ldots\ldots \text{eq.(1).}$$

Where

$m_i \longrightarrow$ is the mass of atom i

$\underline{x}_i(t) \longrightarrow$ is position of atom i

$\underline{F}_i \longrightarrow$ is force acing on atom i

$\underline{\nabla}_i \longrightarrow$ is a gradient with respect to $\underline{x}_i$

The implementation of molecular dynamics in SYBYL allows a choice of force fields (like tripos, kollman all atom, kollman united, or kollman hybrid) and uses the verlet method [9] also known as the leapfrog method, for the integration of the equations of the motion. As in any MD method implemented in a digital computer, the calculations of motion are done at discrete intervals; the length of these intervals defines the time step. The displacement of an atom over a time step Δt is given by:

$$\underline{x}(t + \Delta t) - \underline{x}(t) = \frac{\partial \underline{x}(t^*)}{\partial t} \Delta t = \underline{v}(t^*) \Delta t \quad \ldots\ldots.(2)$$

where $\underline{v}(t^*)$ is velocity at time t^*

The verlet method uses the velocity at the mid point of the time interval in equation (2), since the velocity is not constant through the interval; i.e. $t^* = t + \Delta t/2$. The velocity at the midpoint can be estimated from the previous time step and from the acceleration $\underline{a}$, which in turn can be calculated directed from the force equation (1).

$$\underline{v}\,(t + (\Delta t/2)) = \underline{v}\,(t - (\Delta t/2)) + \underline{a}\,\Delta t$$

After calculating the new velocity, it is submitted into equation (2) and the cycle is repeated. The algorithms used in sybyl dynamics calculations are refinement of those described by Berendsen [10].

MD generates a thermodynamic ensemble over time as well over space, from which the necessary averaged quantities can be derived. However, Monte Carlo uses a series of random moves along with energy based acceptance criteria to produce a thermodynamically relevant ensemble. There is no formal equivalence between individual moves in the space and time domains, so there is no rigorous way to define the effective simulation time corresponding to a Monte Carlo simulation of a given no. of moves. The various criterias for tRNA MD simulation are discussed in the Encyclopedia of Computational Chemistry [11].

2.2 Section B: Quantum Mechanics Methods

Quantum mechanics [12] describes molecule in terms of interactions among nuclei and electrons, and molecular geometry in terms of minimum energy arrangements of nuclei and electrons. The equation of quantum mechanics is schrodinger equation

$$H\psi = E\psi$$

Where H → is total energy operator of many electron system

ψ → is total wave function of many electron system

E → is total energy of many electron system

The total wave function is constructed through suitable combination of individual one-electron wave functions.

$\psi = \Sigma\, a_i \phi_i$, where N is no. of electrons

ϕ_i → one-electron molecular orbital

and a_i → coefficient

The procedure which allows the determination of the individual molecular orbital is the " Self – Consistent Field" method, the main features of which are as follows.

a) Total Hamiltonian is

$$H = \sum_{\nu} H(\nu) + \sum_{\mu<\nu} 1/r_{\mu\nu}$$

where, H(ν) s the Hamiltonian for one electron ν in the field of all the bare nuclei

b) Total energy for the system is

$$E = \frac{\int \psi^* H \psi \, d\tau}{\int \psi^* \psi \, d\tau}$$

expressed in terms of individual orbitals ϕ, by using the determinantal expression of ψ. Various terms in total energy E according to HF is

$$E^{HF} = E^{Nuclear} + E^{Core} + E^{Coulomb} + E^{exchange}$$

c) One satisfies the variation principle for the energy. i.e. The energy is calculated by the above expression using an approximate wave function which always corresponds to energy higher than the exact energy. Carrying out this procedure yields general "Fock" equation one for each individual orbital ϕ

$$F\phi_i = \varepsilon \phi_i \ldots\ldots\ldots\ldots\ldots\ldots\ldots(a)$$

where F is an operator playing the role of an individual Hamiltonian and ε_i is individual energy of one electron occupying the orbital ϕ_i. The operator F depends on all the orbitals that are occupied in the system: thus each ϕ_i is given by an equation that depends on all the orbitals ϕ's. The way out of this difficulty is to choose a reasonable starting set of 'ϕ's and repeat the operations again and again until the p^{th} set of ϕ's reproduces the $(p-1)^{th}$ set to a good accuracy. Hence the name is "Self-Consistent".

The fock operator and expressing individual molecular orbital ϕ_i as combination of atomic orbital ($\phi_i = \Sigma c_r x_r$, x_r – atomic orbital), yields a system of homogeneous linear equations in the c's, the Roothaan equation

$$\sum_{q} c_{iq} (F_{pq} - \varepsilon S_{pq}) = 0$$

where S_{pq} is overlap integral

F_{pq} is pq matrix element of fock operator.

The practical way of solving the Roothaan equation is to choose an initial set of 'c's, calculate F_{pq}'s, solve the equations for a new set, and iterate again until consistency is attained. This is the theory of Hartree-Fock or (SCF-LCAO-MO) abinitio method. Practical reasons forbid the use of complete basis sets (which may have infinite terms), thus a finite incomplete basis set is used in all computations. The choice of atomic basis set fixes the limits to the accuracy of the results. Higher (more complete) basis sets allow greater flexibility (realism) in presenting molecular orbitals. This also leads to solutions approaching true ground state more closely.

2.2.1 Semi – empirical methods: In order to simplify the quantum mechanical calculations, instead of numerical evaluation of the various integrals, empirical values are used in semi-empirical calculations, while some other integrals deemed small are neglected altogether. Various semi-empirical methods differ in the level of approximations used and the values used for the integrals. Semi-empirical models aim to relate molecular properties with one another using broadly theoretical Hartree - Fock model. Considerable simplification results in all valence electron approaches as the inner electrons become part of the nuclear core and are not treated explicitly. Next, the basis set is restricted to a minimal representation.

Various approximations are useful in reducing overall computation. The central approximation is to insist that atomic orbitals residing on different atomic centers do not overlap.

$? \chi_u \chi_v \, \delta\tau = 0$ ……(a) χ_u and χ_v not on same atom

This is referred as Neglect of Diatomic Differential Overlap or NDDO approximation. The AM1 [13] and PM3 [14] models incorporate essentially the same approximations but differ in their parameterization. The Zero Differential Overlap approximation is same as that of eq.(a) , but considering overlap on same or on different atoms. And it was initiated by Pariser and Parr [15] in case of Π -electrons and was later generalized by Pople et.al.[16] for any pair of valence orbitals. The Roothaan LCAO –SCF equations in the ZDO approximation are thus simplified to

$\sum_q c_{iq} (F_{pq} - \varepsilon \, \delta_{pq}) = 0$ where δ_{pq} is the Kronecker symbol.

The Complete Neglect of Differential Overlap (CNDO) method, adds to ZDO hypothesis

two other fundamental approximations: the first one concerns the values of the Coulomb integrals, which are all approximated as Coulomb integrals over s Slater atomic orbitals.

And the second fundamental hypothesis of the CNDO procedure concerns the core matrix elements. The detailed discussion is available in the references [16,17,18,19].

2.2.2 PCILO method:

Perturbative Configuration Interaction Using Localized Orbitals (PCILO) method [19,20] is an all valence electron molecular orbital approach. Realizing the utility of usual molecular sketch representation in chemistry, it is utilized for the suitable zeroth order wavefunction of the molecule. The molecular wavefunction is built from orbitals localized (bonding orbitals) on the chemical bonds and lone pairs of the molecule. The method introduces the following simplifications: a) use of full ZDO hypothesis b) integral approximations based on CNDO/2, both for the coulomb integrals and for the core matrix elements. Empirical values of ionization potential and electron affinity utilized for evaluation of core matrix elements in CNDO/2 approximations.

Suitable combination of atomic hybrids gives bonding orbitals as:

$$i = \alpha\chi_1 + \beta\chi_2$$

And the corresponding antibonding orbital is:

$$i^* = -\beta\chi_1 + \alpha\chi_2$$

Bonding orbitals form zeroth order wavefunction and antibonding orbitals are used to build excited states (mono-, di-excited states). The Configuration Interaction (CI) matrix is constructed on such basis of configurations.

$$\Omega = \sum_k C_k \psi_k \quad \text{where } \Omega \text{ total resultant wave function}$$

$$\psi_k = \text{various configurations}$$

This CI takes into account the correlation energy, which is built-in error in HF-SCF model. The use of localized molecular orbitals (MOs) for correlation problem is useful to give local structure to CI matrix as suggested by Sinanoglu [25]. Almost all correlation energy contribution comes from local excitations. Rayleigh - Schrodinger perturbation [12] technique is used to truncate CI matrices [21]. This truncation is necessary to save computational time and memory, and major contribution to energy comes from the first few terms of full CI expansion. Energy correction upto the third order is included in

PCILO method. In the Rayleigh-Schrodinger perturbation, exact hamiltonian *H* is expressed as

$H = H_o + \lambda V$ where H_o is unperturbed hamiltonian (with ψ_k eigenvectors) which differs from exact hamiltonian by a small perturbation term λV. Taylor expansion in the neighbourhood of $\lambda=0$ gives total energy and total wavefunction as:

$$E = E_k + \lambda E'_1 + \lambda^2 E'_2 + \ldots$$

$$\Omega = \psi_k + \lambda \phi'_1 + \lambda^2 \phi'_2 + \ldots$$

The energy formulae for the first, second and third order energy corrections are given as:

$$E'_1 = V_{oo}$$

$$E'_2 = \sum_{k \neq 0} \frac{|V_{ok}|^2}{E_o - E_k}$$

$$E'_3 = \sum_{k \neq 0} \sum_{l} \frac{V_{ko} V_{lo} V_{ok}}{(E_o - E_k)(E_o - E_l)}$$

The partial charges obtained using method of Del Re [26] have been utilized in PCILO approach.

PCILO is found to be very useful to do conformational search for biomolecules. The rigid-body rotation is assumed for internal rotation around exo-cyclic chemical bonds. Thus the molecular structure problem for a molecule having N atoms gets greatly simplified from 3N-6 degrees of freedom to just few exocyclic torsion angles. Typical bond distances and bond angles are found to essentially retain constant values, across vast structural data encompassing a large number of molecules in different conformations. Thus the assumption of fixed bond distance and bond angle values for conformational search is valid and has great value for computational simplification. We preferred PCILO to span whole conformational space instead of molecular mechanics based limited geometry optimization. Also, PCILO method has been tested successfully in predicting the preferred conformational structures for a large number of biomolecules.

2.2.3 Density Functional Theory (DFT):

Density Functional Models [22] provide an alternative approach to the treatment of correlation (which is difference between Hartree-Fock energy and the experimental

energy) in many-electron systems. The total energy in DFT, is unique functional of the total electron density. The energy according to DFT is

$$E^{DFT} = E^{Nuclear} + E^{Core} + E^{Coulomb} + E^{X}(p) + E^{C}(p)$$

The first three terms represent Hartree-Fock energy, and Hartree-Fock exchange term is replaced by exchange functional $E^{X}(p)$ and in addition a correction functional $E^{C}(p)$. Both the latter terms are functions of electron density p. The local density or non-local density models are included in DFT.

The local density models will be referred to as SVWN (Slater, Vosko, Wilk, Nusair) models. Here, the form of the exchange and correlation functionals follows from the exact (numerical) solution of a many-electron gas of uniform density, as a function of the density, by subtracting E^{Core} and $E^{Coulomb}$ from the total energy (there is no $E^{Nuclear}$ term).

The SVWN model would not be satisfactory for molecular system of non-uniform electron density. The model may be improved by introducing explicit dependence on the gradient of the electron density, in addition to the density itself. Such procedures are termed gradient –correlated or non-local density functional models. An alternative to local density model is the so-called generalized gradient approximation proposed by Becke and Perdew [23,24].

In the Becke – Perdew (BP or BP86) model, a new potential is used in place of the local potential in the Self-Consistent-Field (SCF) procedure. This actually comprises a local part and a gradient correction. The latter needs to be recalculated at every SCF iteration. An alternative, and computationally simpler approaches, is to introduce gradient correction only after convergence based on the local potential alone has been achieved. This procedure is referred to as a perturbative Becke –Perdew model (or pBP).

The basis sets for DFT calculations in spartan are tabulated atomic solutions, supplemented by d-type functions on heavy atoms and p-type functions (optionally) on hydrogen. The numerical polarizations DN* and full polarization (DN**) are basis set for DFT calculations.

2.3 References:

1) Weiner, S. J.; Kollman, P. A.; Nguyen, D. T. and Casem, D. A. J. Comput. Chem. 1986, 7, 230-252.
2) Cornell, W. D.; Cieplak. P.; bayly, C. I.; Gould, I. R.; Merz, K. M.; Jr. Ferguson, D. M.; Spellmeyer, D. C.; Fox, T.; Caldwell, J. W. and Kollman, P. A. J. Am. Chem. Soc 1995, 117, 5179-5197
3) Maple, J. R.; Hwang, M.. J.; Stockfisch, T. P.; Dinur, U.; Waldman, M.; Ewig, C. S.; and Hagler, A. T. J. Comput. Chem. 1994, 15, 162-182
4) Hwang, M. J.; Stockfisch, T. P. and Hagler, A. T. J. Am. Chem. Soc 1994, 116, 2515-2525
5) Nilsson, L. and Karplus, M. J. Comput. Chem. 1986, 7, 591-616
6) Halgren, T. A. J. Comput. Chem 1996, 17, 490-519
7) Allinger, N. L.; Yuh, Y. H. and Lii, J. H. J. Am. Chem. Soc 1989, 111, 8551-8566.
8) Symon, K. R.; Mechanics, 3rd edition, Addison-Wesley Reading, M.A. 1971
9) Verlet, L. Phys. Rev. 1967, 159, 98 - 103
10) Berendsen, H. J. C; Postma, J. P. M.; vanGunsteren, W. F.; Dinola, A.; Haak, J. P.; J. Chem. Phys. 1984, 81, 3684- 3690
11) Auffiger, P. and Westhof, E. in Encyclopedia of Computation Chemistry by P. V. R. Schleyer; John Wiley and suns, 1998, 3, 1628-1639
12) Szabo, A. Ostlund, N. S. Modern Quantum Chemistry, Mc-Graw Hill Publishing company 1982.
13) Dewar, M.. J. S.; Zoebisch, E. G.; Healy, E. F.; and Stewart, J. J. P. J. Am. Chem. Soc 1985, 107, 3902- 3909
14) Stewart, J. J. P. J. Comput. Chem 1989, 10, 209- 220
15) Pariser, R. and Parr, R. G. J. Chem. Phys. 1953, 21,466- 471
16) Pople, J. A.; Santry, D. P.; and Segal G. A. J. Chem. Phys, 1965, 43, S129- S135
17) Pople, J. A and Segal G. A. J. Chem. Phys, 1965, 43, S136- S149
18) Pople, J. A and Segal G. A. J. Chem. Phys, 1966, 44, 3289-3296
19) Diner, S; Malrieu, J. P. and Claverie, P. Theor. Chim. Acta 1969, 13, 1- 17
20) Diner, S; Malrieu, J. P.; Jordan, F. and Culbert, M. Theor. Chim. Acta 1969, 15, 100-110

21) Claverie, P.; Diner, S. and Malrieu, J. P. Int. J. Quantum Chem. 1967, 1, 751

22) Jones, R. O. and Gunnarsson, O. Reviews of density functional theory Revs. Mod. Phys. 1989, 61, 689; Parr, P. G. and Yang, W. Density Functional Theory of atoms and molecules, Oxford Univ. Press, Oxford, 1989 ; Labanowski, J. K. and Andzelm, J. W. Eds., Density Functional Methods in Chemistry, Springer-Verlag, New York, 1991.

23) Becke. A. P. Phys. Rev. A. 1988, 38, 3098-3100

24) Perdew, J. P. Phys. Rev. B.1986, 33, 8822-8824

25) Sinanoglu, O. in Adv. Chem. Phys. VI, (I. Prigogine, ed.), Interscience, New york 1964, 315

26) Del Re,G. J. Chem. Soc. 1958, 4031-4040

Chapter –3(A): Conformational preferences of wobble nucleoside 5 - methoxy carbonyl methyl – 2 thiouridine (mcm^5s^2U)

3(A).1 Introduction: Uridines, modified at base ring carbon-5 and many times also thiolated at carbon-2 are often found at anticodon first (wobble) position in tRNA. All modified uridines are synthesized post transcriptionally in prokaryotes and eukaryotes [1,2]. Modification at 5-position of wobble uridine is variable from short methoxy (mo^5U) group to long like methyl carboxy methyl uridine (mcm^5U). However, 2-thiouridine (s^2U) without some sort of modification at the 5-position has only been found in only one of the anticodon out of hundreds of mature tRNAs that have been sequenced [1]. Thiolation and the 5-position substituents have been shown to influence codon - recognition [3,4] and aminoacylation [5,6] and thus are of chemical and structural importance to the tRNA function.

The 2-thio-5-uridine acetic acid methyl ester (mcm^5s^2U), modified uridine, is present at wobble position of anticodon in $tRNA^{Arg}$ from bovine liver [7], rat liver $tRNA^{Lys}$ [8] as well in human $tRNA^{Lys}$ [9]. The esterified acetic acid side chain adds to the biological interest of this nucleotide [10]. This wobble position modified uridine restricts the recognition to only A. The $tRNA^{Arg}$ from bovine liver recognizes AGA codon [7]. The mcm^5s^2U of tRNA is involved in stabilization of a loop-loop interaction between the anticodon loop of $tRNA^{Lys}$ and an A-rich loop located upstream of the Primer Binding Site (PBS) in the genomic RNA of HIV [11]. Thus, it is important to study the conformational preferences of mcm^5s^2U-modified uridine and its role in codon recognition. Here, structural investigations on 5-methoxy carbonyl methyl -2-thiouridine (mcm^5s^2U) are presented.

3(A).2: Nomenclature, Convention and Procedure:

Figure 1. illustrates the atom numbering and identifies the torsion angles for rotation around the acyclic single chemical bonds required for describing the molecular conformation. The torsion angle α [C(6)-C(5)-C(7)-C(8)] is measured with respect to C(6) from the cis (eclipsed, 0°) position in the right-hand sense of rotation.

Fig.1. Wobble nucleotide 5- methoxy carbonyl methyl –2 thiouridine (mcm^5s^2U)

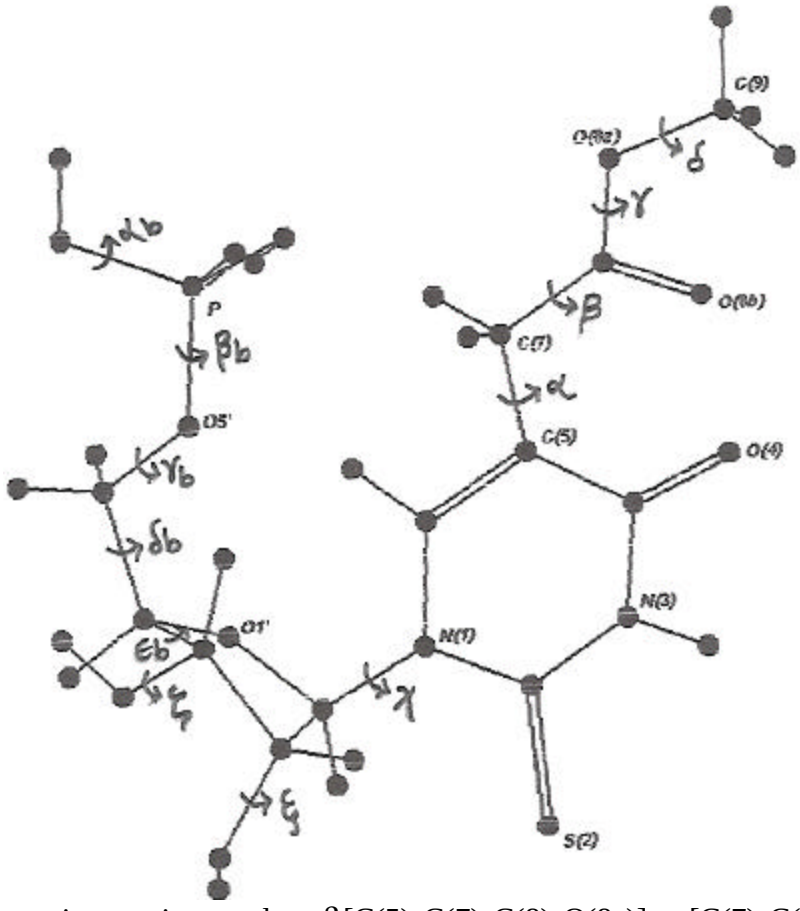

Likewise, the successive torsion angles β[C(5)-C(7)-C(8)-O(8a)], γ[C(7)-C(8)-O(8a)-C(9)] and δ[C(8)-O(8a)-C(9)-H] define the 5-position substituent and glycosidic torsion angle χ is defined as [O1'-C1'-N(1)-C(6)]. However, for torsion angles in the ribose - 5' -phosphate backbone, values have been adopted from Holbrook's model of tRNA [12]. The torsion angles in the ribose- phosphate backbone are distinguished by the subscript b for the backbone. Except for the above mentioned subscript, the same nomenclature is retained as in tRNA model [12] for these backbone torsion angles. The definitions for these backbone torsion angles are α_b [H-O3'-P-O5'], β_b [O3' -P -O5'-C5'], γ_b [P-O5'-C5'-C4'], δ_b [O5'-C5'-C4'-C3'], ε_b [C5'-C4'-C3'-O3'] , ζ_b [C4'-C3'-O3'-P] and ξ_b [C3'-C2'-O2'-H]. The trans (180) arrangement of C(5) substituent is taken as the starting structure.

The perturbative configuration interaction using localized orbitals (PCILO) methods [13] was used for all the energy calculations of the molecular conformation. For each conformation, the polarity of the chemical bonds was optimized and the correction terms up to the third order are included in the calculation of total ground state energy. The logical selection of grid point approach [14] was used for searching the most stable and alternative stable structures in the multidimensional conformational space.

Full geometry optimization, for PCILO most stable and alternative structures, by molecular mechanics force field MMFF [15], parameterized modified neglect of differential overlap framework based PM3 [16-17] and Hartree Fock HF [18,19] approaches has been examined. These methods are implemented in commercially available PC Spartan Pro (Version 6.06 Wavefunction, Inc. 18401 Van Karman Ave., Suite 370 Irvine, CA 92612) and Sybyl 6.4beta (Tripos Inc.) molecular modelling softwares.

Fig.2 The preferred base substituent orientation for mcm^5s^2U by PCILO

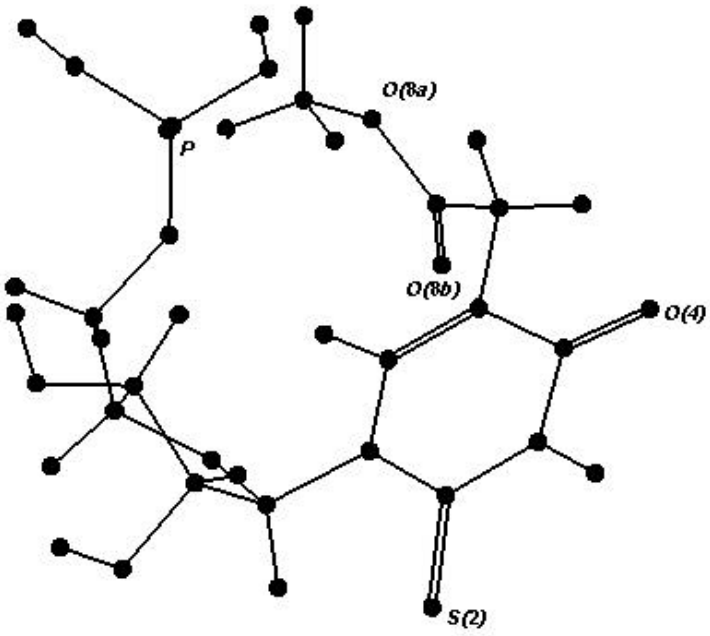

3(A).3: Results and discussion:

Figure 2 depicts the most stable conformation, obtained from PCILO calculations on 5'-monophosphate of mcm^5s^2U. The preferred torsion angles are $\alpha = 330^\circ$, $\beta = 120^\circ$, $\gamma = 180^\circ$, $\delta = 180^\circ$ for the C(5) substituent orientation. The structure is stabilized because of intramolecular hydrogen bonding interaction of C(9)H with the phosphate group oxygen (Table 3a). The other C(6)H...O5' interaction can also stabilize the preferred molecular structure. In this conformation, the C(5)-position substituent orientation does not obstruct the Watson-Crick sites which remain accessible for codon - anticodon interactions.

Table :1 Predicted most and alternative stable conformations for single nucleotide 5-methoxy carbonyl methyl 2-thiouridine.

Torsion angles in (°)	PCILO Rel. energy kcal/mol
a] $\alpha = 180, \beta = 180, \gamma = 180, \delta = 180, \chi = 3$	16.5
b] $\alpha = 330, \beta = 120, \gamma = 180, \delta = 180, \chi = 3$	0.0
c] $\alpha = 330, \beta = 300, \gamma = 330, \delta = 180, \chi = 3$	0.3
d] $\alpha = 90, \beta = 180, \gamma = 0, \delta = 180, , \chi = 3$	2.5
e] $\alpha = 270, \beta = 150, \gamma = 300, \delta = 180, \chi = 3$	5.3

The PCILO predicted alternative structure for 5'-monophosphate mcm^5s^2U are given in Table 1. The first alternative is 0.3 kcal/mol higher in energy than the most stable conformation. The torsion angles describing this alternative are $\alpha = 330^\circ$, $\beta = 300^\circ$, $\gamma = 330^\circ$, $\delta = 180^\circ$. The next alternative ($\alpha = 90^\circ$, $\beta = 180^\circ$, $\gamma = 0^\circ$, $\delta = 180^\circ$) is 2.5kcal/mol higher in energy than the most stable structure. This alternative structure places the C(5)-position substituent over and perpendicular to the plane of uridine base. However, in the next higher energy alternative ($\alpha = 270^\circ$, $\beta = 150^\circ$, $\gamma = 300^\circ$, $\delta = 180^\circ$), C(5)-position substituent is placed below the plane of the uridine base. The alternative structure retains the intramolecular hydrogen bonding between C(9)H...O3'p and C(7)H...O3'p (see Table 3(a)).

Table3(a): Geometrical Parameters for hydrogen bonding for PCILO structures of 5'-monophosphate mcm^5s^2U

Atoms Involved (1-2-3)	Atom pair (1-2) A	Atom pair (2-3) A	Angle (1-2-3)	Reference
C(7)H...O2P	1.091	2.320	135.1	Table1[a]
O2'H...O3'	0.97	2.110	110.0	Table1[a,b,c,d,e]
C(6)H...O5'	1.091	2.330	145.5	Table1[a,b,c,d,e]
C(9)H...O2P	1.091	0.910	159.3	Table1[b]
C(9)H...O3'p	1.091	2.140	112.8	Table1[e]
C(7)H...O3'p	1.091	2.360	169.5	Table1[e]

Interdependence of torsion angle α and β is depicted as isoenergy contour map in fig.3. The most stable conformation is shown by cross 'x' mark at torsion angle values $\alpha=330^\circ, \beta=120^\circ$.

Fig.3 Isoenergy contour diagram for α and β

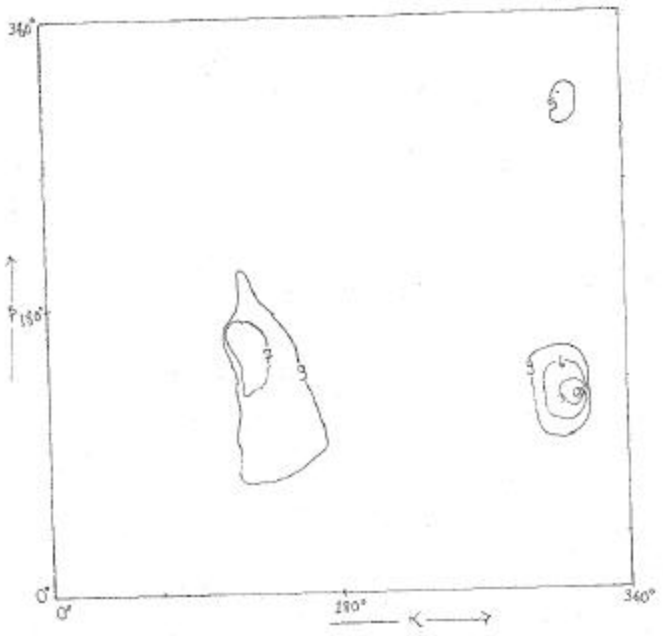

Another stable region within 5kcal/mol energy contour is located at α=330° and β=300°. The contour diagram shows sudden increase in energy when α<120° and α>330°.

Correlation of rotation around bonds C(7)-C(8) and C(8)-O(8a) (torsion angles β and γ) is shown as isoenergy contour map in fig.4. β=120°, γ=180° values represent the most stable conformation denoted by 'x'. The isoenergy contour map shows greater rotational freedom for torsion angle 'γ' as compared to torsion angle 'β' with β=120°, the accessible range for γ is between 60°-210°. The alternative stable region is located around β=300° and γ=330° in the isoenergy contour map of β and γ.

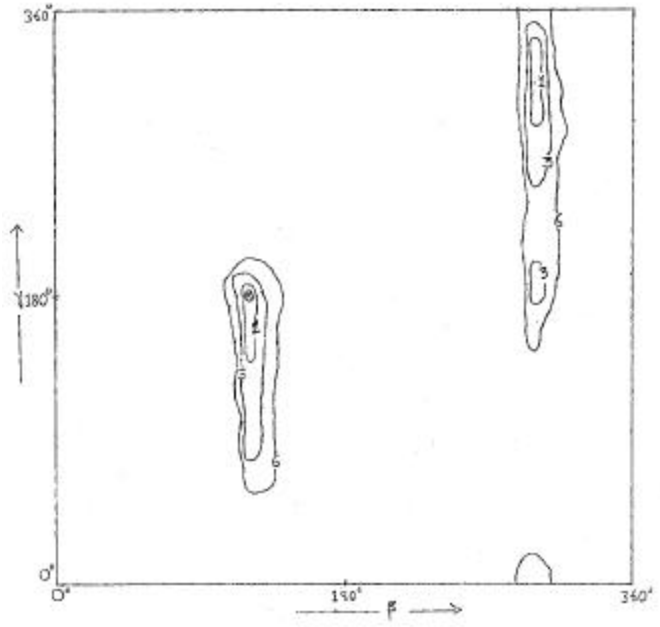

Fig.4 Isoenergy contour diagram for β and γ

The automatic full geometry optimization has been performed, using MMFF, PM3 and HF methods, for all PCILO structures in Table 1. Geometry optimization results using MMFF indicate that the optimized PCILO starting structure (Table 2(1)) leads to the most stable optimized structure amongst all MMFF optimized structures in Table 2. The optimized torsion angle α is significantly different than the starting PCILO geometry for this optimized structure. The C(5) substituent in mcm^5s^2U is placed above but is perpendicular to the plane of uracil. The optimized PCILO most

stable structure is 2.7 kcal/mol higher than the optimized PCILO starting structure.

Table 2: Optimized values of the torsion angles by automatic optimization using MMFF, PM3, and HF methods for mcm^5s^2U

Molecule	Torsion angles in (°)												Rel.	Starting
	α	β	γ	δ	χ	α_b	β_b	γ_b	δ_b	ε_b	ζ_b	ξ_b	energy	geometry
A]MMFF Results:														
1]	97.6	-176.9	175.8	178.8	19.1	-57.7	176.7	156.5	51.2	74.7	-78.5	-44.5	0	Table1[a]
2]	-90.9	169.8	-175.4	170.7	20.7	-60.2	171.5	155.6	43.2	74.4	-74.3	-45.4	2.7	Table1[b]
3]	-56.6	-89.5	-5.2	–175.7	26.3	-53.7	-179.1	169.9	48.6	76.3	-73.3	-41.7	15.9	Table1[c]
4]	90.3	134.0	-2.8	174.9	9.7	-46.6	-163.4	-166.5	56.4	82.6	-77.8	-43.0	6.8	Table1[d]
5]	-101.3	176.5	-5.2	175.5	19.2	-61.4	172.6	154.3	46.9	75.6	-74.8	-44.3	11.9	Table1[e]
B] PM3 Results:														
6]	71.3	130.5	180.0	178.1	67.3	-56.3	-175.5	179.8	41.5	89.6	-59.0	-54.3	0	Table1[a]
7]	-103.3	-177.6	179.1	-179.2	43.0	-56.0	-168.0	-152.5	23.3	93.4	-67.4	-58.3	3.0	Table1[b]
8]	-60.2	-91.8	-1.9	176.0	6.4	-47.5	176.6	-137.6	35.3	93.9	-76.0	-66.9	44.4	Table1[c]
9]	61.3	112.8	-2.9	177.2	60.8	-46.3	-177.0	-170.9	47.6	94.1	-69.2	-57.4	0.3	Table1[d]
10]	-81.8	175.8	-2.5	176.7	5.9	-51.2	156.8	160.5	15.2	92.9	-65.0	-69.7	5.9	Table1[e]
C]HF(Full Optimization) Results:														
11]	109.5	160.7	179.5	175.4	10.2	-15.0	149.4	121.5	47.4	78.2	-154.0	-42.4	8.0	Table1[a]
12]	-85.6	116.1	176.8	-179.9	11.3	-42.4	-70.6	140.5	43.6	84.7	-146.4	-40.5	3.6	Table1[b]
13]	-64.1	-69.1	-15.1	143.0	19.8	27.4	-154.1	-129.1	50.8	89.5	-139.3	-39.3	4.8	Table1[c]
14]	107.7	122.6	-15.4	-167.5	15.9	81.6	122.3	-100.2	42.8	85.2	-87.0	-47.2	0	Table1[d]
15]	-97.1	169.4	-14.5	-174.6	15.0	-139.6	22.7	109.9	48.4	75.1	-154.2	-42.2	18.9	Table1[e]

However, 5 - position substituent of uridine is below the uracil plane but is at perpendicular inclination. The intramolecular hydrogen bonding interaction O2'H...O3' is maintained in all MMFF optimized structures. In all the optimized structures, obtained using MMFF, PM3 and HF methods, no O2'H…S(2) interaction is found. This may be due to the influence of thio group in maintaining C3'-endo ribose puckering in all optimized structures obtained using MMFF, PM3 and HF methods alike. The geometrical parameters for hydrogen bonding of all optimized structures obtained through MMFF, PM3 and HF methods are included in Table 3(b).

Table3 (b): Geometrical Parameters for hydrogen bonding for optimized structures of 5'-monophosphate mcm^5s^2U by MMFF, PM3 and HF methods

Atoms Involved (1-2-3)	Atom pair (1-2) A	Atom pair (2-3) A	Angle (1-2-3)	Reference
O2'H...O3'	0.980	2.112	113.6	Table2[1,2,3,4,5]
C(9)H...O(4)	1.098	2.720	123.2	Table2[3]
O3'pH...O(8b)	0.970	1.694	152.4	Table2[4]
O2'H...O3'	0.970	2.407	103.8	Table2[6,7,8,9,10]
C(6)H...O5'	1.097	2.586	169.5	Table2[7]
C(6)H...O5'	1.097	2.550	140.4	Table2[8]
O3'pH...O(8b)	0.970	2.578	153.2	Table2[9]
C(6)H...O5'	1.097	2.550	141.7	Table2[9]
C(7)H...O2P	1.098	2.610	158.3	Table2[10]
C(7)H...O2P	1.098	2.168	152.1	Table2[11]
C(6)H...O2P	1.097	2.249	143.0	Table2[11,15]
O2'H...O3'	0.970	2.075	114.8	Table2[11,12,13,14,15]
O3'pH...O(8b)	0.970	1.597	166.9	Table2[12,13]
C(7)H...O1P	1.098	2.350	167.9	Table2[12]
C(6)H...O5'	1.097	2.591	143.0	Table2[12]
C(6)H...O3'p	1.097	2.320	144.3	Table2[12]
C(6)H...O5'	1.097	2.095	161.8	Table2[13]
C(9)H...O(4)	1.098	2.250	171.0	Table2[13,14]
C3'H...O3'p	1.097	2.367	155.4	Table2[14]
C(6)H...O5'	1.097	2.260	153.5	Table2[14]
O3'pH...O(8b)	0.970	1.550	174.6	Table2[14]
C(9)H...O2P	1.098	2.570	147.4	Table2[15]
C(7)H...O2P	1.098	2.168	144.1	Table2[15]

PM3 optimization of PCILO starting structure (Table 2(6)) yields most stable optimized conformation. This optimized stable conformation has nearly perpendicular (above the uracil plane) orientation of C(5)-substituent. The optimized PCILO second alternative structure is just 0.3 kcal/mol higher in energy to optimized PCILO starting structure, while, PM3 optimized

PCILO most stable structure is 3.0 kcal/mol higher in energy. The orientation of C(5)-substituent in PM3 optimized PCILO most stable structure is below uracil plane, but is at nearly perpendicular inclination.

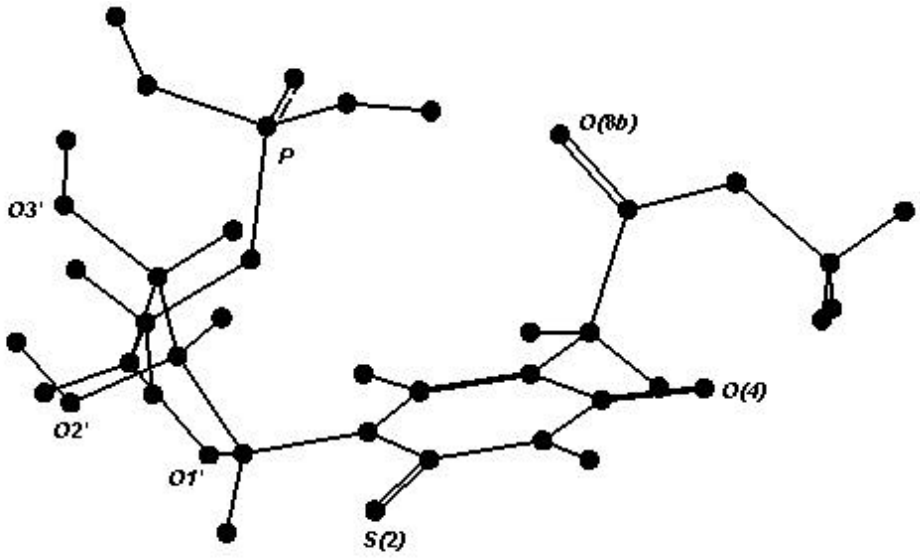

Fig.5 HF-Optimized second PCILO alternative (Table 2[14])

Optimization using HF does not give results (Table -2) similar to those obtained using PM3 and MMFF. The optimized second PCILO alternative stable structure turns out to be the most stable optimized structure using HF. This conformation is stabilized due to various intramolecular hydrogen bonds like C(9)H...O(4), O3'H...O1P, C3'H...O3'p, C(6)H...O5' (Table 3). This most stable optimized structure keeps C(5) substituent orientation tilted perpendicular to but over the plane of uracil base. The optimization of PCILO most stable structure turns out to be 3.6 kcal/mol higher than the lowest energy optimized structure. The relative energy and torsion angle values are included in Table 2.

All the optimized structures keep the C(5)-substituents oriented away from the Watson -Crick base pairing sites of uracil base. The optimization of ribose-phosphate backbone also contributes to the stability of the optimized structure. However, optimized torsion angles of ribose-phosphate backbone also show expected flexibility of wobble nucleotide to enable the backbone turn and provide alternative modes for non-cognate

wobble base pairing. In view of this flexibility the fully optimized structure in Table 2 may conveniently be accommodated in the anticodon loop.

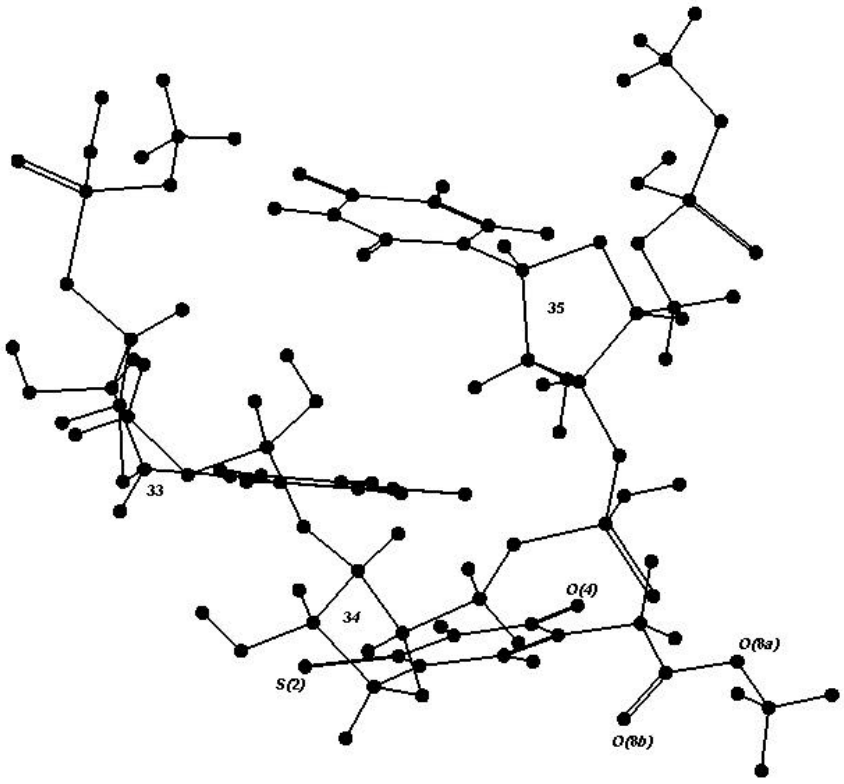

Fig.6 The preferred most stable conformation by PCILO, for substituent of $mcm^5s^2U_{34}$

3(A).4: Trinucleotide mcm^5s^2U ($U_{33}mcm^5s^2U_{34}U_{35}$): To model interactions of hypermodified nucleoside with adjacent neighbours calculations on the trinucleotide segment have been made using PCILO and MMFF methods. During PCILO conformational search the backbone torsion angles are kept as in Holbrook's [12] data. However, full geometry optimization using MMFF is made to study the salient features of stable conformations (Table 4).

The most stable conformation obtained by PCILO for the trinucleotide model segment is shown in fig. 6. The torsion angles describing most stable conformation

are α =330°, β=180°, γ=180°, δ=180° for the C(5) - substituents. The intramolecular hydrogen bonding between $C(6)H_{34}...O5'_{34}$, $C(6)H_{34}...O(8b)_{34}$ and bifurcated hydrogen bonding $O1'_{34}...C(6)H_{34}...O(8b)_{34}$ may provide stability to the most stable conformation (see table 6).The C(5) substituent orientation is not perpendicular to the uracil plane for the most stable conformation.

Table 4: PCILO results for most stable and alternative stable conformations of the trinucleotide

	α	β	γ	δ	χ	Rel. energy	Reference
	in (°)						
a]	180	180	180	180	3	140.0	The starting extended
b]	330	180	180	180	3	0.0	PCILO most stable
c]	210	120	180	300	3	0.5	PCILO alternative-I
d]	120	180	180	300	3	1.4	PCILO alternative-II

The first alternative (α =210°, β=120°, γ=180°, δ=300°) stable structure has 0.5 kcal/mol higher energy than the most stable structure. The interaction between C(7)H group of C(5) substituent and phosphate oxygens of 34th nucleotide (Table 6) are the stabilizing factors for this conformation.

The second alternative structure is 1.4 kcal/mol higher in energy than the most stable structure and is described by torsion angles α =120°, β=180°, γ=180°, δ=300°. The intramolecular hydrogen bonding between carboxyl oxygen O(8b) and hydroxyl $O2'H_{33}$ group of ribose 33rd is noteworthy (Table 6).

Table 5: Optimized torsion angles of C(5) substituent present in trinucleotide U33-mcm^{5}s^{2}U34-U35

	α	β	γ	δ	χ	Rel. energy	Reference
		in (°)					
1]	7.6	138.5	14.4	156.8	14.0	37.8	Table4[a]
2]	-101.1	156.5	179.9	173.9	18.4	16.4	Table4[b]
3]	-105.8	32.1	172.5	-175.2	7.6	36.4	Table4[c]
4]	89.1	159.4	-177.4	-160.4	10.4	0.0	Table4[d]

The results of MMFF optimization for the various conformations included in Table 4 are listed in Table 5. The optimization of the second PCILO alternative (fig.7, Table 5) yields the lowest energy optimized structure. The optimized PCILO alternative (Table 5(4)) keeps (fig.7) the C(5)-substituent oriented above and perpendicular to the plane of uracil base. Thus it can form hydrogen bonding with the hydroxyl O2'H group of ribose 33. Other hydrogen bonding interaction namely $C(5)H_{34}...O(8b)_{34}$, $C(9)H_{34}...O2'H_{33}$ and $C(6)H_{34}...O2P_{34}$ may also stabilize the structure (Table 6).

Optimization of the PCILO most stable conformation leads to 16.4-kcal/mol higher energy optimized structure than the most stable optimized structure arising from the PCILO alternative stable structure. This conformation has C(5) substituent placed down the plane of uridine. Various likely intramolecular hydrogen bonding interactions are listed in Table 6. The hydrogen bonding of $N(3)H_{33}$ with phosphate group 35p36 is present in all the optimized geometries and may help maintain the U-turning feature of the anticodon loop.

Table 6: Geometrical Parameters for hydrogen bonding for trinucleotide U33-mcm^{5}s^{2}U34-U35

Atoms Involved (1-2-3)	Atom pair (1-2) A	Atom pair (2-3) A	Angle (1-2-3)	Reference
C(6)H_{34}...O5'$_{34}$	1.097	2.456	112.5	Table4[b]
C(6)H_{34}...O(8b)$_{34}$	1.097	1.819	118.3	Table4[b]
O1'$_{34}$...C(6)H_{34}...O(8b)$_{34}$	2.140	1.819	125.0	Table4[b]
C(7)H_{34}...O2P$_{34}$	1.098	2.334	112.5	Table4[c]
C(7)H_{34}...O3'$_{33}$	1.098	2.610	141.6	Table4[c]
O2'H_{33}...O(8b)$_{34}$	0.980	1.499	127.3	Table4[d]
C(7)H_{34}...O2P$_{34}$	1.098	1.934	150.2	Table4[d]
N(3)H_{33}...O1P$_{36}$	1.090	1.729	152.9	Table5[1,3]
O2'H_{33}...O(8b)$_{34}$	0.980	2.130	132.2	Table5[1]
C(6)H_{34}...O(8b)$_{34}$	1.097	2.336	117.9	Table5[1]
C(5)H_{35}...O2'$_{33}$	1.097	2.552	141.8	Table5[1]
O1'$_{34}$...C(6)H_{34}...O(8b)$_{34}$	2.270	2.336	136.3	Table5[1]
C(6)H_{34}...O2P$_{34}$	1.097	2.740	154.3	Table5[2]
N(3)H_{33}...O1P$_{36}$	1.090	1.868	156.4	Table5[2]
C(6)H_{34}...O2P$_{34}$	1.098	2.491	159.2	Table 5[3]
N(3)H_{33}...O1P$_{36}$	1.090	2.076	148.9	Table5[4]
O2'H_{33}...O(8b)$_{34}$	0.980	1.695	161.2	Table5[4]
C(6)H_{34}...O2P$_{34}$	1.098	2.385	153.2	Table5[4]
C(5)H_{34}...O(8b)$_{34}$	1.098	2.606	148.1	Table5[4]
C(9)H_{34}...O2'$_{33}$	1.098	2.553	143.1	Table5[4]

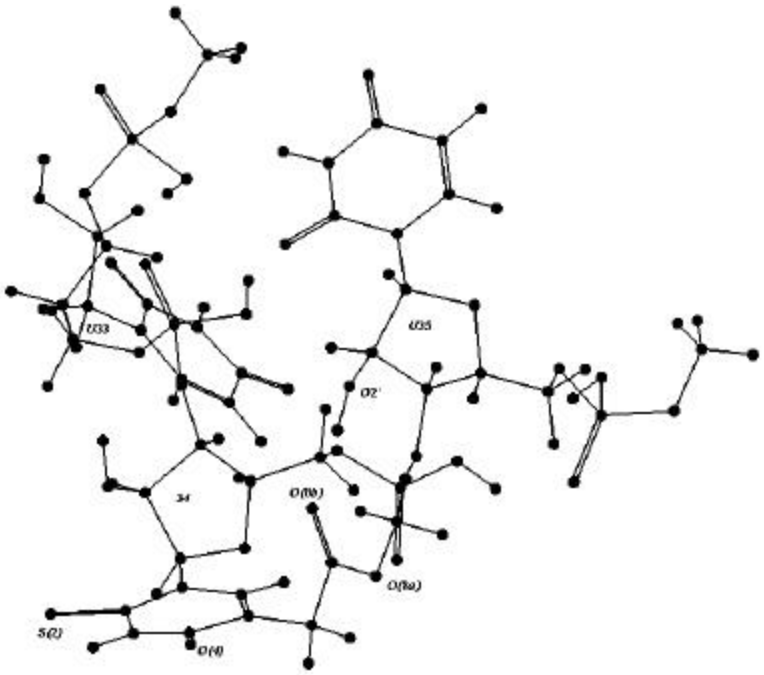

Fig.7 MMFF optimized structure from the second alternative stable PCILO structure.

3(A).5: Conclusions: The C(5) substituent is found to be oriented above or below the plane of uracil base and is perpendicular to it in the preferred and alternative stable conformations of mcm^5s^2U . Although, several different conformations for C(5)-substituent of mcm^5s^2U are indicated, but in each case prospective codon - anticodon base pairing sites remain unobstructed.

3(A).6: References:

1) Agris, P. F; Kopper, R. A. The Modified Nucleosides of Transfer RNA-II; Alan, R.; Liss: New York;1983.
2) Bjork, G. R. In Processing of RNA; Apirion, D.; Ed; CRC Press: Boca Raton, F. L., 1984 , 291- 329.
3) Agris, P. F.; Soll, D.; Seno, T. Biochemistry 1973, 12 , 4331-4337.
4) Elseviers, D.; Petrullo, L. A.; Gallagher, P. J. Nucleic Acid Res. 1984, 12, 3521-3534.
5) Singhal, R. P. Biochemistry 1974, 13, 2924-2932
6) Seno, T.; Agris, P. F.; Soll, D. Biochem.Biophys.Acta 1974, 349, 328-338
7) Keith, G. Nucleic Acid Res. 1984,12,2553-2547
8) Hedgcoth, C.; Harrison, M.; Nayenga, K.; Ortwerth, B. J. Nuclei. Acid. Res 1984, 12,

2535-2541

9) Benas, P.; Bec, G.; Keith, G.; Marquet, R.; Ehresmann, C.; Ehresmann, B.and Dumas, P. RNA, 2000, 6, 1347-1355

10) Baczynskyj, I.; Biemann, K. and Hall, R. H. Science 1968, 159,1481-1483

11) Isel, C.; Marquet, R..; keith, G.; Ehresmann, C.; Ehresmann, B.; J. Biol. Chem. 1993, 268, 25269 - 25272

12) Holbrook, S. R.; Sussman, J. L.; Warrant, R. W.; Kim, S. H. J. Mol. Biol. 1978, 123, 631- 660

13) Pullman, B.; Saran, A. Prog. Nucleic Acid. Res. Mol. Biol. 1976, 18, 216-326

14) Tewari, R. Int. J. Quantum Chem. 1987, 31, 611-624

15) Halgren, T. A. J. Comp. Chem. 1996, 17, 490-519

16) Dewar, M. J. S.; Thiel, W. J. Am. Chem. Soc. 1977, 99, 4899-4907

17) Stewart, J. J. P. J. Comp. Chem. 1991, 1, 320-341

18) Szabo, A. and Ostlund, N. S. Modern Quantum Chemistry, 1989

19) Levine, I. N. Quantum Chemistry, 4th ed., Prentice Hall, 1991

20) Hehre, W. J.; Yu, J.; Klunzinger, P. E.; Lou, L. `A Brief Guide to Molecular Mechanics and Quantum Chemical Calculations', 1998 Wavefunctions Inc., Irvine, CA 92612 USA

Chapter -3(B): Conformational Preferences of another wobble nucleoside queuosine(Q) and its analogs.

3(B).1 Introduction:

Queuosine `Q' is one of the most extensively modified [1-3] complex nucleosides, which naturally occurs in the first 'wobble' position of anticodon [4-5] in specific tRNAs. The 7-deazaguanine of queuosine in place of unmodified guanine ring may exclude wobble G-G base pairing and eliminate the trace recognition [4] of G(codon) by G(anticodon), but the role of cyclopentenediol and aminomethyl linkage is not clear. Absence of queuosine modification is associated with rapidly proliferating cells [6] and malignant growth. Queuosine is synthesized in bacteria by the insertion of the base of pre Q1 by tRNA (Q34) transglycosylase (the TGT-enzyme). This incorporated base is then modified to Q. The bacterial enzyme only inserts the base of preQ1 and not queuine (the base of Q), whereas the eukaryotic enzyme inserts queuine [7]. Temperature - jump relaxation experiments have shown that guanosine - containing and queuosine modified tRNAs are equally stable in complexes with NAU codons, however guanosine containing tRNAs are significantly more stable in complexation with NAC codons (8, 9, 10). Therefore, it is likely that modifications at the wobble position may restrict or enlarge the recognition of the third codon base thus determining the synonymous codon family. The cyclopentenediol moiety and the aminomethyl linkage to 7-deazaguanine ring in queuosine may enable extended intramolecular interactions. Base substituent may also probe molecular environment of the anticodon loop. Present study aims at understanding the significance of wobble nucleoside modifications as well.

3(B).2 Nomenclature Convention and Procedure:

Fig. 1 illustrates the atom numbering and identification of the torsion angles, which determine the relative orientation of various atoms - groupings (conformational preferences) in hypermodified nucleotide queuosine 5`-monophosphate, pQ. The torsion angle α[C(8)-C(7)-C(12)-N(13)] is measured with respect to C(8) from the eclipsed (0°) position between the terminal bonds C(7)-C(8) and C(12)-N(13) in the right hand sense of rotation around the central bond C(7)-C(12). The other torsion angles β [C(7)-C(12)-N(13)-C3"], γ [C(12)-N(13)-C3"-C2"], δ [C5"-C4"-O4"-H], ε [C4"-C5"-O5"-H] and

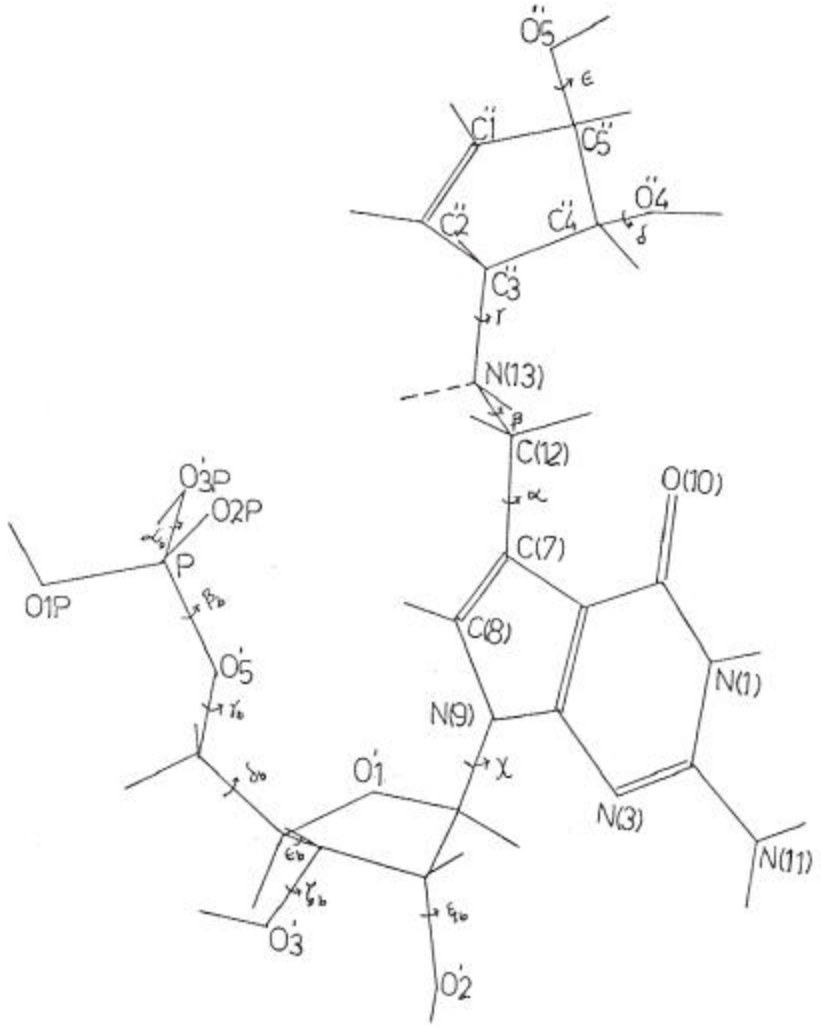

Fig.1 Complex modified nucleotide queuosine 5`-monophosphate, pQ. Identification of atoms and the torsion angles which determine base substituent orientation. The depicted base substituent orientation is as observed in the crystal structure of pQH+.

χ [O1'-C1'-N(9)-C(8)] are likewise measured from the cis (eclipsed, 0°) position in the right hand sense of rotation. Steric arrangement of the various functional groups of the base substituent as observed in the crystal structure of protonated pQH+ [11] is taken for starting structure. However, to represent the anticodon loop situation instead of free nucleotide, pertinent values for the wobble nucleotide (34^{th} position) in Holbrook's model of tRNA [12] have been taken for torsional angles in the ribose -5`-phosphate backbone. The torsion angles in the ribose - phosphate backbone are distinguished by the subscript b to refer to the backbone. These backbone torsion angles retain the same nomenclature as in the tRNA model [12] - referring likewise to the right hand sense of rotation around the central bond, measured from the eclipsed position of the outer bonds. The torsion angles α_b [H-O3'-P-O5'], β_b [O3'-P-O5'-C5'], γ_b [P-O5'-C5'-C4'], δ_b [O5'-C5'-C4'-C3'], ε_b [C5'-C4'-C3'-O3'], ζ_b [C4'-C3'-O3'-P] and ξ_b [C3'-C2'-O2'-H] description may likewise be understood.

Conformational energy calculations have been made using quantum chemical Perturbative Configuration Interaction with Localized Orbitals (PCILO) method [13-15]. Polarity of each bond in the molecule is optimized throughout the conformational energy calculations. Energy correction terms upto the third order are included for each calculation. Variation of total energy with respect to torsional angles determining the base substituent orientation in the modified nucleotides pQ, pQH+ and p̄QH+ have been studied. Logical selection of grid points approach [16] is utilized for searching the most stable and alternative stable structures in multidimensional conformational space. Relative stability of salient points has also been examined using automatic geometry optimization by molecular mechanics force field MMFF [17], parametrized modified neglect of differential overlap framework based PM3 [18-19] and Hartree Fock - density functional theory HF-DFT [20, 21] approaches. These methods are implemented in commercially available PC Spartan Pro (Version 6.06 Wavefunction, Inc. 18401 Van Karman Ave., Suite 370 Irvine, CA 92612) software. Non local perturbative Becke - Perdew DFT model for explicitly taking into account electron inhomogeneities [20,21] and numerical polarization basis set DN* was used for (pBP/DN*) DFT calculations [22]. The reported HF - DFT calculations here refer to single point DFT calculations following geometry optimization at Hartree Fock (3-21G*) level. In this manner salient

features of the preferred and the alternative stable conformations of queuosine 5`-monophosphate pQ, protonated form pQH+ as well as zwitterionic form $p^{-}QH+$ have been studied.

Fig.2 The preferred base substituent orientation for pQ by PCILO.

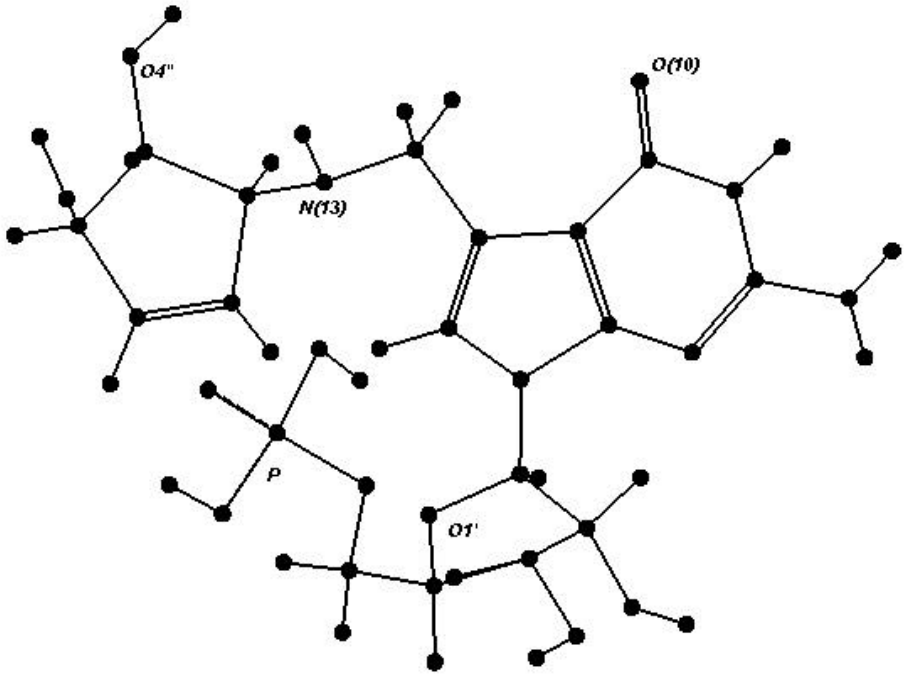

3(B).3 Results and Discussion:

Besides the PCILO most stable conformation, higher energy stable alternative conformations for pQ, pQH+ and $p^{-}QH+$ are listed in Table I. The results of automatic geometry optimization for pQ, pQH+ and $p^{-}QH+$, starting with the base substituent orientation as (a) in the observed pQH+ crystal structure, or (b) as the PCILO preferred conformation, or (c) as the alternative stable conformation are included in Table II. The molecular mechanics force field MMFF, semi empirical parametrized PM3 molecular orbital approach and Hartree- Fock -Density Functional Theory HF-DFT method have

been used for this. The geometrical parameters for likely hydrogen bonding are included in Table III.

3(B).3.1 Neutral queuosine -5'-monophosphate(pQ): The preferred most stable base substituent orientation by PCILO for unprotonated queuosine-5`-monophosphate, pQ is shown in Fig. 2. The torsion angles describing the base substituent orientation are (α=31°, β=264°, γ=107°, δ=180°, ε=300°). The glycosyl orientation is held anti (χ= 3°) and the ribose ring puckering is C3'-endo, similar to the wobble nucleotide in the Holbrook model for tRNA. The 5'-phosphate group orientation is likewise retained as in Holbrook model. The deazaguanine base in Q can participate in the usual Watson - Crick base pairing, as no obstruction from the base substituent is indicated. The preferred pQ conformation has no strong interaction of the base substituent with the ribose phosphate chain or with the deazaguanine base. No intramolecular hydrogen bonding of N(13)H

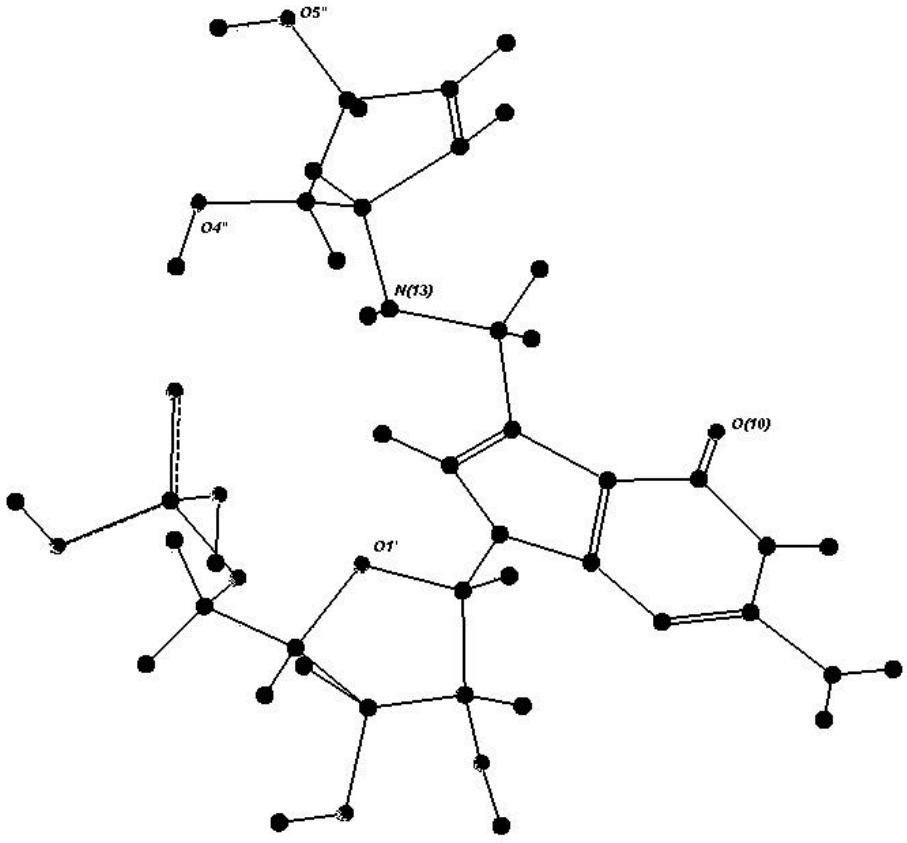

Fig.3 The alternative base substituent orientation for pQ by PCILO.

with the O(10) is predicted for unprotonated pQ (Figs 2,3). This is due to the absence of the quaternary nitrogen, in the aminomethyl group of the base substituent in pQ, for intramolecular hydrogen bonding with O(10).

Table I. Predicted most and alternative stable conformations for queuosine (pQ) , protonated queuosine (pQH+) and zwitterionic queuosine (p^-QH^+)analogs.

Torsion Angles in (°)	PCILO Rel. Energy (kcal/mol)	Fig. Ref.
Queuosine (pQ) :		
1.α=121, β=174, γ=167, δ=90, ε=270, χ=3	9.50	1
2. α=31, β=264, γ=107, δ=180, ε=300, χ=3	0.00	2
Alternatives of Queuosine (pQ) :		
3. α=241, β=54, γ=287, δ=180, ε=300, χ=3	3.24	
4. α=91, β=24, γ=317, δ=180, ε=300, χ=3	3.66	
5. α=31, β=234, γ=347, δ=180, ε=300, χ=3	3.06	3
6. α=61, β=234, γ=77, δ=180, ε=300, χ=3	3.09	
7. α=91, β=54, γ=317, δ=180, ε=300, χ=3	4.20	
Protonated Queuosine (pQH+):		
1. α=121, β=174, γ=167, δ=90, ε=270, χ=3	10.20	1
2. α=151, β=174, γ=317, δ=60, ε=270, χ=3	0.00	7
Alternatives of Protonated Queuosine (pQH+):		
3. α=151, β=294, γ=17, δ=60, ε=270, χ=3	0.17	8
4. α=31, β=264, γ=107, δ=60, ε=270, χ=3	1.36	
5. α=61, β=234, γ=77, δ=60, ε=270, χ=3	3.35	
6. α=211, β=84, γ=77, δ=60, ε=270, χ=3	4.23	
7. α=241, β=54, γ=287, δ=60, ε=270, χ=3	4.25	
Zwitterion Queuosine (p^-QH^+) :		
1. α=121, β=174, γ=167, δ=90, ε=270, χ=3	22.0	1
2. α=61, β=174, γ=47, δ=60, ε=240, χ=3	0.0	12
No suitable alternative for Zwitterion Queuosine (p^-QH^+).		

Alternative stable structure by PCILO having 3.1 kcal/mol higher energy than the most stable structure for unprotonated queuosine is shown in Fig. 3. The torsion angles

describing the substituent orientation are (α=31°, β=234°, γ=347°, δ=180°, ε=300°). This structure has no intramolecular hard contacts as the various chemical groups are

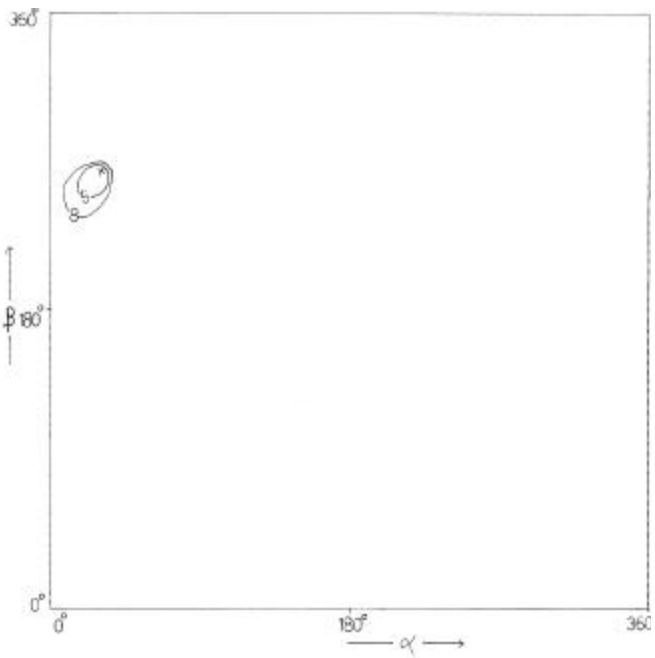

Fig.4 Isoenergy contour map of torsion angle α and β

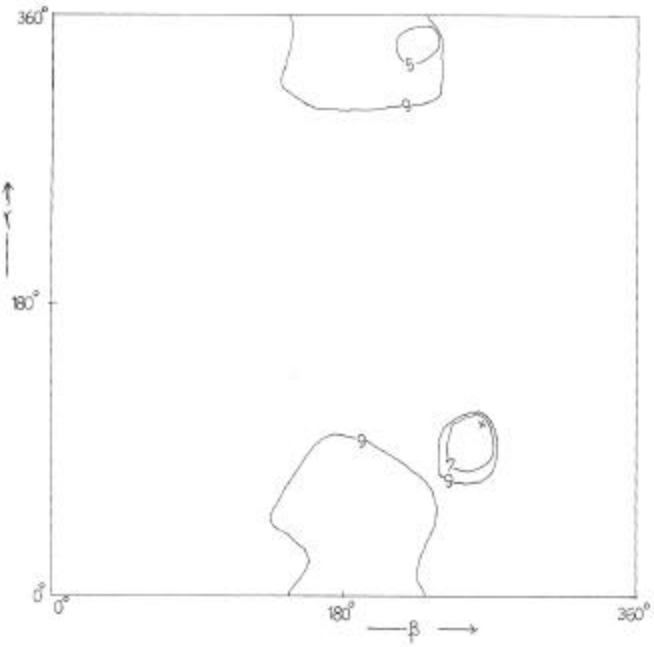

Fig.5 Isoenergy contour map for torsion angle β and γ

well spread out. Hydrogen bonding interaction between the hydroxyl group O4"H in cyclopentenediol moiety and the phosphate group O2P (Table III) may provide stabilization to this conformation. This alternative structure also permits unhindered access to all the usual Watson - Crick sites for base pairing.

The other comparable higher energy alternative stable structures for pQ and pQH+ are included in Table I. An alternative stable structure for pQ, also having about 3.1 kcal/mol higher energy as compared to the most stable structure, is predicted by PCILO for (α=61°, β=234°, γ=77°, δ=180°, ε=300°). Next higher energy stable structure at 3.2 kcal/mol is predicted for (α=241°, β=54°, γ=287°, δ=180°, ε=300°). Another stable conformation at 3.7 kcal/mol is predicted for (α=91°, β=24°, γ=317°, δ=180°, ε=300°). Next higher energy alternative conformation at 4.2 kcal/mol is predicted for (α=91°, β=54°, γ=317°, δ=180°, ε=300°). These alternative conformations arise from different combinations of torsion angles α, β, and γ.

Interdependence of the torsional angles α and β is shown as isoenergy contour map in Fig. 4. It is clear that there is a unique combination (α=30°, β=270°) favored for these torsion angles and the conformational energy rises rapidly on moving away from the preferred most stable structure.

Interdependence with respect to torsion angles β and γ is shown as isoenergy contour map in Fig. 5. A unique preferred combination is seen for β=270°, γ=105°. The conformational energy rises quickly on moving away from this lowest energy conformation. Another stable conformation having higher energy occurs around β=240°, γ=345°. Energy variation is steep around this alternative conformation as well.

Relative energies of the fully optimized pQ structures have been calculated (Table II) using MMFF, PM3 and Hartree Fock - density functional theory HF-DFT (pBP/DN*) methods starting from structures in Fig. 1, Fig. 2 and Fig. 3. These structures correspond to the preferred pQ conformation by PCILO (fig. 2), the alternative stable PCILO

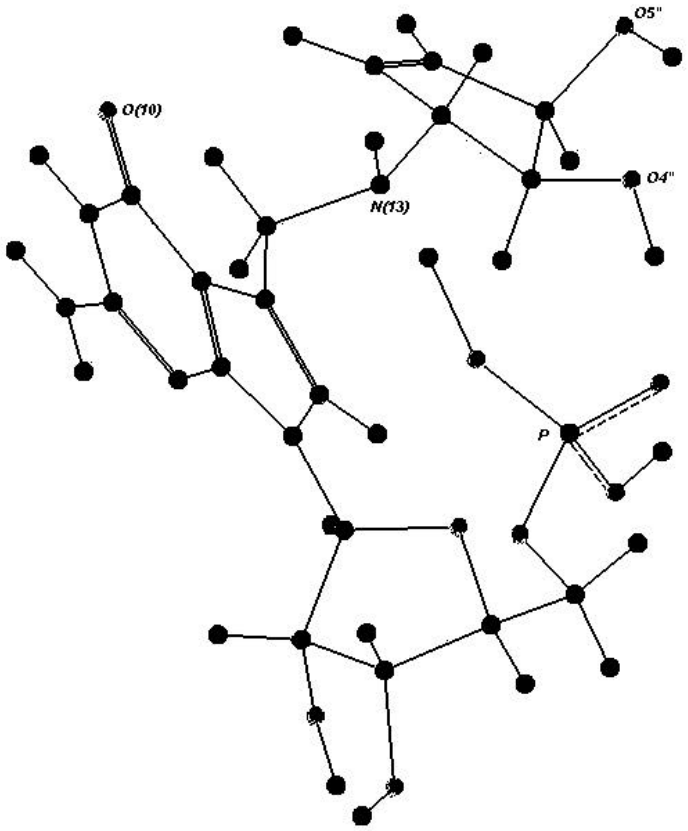

Fig.6 HF-DFT optimized PCILO most stable conformation for pQ

conformation (fig. 3) and with the base substituent orientation as observed in the crystal structure conformation (fig. 1). Irrespective of the optimization method employed, starting from the PCILO preferred base substituent conformation results in lowest energy optimized structure. MMFF optimized structures starting from the alternative stable PCILO structure as well as from the observed base substituent orientation in crystal structure are equally stable at 6.3 kcal/mol higher energy over the more stable optimized structure arising from the preferred PCILO conformation. However, PM3 optimized structure from the base substituent orientation as in crystal structure turns out to be closer than the higher energy optimized structure yielded from the PCILO alternative stable conformation. This may be contrasted with the opposite trend shown by HF-DFT calculations. The DFT results instead prefer the optimized most stable PCILO conformation compared to the optimized PCILO alternative structure by 2.1 kcal/mol and by even more 22.8 kcal/mol compared to the optimized crystal structure conformation. The overall geometry optimization results indicate that intramolecular hydrogen bonding interactions involving the cyclopentenediol hydroxyl group, O4”H and O(10) or O2P (Table III) may provide conformational stabilization. The N(13)H group in the base substituent is capable of hydrogen bond donor acceptor role and may also interact with the phosphate group. However, the ribose - phosphate backbone orientation in the anticodon loop is clearly constrained and thus can limit the interactions between the phosphate group and the base substituent. As compared to pQH+, stronger interaction of the base substituent with the 5’-phospate is indicated (Table III) for pQ.

3(B).3.2 Protonated queuosine-5'-monophosphate (pQH+) : The most stable PCILO structure for protonated queuosine-5`-monophosphate, pQH+, specified by torsion angles (α=151°, β=174°, γ=317°, δ=60°, ε=270°) is shown in Fig. 7.

Fig. 7 The PCILO preferred base substituent orientation for pQH+.

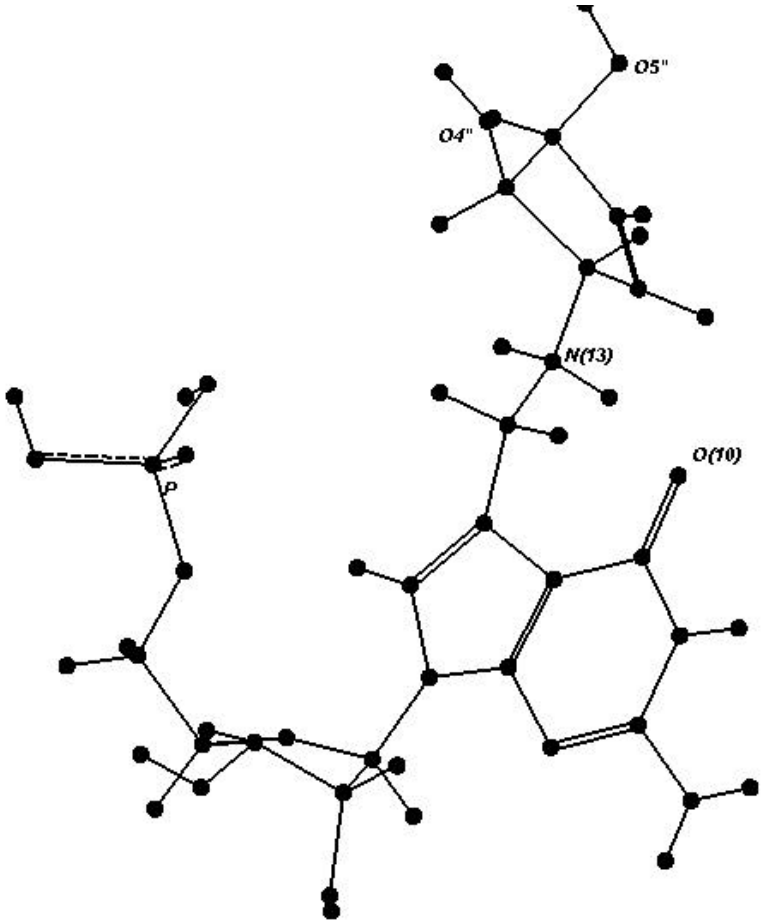

The base substituent spreads along the direction nearly parallel to C(6)-O(10). This leaves access to Watson - Crick base pairing sites unobstructed. Other than $HN(13)^{+}H$---O(10) hydrogen bonding, no strong intramolecular interaction is indicated at mononucleotide level. The PCILO preferred torsion angles for protonated queuosine-5`-monophosphate, pQH+, (α=151°, β=174°, γ=317°, δ=60°, ε=270°) may be compared with the observed values in crystal structure (α=121°, β=174°, γ=167°, δ=90°, ε=270°). The preferred value for γ is substantially different in the crystal structure, and the values of α and δ differ by 30°, but β agrees with the preferred value. In the crystal structure the $HN(13)^{+}H$ group besides interacting with the O(10) also interacts with the phosphate group. Crystal structure orientation of the ribose phosphate backbone and α=121° enable this. The predicted change in α to 151° instead of the observed 121° results in improved geometry for $HN(13)^{+}H$---O(10) hydrogen bonding as evident from parameters in Table III. The chosen model for wobble nucleotide backbone orientation [32] keeps the base substituent and the backbone apart, thus reducing interaction between $HN(13)^{+}H$ and 5'-phosphate.

Fig.8 The alternative stable base substituent orientatic for pQH+ by PCILO.

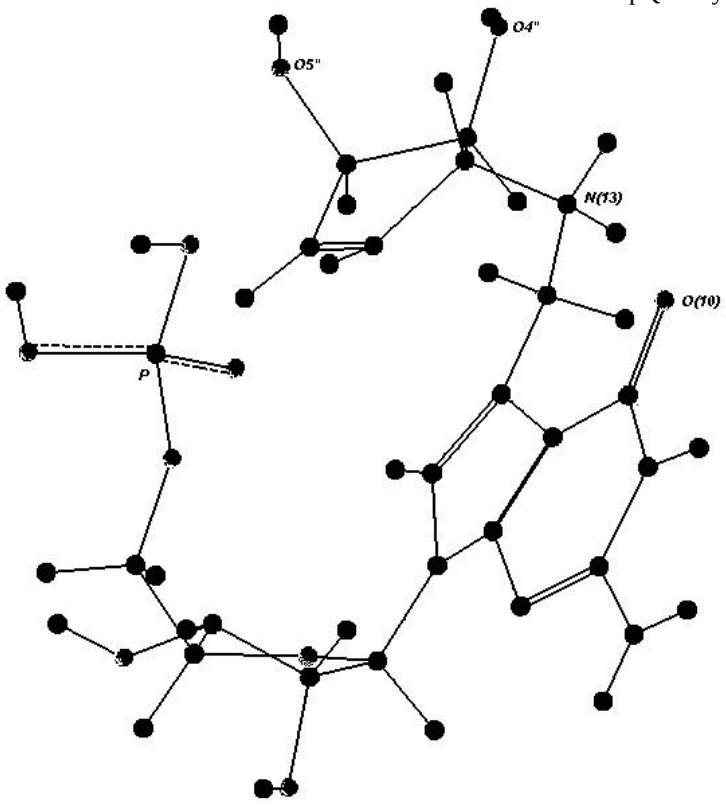

The alternative stable conformation (α=151°, β=294°, γ=17°, δ=60°, ε=270°) having 0.2 kcal/mol higher energy for pQH+ is shown in Fig. 8. Although the hydrogen bonding between $HN(13)^{+}H$---O(10) is maintained, noteworthy difference as compared to Fig. 6 is that the base substituent folds back towards the 5'-phosphate group instead of spreading farther along parallel to C(6)-O(10). Such an orientation may allow for interaction of the base substituent with the ribose phosphate backbone.

The other alternative stable conformations of higher energy for pQH+ are included in Table I. Next higher energy stable structure for pQH+ at 1.4 kcal/mol is predicted for (α=31°, β=264°, γ=107°, δ=60°, ε=270°). The next stable structure at 3.3 kcal/mol arises for (α=61°, β=234°, γ=77°, δ=60°, ε=270°). Another higher energy stable structure at 4.2 kcal/mol is predicted for (α=211°, β=84°, γ=77°, δ=60°, ε=270°). The next stable structure at 4.2 kcal/mol has (α=241°, β=54°, γ=287°, δ=60°, ε=270°). These alternative structures arise through different combinations of torsion angles α, β, and γ.

Interdependence of torsion angles α and β is shown as isoenergy contour map in Fig. 9. A unique combination at α= 150° and β= 180° is distinctly favored. However, higher energy alternative conformations are indicated around (α=90°, β=60°) and also around (α=210°, β=180°). The area inside the 3 kcal/mol contour is not much - signifying limited conformational freedom. Nevertheless, as compared to pQ in Fig. 4, somewhat larger flexibility is evident in Fig. 9.

Correlation of rotation around bonds C(12)-N(13) and N(13)-C"3 (torsion angles β and γ) is shown as isoenergy contour map in Fig. 10. The most stable structure occurs for β= 180° and γ=315°. Another alternative structure having energy within 1 kcal/mol of the most stable structure is predicted for β= 180° and γ= 165°. Another higher energy alternative within 2 kcal/mol is indicated around β=300° and γ= 15°. In Fig. 10, for β=180°, all values of γ are within 5 kcal/mol contour. Considerably greater range for γ is thus permissible when β is trans (180°).

Table II. Optimized values of the torsion angles by automatic geometry optimization using MMFF, PM3 and HF-DFT methods

Molecule	Torsion Angles in (°)													Rel. Energy	Starting Geometry
	α	β	γ	δ	ε	χ	α_b	β_b	γ_b	δ_b	ε_b	ξ_b	ξ'_b		
1) MMFF Results :															
Queuosine (pQ)															
a.	97.9	-179.7	150.8	172.6	-23.2	5.4	-96.8	166.6	153.2	41.3	82.5	-88.4	-40.8	6.3	fig.1
b.	-3.2	-99.0	50.9	169.3	-23.1	0.8	-109.0	173.1	141.1	22.1	70.6	-86.0	-49.7	0.0	fig.2
c.	9.9	-106.6	-50.9	178.9	-15.7	-4.1	-103.5	175.6	140.0	37.0	76.8	-93.8	-43.0	6.3	fig.3
Protonated Queuosine (pQH+)															
d.	97.8	-174.4	173.1	76.7	-41.7	-1.1	-103.1	161.5	152.6	43.6	80.0	-81.3	-42.7	21.3	fig.1
e.	123.5	-143.7	-25.0	-5.6	-173.0	16.6	-105.6	-178.3	-138.8	-22.5	78.2	-68.9	-43.8	0.0	fig.7
f.	132.0	-85.1	35.9	-7.8	178.9	11.9	-97.4	162.3	147.2	42.7	77.6	-79.4	-43.8	10.0	fig.8
Zwitterionic Queuosine(p^-QH^+)															
g.	90.6	152.5	164.2	142.4	-36.1	-2.3	-115.8	75.9	155.5	46.7	90.6	-75.7	-37.2	0.4	fig.1
h.	39.1	171.4	59.3	127.2	-38.7	-2.5	-80.3	-121.8	117.1	11.6	86.0	-71.3	-38.3	0.0	fig.12
2) PM3 Results :															
Queuosine (pQ)															
i.	103.4	161.3	163.2	125.8	-1.1	79.5	-57.8	176.1	161.5	25.3	93.9	-53.7	-79.1	17.8	fig.1
j.	-3.4	-75.9	124.9	-58.5	-61.4	-28.8	-58.6	-161.8	165.9	22.7	98.7	-85.1	-88.7	0.0	fig.2
k.	32.4	-128.4	-27.8	178.3	-13.2	3.3	-57.8	175.5	161.6	22.0	92.3	-45.8	-94.5	74.0	fig.3
Protonated Queuosine (pQH+)															
l.	115.3	171.2	166.5	72.0	-69.1	-3.6	-58.5	178.4	160.8	22.5	82.8	-37.8	-80.1	6.1	fig.1
m.	145.2	178.1	-54.1	23.0	-121.6	10.0	-56.9	176.5	162.5	24.3	95.4	-60.0	-83.9	0.0	fig.7
n.	150.5	-86.1	36.8	57.4	-70.3	9.0	-57.7	175.5	161.7	24.6	107.9	-58.6	-83.6	5.9	fig.8
Zwitterionic Queuosine(p^-QH^+)															
o.	63.7	162.9	-169.5	67.0	64.0	-3.0	-74.3	140.7	133.5	41.7	88.5	-55.4	-49.2	2.8	fig.1
p.	55.3	174.0	73.4	-3.3	95.0	-7.2	-72.2	152.9	129.5	47.0	85.8	-54.1	-52.0	0.0	fig.12
3) HF(full optimization) – DFT(single point) :															
Queuosine (pQ)															
q.	98.3	143.2	159.2	147.7	-28.5	6.9	-11.1	151.8	125.4	44.1	83.4	-101.6	-45.7	22.8	fig.1
r.	–58.4	-61.4	-16.7	127.3	-29.0	37.3	104.8	-148.5	142.3	44.8	91.1	-140.0	-32.6	0.0	fig.2
s.	70.7	-145.2	-55.1	141.0	-21.8	-12.4	105.2	-160.9	139.2	40.1	93.3	-138.7	-35.0	2.1	fig.3
Protonated Queuosine (pQH+)															
t.	139.9	163.9	170.1	89.9	-36.3	4.6	-46.6	130.5	139.6	43.9	86.2	-151.0	-38.0	2.1	fig.1
u.	132.3	-170.5	-40.6	-27.5	-178.6	1.9	-40.6	122.2	147.1	44.5	86.8	-155.2	-37.9	0.0	fig.7
v.	150.0	-87.5	47.7	-26.1	-177.5	-2.6	-49.5	130.7	134.4	39.8	88.0	-107.5	-45.9	5.8	fig.8
Zwitterionic Queuosine(p^-QH^+)															
w.	97.1	151.6	160.5	143.6	-39.3	-1.5	-148.1	63.5	141.4	34.2	94.9	-84.5	–39.8	0.0	fig.1
x.	48.6	172.4	39.5	125.2	-34.8	4.5	-89.8	-110.8	106.6	0.9	86.1	-74.2	-42.4	5.2	fig.12

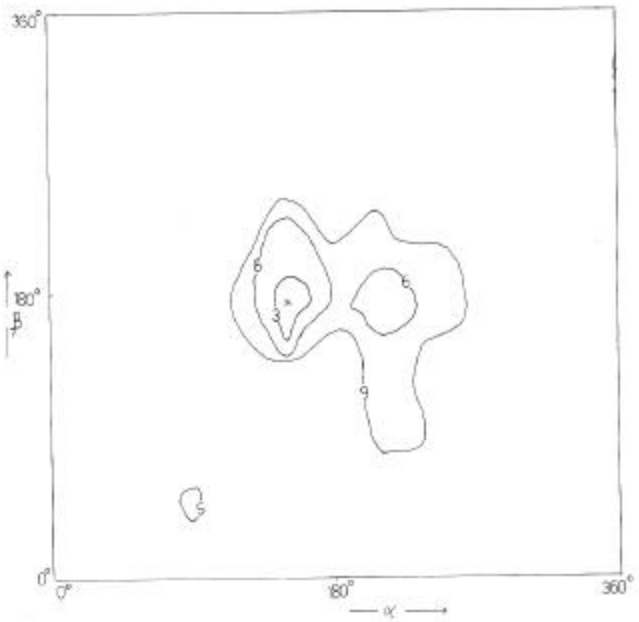

Fig.9 Isoenergy contour map of torsion angles α and β

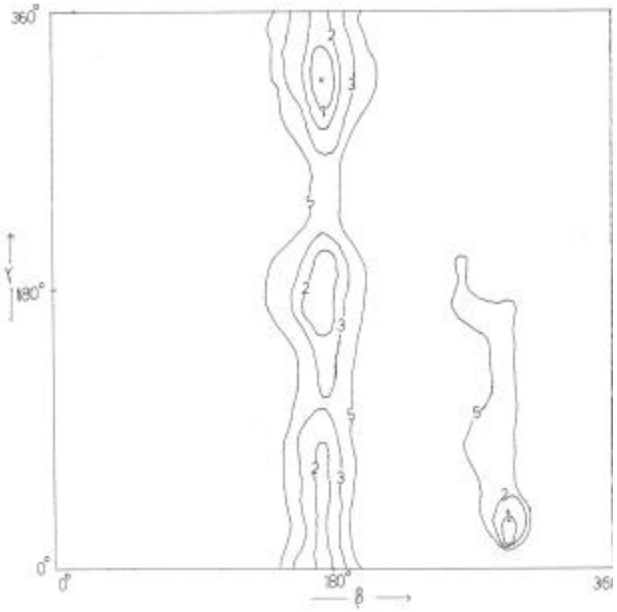

Fig.10 Isoenergy contour map of β and γ

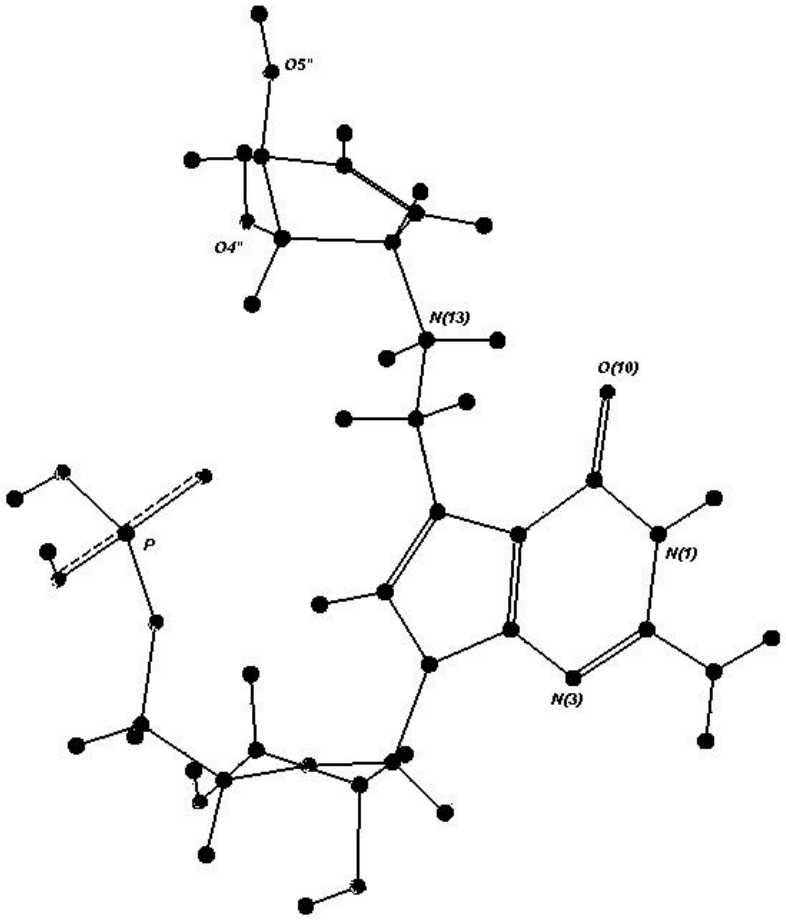

Fig. 11 HF-DFT optimized PCILO most stable conformation for pQH+

Relative energies of full geometry optimized pQH+ using MMFF, PM3 and HF - DFT (pBP/DN*) methods, starting with the PCILO preferred structure (Fig. 7), alternatve stable structure (Fig. 8), or from the crystal structure base substituent orientation (Fig. 1) have been calculated (Table II). The optimization starting from the PCILO preferred conformation turns out to remain stabler irrespective of the utilized optimization method. However, the relative stability of optimized structures starting from the alternative stable structure or starting from the base substituent orientation as in crystal structure depends upon the utilized optimization method. While the alternative stable structure comparatively yields lower energy (stabler) optimized structures, by MMFF and PM3 methods, than the optimization starting from the base substituent orientation taken as in the crystal structure [11], the reverse comparative stability order is indicated by HF-DFT method. Besides the HN(13)$^{+}$H---O(10) interaction in pQH+, stabilization may also arise from possible O4”H---O(10) interaction or by O4”H---O2P hydrogen bonding interaction (Table III). However, in the anticodon loop situation the ribose - phosphate backbone orientation is likely to be constrained by loop closure considerations and this may also limit the interactions between the base substituent and the 5’-phosphate group.

3(B).3.3 Zwitterionic queuosine 5'-monophosphate (p^{-}QH+):

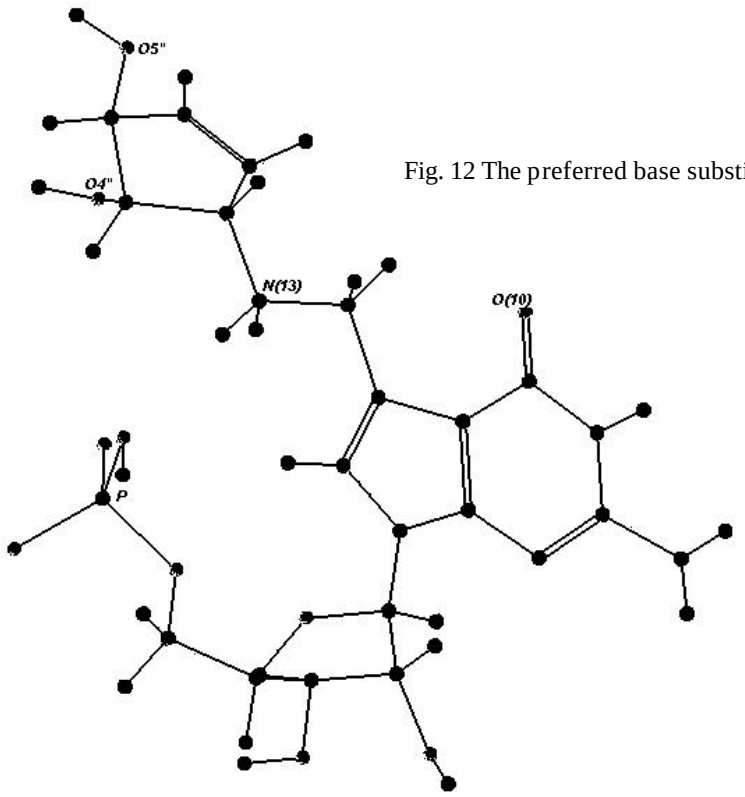

Fig. 12 The preferred base substituent orientation for p^{-}QH+ by PCILO.

Fig.12 shows the preferred most stable base substituent orientation by PCILO for zwitterionic queuosine 5'-monophosphate (p^-QH+). The torsion angles favoured for the most stable structure of base substituent are (α=60°, β=174°, γ=47°, δ=60°, ε=240°). No intramolecular hydrogen bonding of $N^+(13)H$ with the O(10) is predicted for zwitterionic p^-QH+ (fig.12). But, the weak intramolecular hydrogen bonding of $N^+(13)H$ with the O2P is preferred. This structure does not affect the participation of Q in usual Watson – Crick base pairing.

No alternative stable structure by PCILO is obtained within 6 kcal/mol higher energy than the most stable structure for zwitterionic queuosine. Interdependence of the torsion angles α and β as isoenergy contour map (fig.13) also suggests restricted conformational freedom for these torsion angles. Unique combination (α=60°, β=180) is favoured for these torsion angles and the conformational energy rises quickly on moving away from the preferred most stable structure.

Interdependence of the torsion angles β and γ as isoenergy contour map shown in fig.14 has some conformational freedom for torsion angle γ but no alternative stable region within 6kcal/mol of the most stable structure for zwitterion queuosine molecule is seen.

Fig.13 Isoenergy contour map of α and β

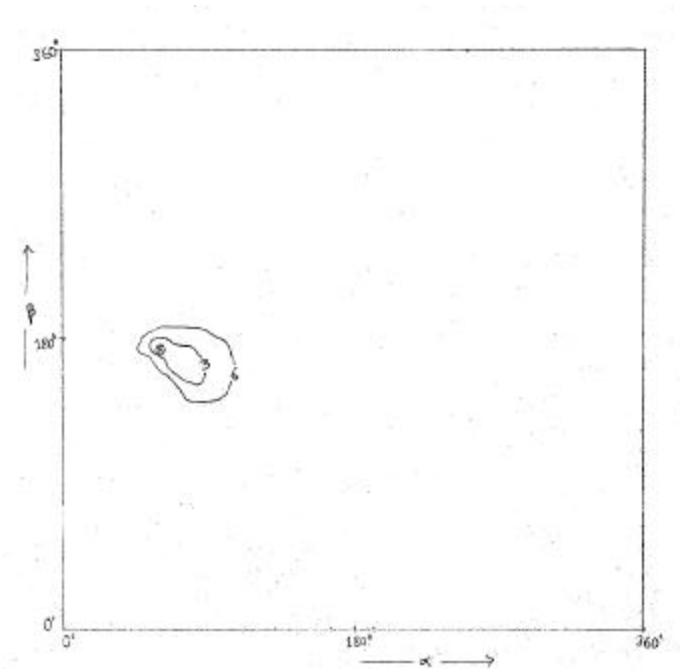

Fig.14 Isoenergy contour map of β and γ

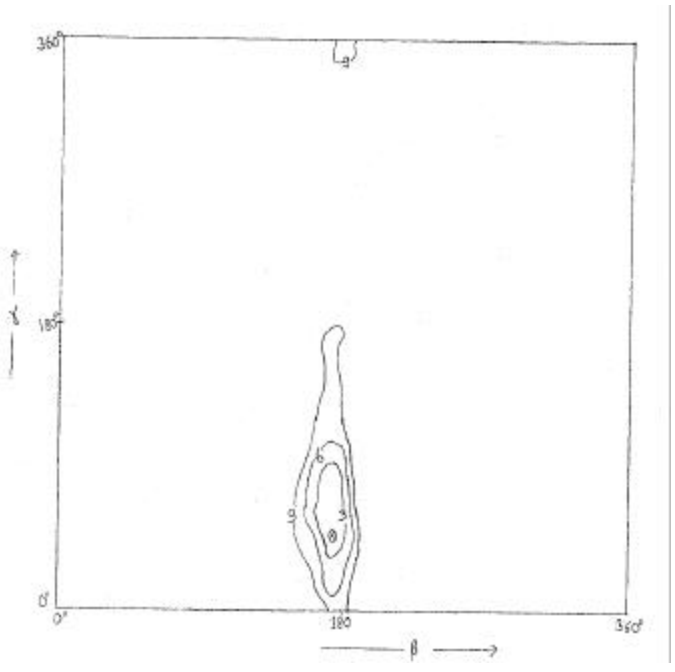

Relative energies of full geometry optimized p^-QH+ using MMFF, PM3 and HF-DFT (pBP/DN*) methods, starting with the crystal structure base substituent orientation (fig.1) and the PCILO preferred structure (fig.12) have been calculated (Table-II). The optimization starting from the PCILO preferred conformation turns out to remain stabler for MMFF and PM3 optimization methods, while reverse trend is noticed for HF-DFT optimization method. The stabilization may arise from the $N(13)^+H$...O2P intramolecular hydrogen bonding, (Table III), additionally supplemented by interaction of O4''H donor group with either phosphate group or O(10) of the deazaguanosine.

Table III. Geometrical parameters for hydrogen bonding in the preferred conformations of queuosine (pQ), protonated queuosine (pQH+) and Zwitterionic queuosine (p^-QH^+) molecules.

Atoms Involved (1-2-3)	Distance atom pair 1-2 (A°)	Distance atom pair 2-3 (A°)	Angle 1-2-3 (deg.)	Figure References
N^+(13)H…O(10)	1.009	2.388	136.2	1
C4”H…O(10)	1.010	2.580	140.6	1
O4”H…O2P	0.950	1.640	154.9	3
N^+(13)H…O(10)	1.009	1.610	150.0	6
C2”H…O3’p	1.010	1.860	141.2	7
C4”H…O(10)	1.010	2.240	132.6	7
N^+(13)H…O(10)	1.009	1.610	158.0	7
N^+(13)H…O2P	1.009	2.703	160.5	10
N(13)H…O(10)	1.037	2.595	124.3	Table-II(a)
O4”H…O2P	0.977	2.100	170.6	Table-II(c)
N^+(13)H…O(10)	1.037	2.330	129.5	Table-II(d)
N^+(13)H…O(10)	1.037	2.250	120.8	Table-II(e)
N^+(13)H…O(10)	1.037	1.650	152.3	Table-II(f)
N^+(13)H…O2P	1.037	1.355	161.6	Table-II(g)
O4”H…O(10)	0.977	1.860	159.6	Table-II(g)
N^+(13)H…O2P	1.037	1.539	140.3	Table-II(h)
N^+(13)H…O3’p	1.037	1.785	152.1	Table-II(h)
O4”H…O1P	0.977	1.700	158.8	Table-II(h)
O4”H…O2P	0.977	1.743	167.11	Table-II(k)
N^+(13)H…O(10)	1.009	2.300	137.5	Table-II(l)
C(12)H…O4”	1.098	2.500	119.2	Table-II(l)

N^+(13)H…O(10)	1.009	1.758	156.3	Table-II(m)
N^+(13)H…O(10)	1.009	1.770	164.9	Table-II(n)
C(8)H…O2P	1.099	2.750	150.0	Table-II(n)
N^+(13)H…O2P	1.037	1.705	156.6	Table-II(o)
N^+(13)H…O2P	1.037	1.680	164.3	Table-II(p)
O4"H…O(10)	0.970	1.760	158.2	Table-II(q)
C(8)H…O2P	1.098	2.150	158.8	Table-II(q)
O4"H…O2P	0.977	1.600	165.2	Table-II(r)
O4"H…O2P	0.977	1.590	160.0	Table-II (s)
N^+(13)H…O(10)	1.037	1.700	164.2	Table-II (t)
C(12)H…O2P	1.099	2.220	146.0	Table-II (t)
C4"H…O(10)	1.098	2.540	138.9	Table-II (t)
N^+(13)H…O(10)	1.037	1.770	155.9	Table-II (u)
C(12)H…O2P	1.098	2.120	149.2	Table-II (u)
C4"H…O2P	1.098	2.580	169.2	Table-II (u)
N^+(13)H…O(10)	1.037	1.640	170.2	Table-II (v)
C(12)H…O2P	1.098	2.240	142.9	Table-II (v)
C2"H…O2P	1.098	2.680	137.2	Table-II (v)
C4"H…O(10)	1.098	2.680	136.0	Table-II (t)
N^+(13)H…O2P	1.037	1.401	175.6	Table-II(w)
O4"H…O(10)	0.970	1.784	156.6	Table-II(w)
N^+(13)H…O2P	1.037	1.607	157.1	Table-II(x)
O4"H…O2P	0.977	1.713	158.5	Table-II (x)
N^+(13)H…O3'p	1.037	2.130	130.6	Table-II(x)

3(B).4 Trinucleotide ($U_{33}Q_{34}U_{35}$):

PCILO energy calculations have been made to find preferred most stable conformation of protonated trinucleotide ($U_{33}Q_{34}U_{35}$). Also interaction of base substituent of queuosine with adjacent nucleotides is studied. For these calculation backbone is maintained throughout the calculation as in Holbrook [12] data. The 3' and 5' ends of molecule have been methylated for termination. MMFF full optimizations have been done for the selected stable structures obtained through PCILO calculations; just to compare the salient features concerning the preferred and the alternative stable conformations of protonated trinucleotide queuosine.

3(B).4.1 Protonated trinucleotide queuosine (U33Q34U35)

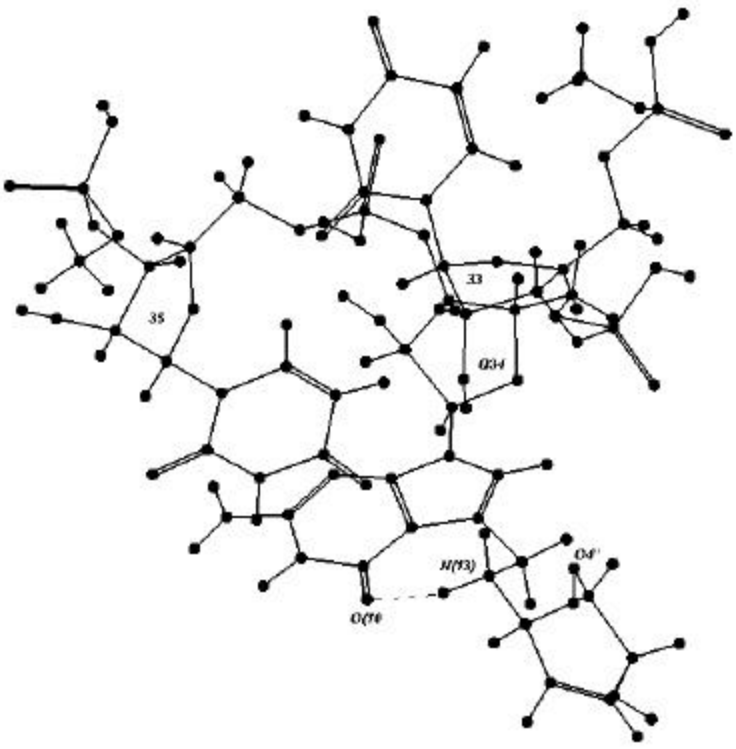

Fig.15 PCILO most stable structure for $U_{33}Q_{34}U_{35}$

Fig.16 MMFF optimized PCILO most stable structure

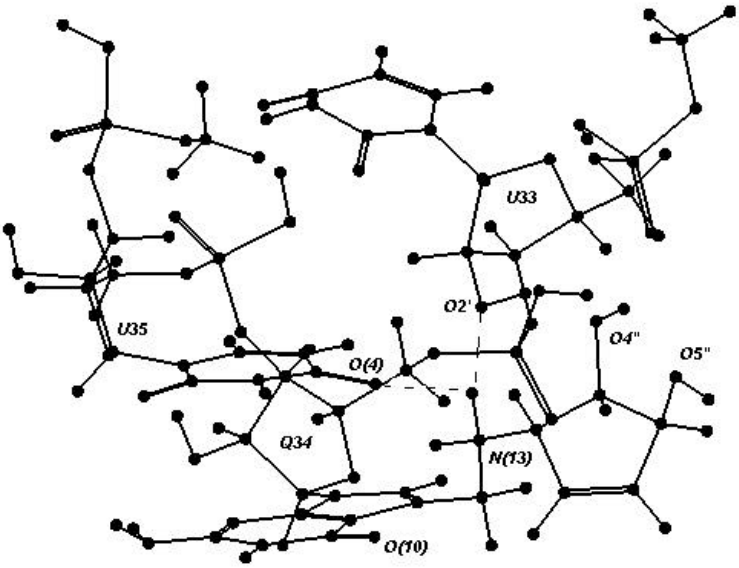

The most stable base sustituent orientation (fig.15) by PCILO for protonated trinucleotide queuosine segment is for torsion angle values $\alpha = 151°$, $\beta = 174°$, $\gamma = 317°$, $\delta = 330°$, $\varepsilon = 210°$. Except for remarkable differences in δ and ε torsion angles, this is similar to that of protonated queuosine 5'-monophosphate. The intramolecular hydrogen bonding between the base substituent imino group with O(10) of 7-deazaguanine is maintained. This is in agreement with the observed crystal structure of queuosine (see Table V).

MMFF geometry optimization prefers optimized alternative PCILO structure as more stable than the optimized PCILO most stable structure (fig.16). The hydrogen bonding geometrical parameters for these optimized structures are given in Table(V).

Table IV(1): PCILO results for protonated trinucleotide queuosine

	Torsion angles in (°)					Rel.	Reference
	α	β	γ	δ	ε	energy	
a)	121	174	167	90	270	9.1	starting
b)	151	174	317	330	210	0.0	most stable
c)	151	264	197	330	210	3.0	alternative

Table IV(2): Optimized values of the torsion angles for base substituent orientation of queuosine by automatic geometry optimization using MMFF method.

	Torsion angles in (°)					Rel.	starting
	α	β	γ	δ	ε	energy	
d)	133.8	177.0	-168.9	66.4	-40.4	4.9	Table IV(1)[a]
e)	113.8	174.5	-41.9	-18.4	169.9	3.7	Table IV(1)[b]
f)	118.7	-85.9	171.6	-51.2	-157.8	0.0	Table IV(1)[c]

Table V: Geometrical Parameters for hydrogen bonding in the preferred PCILO as well as for MMFF optimized conformations of the trinucleotide queuosine segment.

Atoms Involved (1-2-3)	Atom pair (1-2) A	Atom pair (2-3) A	Angle (1-2-3)	Reference
$N^{+}(13)H_{34}...O(10)_{34}$	1.010	1.642	161.8	Table IV(1)[b]
$N^{+}(13)H_{34}...O(10)_{34}$	1.010	1.695	150.4	Table IV(1)[c]
$N^{+}(13)H_{34}...O(4)_{35}$	1.010	2.308	135.7	Table IV(1)[c]
$O4''H_{34}...O3'p_{34}$	0.970	1.893	122.7	Table IV(1)[c]
$N(3)H_{33}...O1P_{36}$	1.008	1.920	138.8	Table IV(2)[a]
$N^{+}(13)H_{34}...O2'_{33}$	1.009	1.942	156.3	Table IV(2)[a]
$N^{+}(13)H_{34}...O(10)_{34}$	1.009	1.740	150.0	Table IV(2)[a]
$O2'H_{33}...O(4)_{35}$	0.977	2.270	126.9	Table IV(2)[a]
$N(3)H_{33}...O5'p_{36}$	1.008	2.100	162.6	Table IV(2)[b]
$N^{+}(13)H_{34}...O(10)_{34}$	1.009	2.190	130.2	Table IV(2)[b]
$N^{+}(13)H_{34}...O2'_{33}$	1.009	1.730	160.2	Table IV(2)[b]
$N^{+}(13)H_{34}...O(4)_{35}$	1.009	1.838	134.3	Table IV(2)[b]
$O2'H_{33}...O4''_{34}$	0.970	1.679	146.0	Table IV(2)[b]
$N(3)H_{33}...O1P_{36}$	1.008	1.730	163.7	Table IV(2)[c]
$N^{+}(13)H_{34}...O(10)_{34}$	1.009	2.240	121.5	Table IV(2)[c]
$N^{+}(13)H_{34}...O(4)_{35}$	1.009	1.999	151.1	Table IV(2)[c]
$O4''H_{34}...O2'_{33}$	0.970	2.074	145.0	Table IV(2)[c]
$O2'H_{33}...O5''_{34}$	0.970	1.660	144.6	Table IV(2)[c]

Interresidue hydrogen bonding between $N(13)^{+}H$ group of base substituent of queuosine with hydroxyl group (O2'H) of 33rd nucleotide ribose is seen. The $N(13)^{+}H$ group also participates in H-bonding interaction with $O(4)_{35}$ (Table V).

The hydrogen bonding $N(3)H_{33}...O1P_{36}$ is retained in MMFF optimization and clearly indicates well maintained backbone conformation in the trinucleotide segment. The interaction of cyclopentenediol group of queuosine with $O2'H_{33}$ group may stabilize the optimized PCILO alternative structure.

3(B).5 Conclusion:

The presence of several polar functional groups in modified nucleotide pQ allows interesting possibilities for intranucleotide interactions as well as interactions with the other nucleotides in the anticodon loop. In pQ and $p^{-}QH^{+}$, the aminomethyl group may have stronger hydrogen bond donor - acceptor interactions with the 5'-phosphate. On protonation, stabilization is provided by $HN(13)^{+}H$---O(10) interaction in pQH+.

The queuosine trinucleotide segment shows not only intramolecular interaction of $HN(13)^{+}H$ with O(10) but also interresidue interaction with $O2'H_{33}$ and / or $O(4)_{35}$.

In each case, prospective sites for usual codon - anticodon base pairing remain unobstructed.

3(B).6 References :

1) Kersten, H. Prog. Nucl. Acid Res. Mol. Biol. 1984, 31, 59-114
2) Bjork, G. R.; Ericson, J. U.; Gustafsson, C. E. D.; Hagervall, T. G.; Jonsson, Y. H.; Wikstrom, P. M. Ann. Rev. Biochem. 1987, 56, 263-287
3) Persson, B. C. Molecular Microbiology 1993, 8, 1011-16
4) Yokoyama, S.; Nishimura, S.; in tRNA Structure Biosynthesis and Function (eds. Soll, D.; RajBhandary, U. 1995 Am. Soc. Microbiol., Washington, DC 20005)
5) Sprinzl, M.; Horn, C.; Brown, M.; Ludovitch, A.; Steinberg, S. Nucleic Acid Res. 1998, 26, 148-153
6) Okada, N. S.; Terada, M.; Nishimura, S. Europ. J. Biochem. 1981, 115, 423-428
7) Bjork, G. R. and Ramuson, T. in Modification and Editing of RNA (eds. Grosjean, H.; Benne, R. 1998 Am. Soc. Microbiol., Washington, DC 20005)
8) Grosjean, H. and Chantrenne, H. in Molecular Biology, Biochemistry and Biophysics ,F,Chapeville. A. Haenni,eds.(Springer Verlag, Berlin),1980, 32, 347-367
9) Labula, D. ;Grosjean,H.; Striker, G. and Porschke, D., Biochimica et.Biophysica Acta 1982,68,230-236
10) Grosjean, H.; Houssier,C. and Cederren,R., in Structure and Dynimics of RNA, P.H.van Knippenberg, C.W.Hilbers. Eds (Plenum Press, New York),1986 161-174
11)Yokoyama, S.; Miyazawa, T.; Itaya, Y.; Yamaizumi, Z.; Kasai, H.; Nishimura, S.

Nature 1979, 282, 107-109

12) Holbrook, S. R.; Sussman, J. L.; Warrant, R. W.; Kim, S. H. J. Mol. Biol. 1978, 123, 631-660

13) Malrieu, J. P. in Semiempirical Methods of Electronic Structure Calculations, Part A, Techniques, Segal, G A.; Ed.; Plenum, New York, 1977, 69-103

14) Pullman, B.; Pullman, A. Advan. Protein Chem. 1974, 16, 347-526

15) Pullman, B.; Saran, A. Prog. Nucleic Acid. Res. Mol. Biol. 1976, 18, 216-326

16) Tewari, R. Int. J. Quantum Chem. 1987, 31, 611-624

17) Halgren, T. A. J. Comp. Chem. 1996, 17, 490-519

18) Dewar, M. J. S.; Thiel, W. J. Am. Chem. Soc. 1977, 99, 4899-4907

19) Stewart, J. J. P.; J. Comp. Chem. 1991, 1, 320-341

20) Becke, A. D. Phys. Rev. A 1988,38, 3098-3100

21) Perdew, J. P. Phys. Rev. B. 1986, 33, 8822-8824

22) Hehre, W. J.; Yu, J.; Klunzinger, P. E.; Lou, L. `A Brief Guide to Molecular Mechanics and Quantum Chemical Calculations', 1998 Wavefunctions Inc., Irvine, CA 92612 USA

Chapter 4: Effect of protonation on the conformational preferences of threonyl carbonyl adenine (tc^6Ade) system.

4.1 Introduction: Extensively (hyper) modified nucleic acid bases are found to naturally occur at strategic locations in the anticodon loop of tRNAs [1-5]. Hypermodification is specially associated with the first position of the anticodon and the anticodon 3'-adjacent position [4-7]. The nature of the chemical modification of the nucleic acid base, occurring 3'-adjacent to the anticodon correlates with the nature of the terminal base of the anticodon [1-5,8,9]. In tRNA molecules with the anticodon ending in adenosine (A), the hydrophobic modified base N6- (Δ^2-isopententenyl) adenine, i^6Ade, or its derivative 2-methyl -thio-N6-(Δ^2-isopententenyl) adenine , ms^2i^6Ade, occurs 3'-adjacent to it [6,8,9]. In contrast to this, in tRNAs with anticodon terminating in uridine (U), the 3'-adjacent hypermodified base is hydrophilic substituted N6-(N-glycyl carbonyl) adenine, gc^6Ade, or N6-(N-threonyl carbonyl) adenine, tc^6Ade, or its methyl derivatives, m^6tc^6Ade, or 2-methyl thio derivative, ms^2tc^6Ade [7-9]. The orientation of the N(6) substituent in i^6Ade, ms^2i^6Ade, gc^6Ade, tc^6Ade, m^6tc^6Ade and ms^2tc^6Ade is found to be "distal" (the substituent spreads away from the five membered imidazole moiety of adenine ring) in the crystal structure observations [10-15] and is also preferred theoretically [16-18]. Consequent to the distal orientation, N(6)H becomes inaccessible for participation in the usual Watson-Crick base pairing with the codon and thus can help define the proper reading frame during translation. The anticodon 3'-adjacent modifications are also implicated in modulation of codon - anticodon interactions for accurate and efficient smooth in-phase protein biosynthesis [19-21] and may also be important for cellular regulation [2,5]. The conformational flipping required for the functioning of tRNA may be triggered by changes in intermolecular hydrogen bond donor-acceptor interactions, which may be simulated by protonation status changes at appropriate sites [14,15].

In nucleoside adenosine N(1), N(3), and N(7) are the possible sites of protonation (fig.2). The alkylation studies of nucleic acids and constituents [22] has shown that the reactivity order of the N(1), N(3), and N(7) sites of adenine can be quite different depending upon the molecular environment and association of these molecules

in solutions. In the context of mRNA codons associating with the tRNA anticodon forming double strand, the N(1) and N(7) sites may be approached from the major groove side. The N(1) and N(7) sites are well known to, respectively, participate in the Watson -Crick and the Hoosteen base pairing [1-3]. The interaction of the 2'-OH with the N(3) is held responsible for the preferred ribose ring puckering and the RNA A form structure[3]. The crystal structure data shows that these sites also participate in intermolecular hydrogen bond donor-acceptor interactions with the neighboring

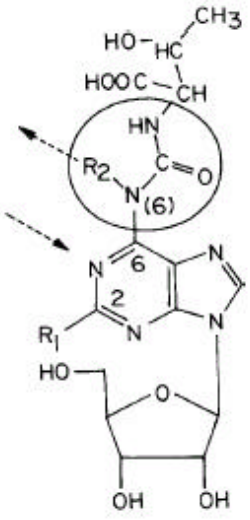

FIGURE 1. Identification of the hypermodified nucleoside N^6-(*N*-threonylcarbonyl) adenosine tc^6A (R_1 = H and R_2 = H), excluding the ribose sugar part the modified base is denoted as tc^6Ade and likewise other related modified bases are m^6tc^6Ade (R_1 = H and R_2 = CH_3) and mS^2tc^6Ade (R_1 = mS^2 and R_2 = H). Arrows indicate the potential hydrogen bonds donor or acceptor groups for canonical base pairing. The ureido linkage is shown encircled.

molecules packed in the crystalline environment [14-15]. The effect of such intermolecular hydrogen bond donor-acceptor interactions could be simulated through protonation of acceptor site in tc^6Ade [14,23]. The protonation status changes of modified bases in tRNA may trigger conformational transitions required for the functioning of tRNA and its chemical modulation.

Conformational flipping induced by diprotonation of gc^6Ade has been reported from crystal structure investigation as well as theoretically [15,26]. Earlier probings for simulating the hydrogen bond donor-acceptor interactions through protonation at the appropriate site on gc^6Ade system [23,24,25,26] has prompted the

current study on singly and doubly protonated tc^6Ade and ms^2tc^6Ade. Since in these molecules, quite often, more than one acceptor site gets involved in hydrogen bond donor-acceptor interactions with the surrounding molecules, diprotonation is required to simulate such a situation. As far as the present investigation is concerned, protonation need not imply physiological pH change. The results of the present investigation should be relevant to biomolecular function as single site and multiple site hydrogen bond donor-acceptor interactions take place under normal physiological condition as well.

Presently, the protonation induced conformational flipping in N(7), N(3) or N(1) protonated tc^6Ade and ms^2tc^6Ade along with preferred conformation of (N(1),N(3)), (N(3),N(7)), and (N(1),N(7)) diprotonated tc^6Ade and ms^2tc^6Ade is reported. Implications of such protonations on codon-anticodon interactions are also discussed.

4.2 Nomenclature, Convention and procedure:

Fig.2 depicts the atom numbering and the identification of the torsion angles (which specify the rotation around the various acyclic single chemical bonds determining the molecular conformation in ms^2tc^6Ade. Besides the 2-methylthio group, which is present only in ms^2tc^6Ade, Fig.2 also illustrates the atoms and the torsion angles which are also present in tc^6Ade. The orientation of 2-methylthio group in ms^2tc^6Ade is defined by the torsion angle χ[N(3)-C(2)-S(2)-C(16)], which specifies the rotation of C(16) about the bond C(2)-S(2) and is measured with reference to the eclipsing of the C(2)-N(3) bond by the S(2)-C(16) bond, and the torsion angle ψ[C(2)-S(2)-C(16)-H], which likewise specifies the placement of one of the three identical hydrogen atoms of the methyl group. In the N(6) substituent the torsion angle α[N(1)-C(6)-N(6)-C(10)] denotes the rotation of C(10) around bond C(6)-N(6) and is measured with respect to N(1) from the cis (eclipsed, 0°) position in the right-hand sense of rotation. Likewise, the successive chemical bonds along the main extension of the substituent define the subsequent torsion angles β, γ, δ, ε, θ, ξ, η, ϕ.

For all the energy calculations of the various molecular conformations, the quantum chemical perturbative configuration interaction with localized orbitals (PCILO) method has been used [27]. The most stable structure and the alternative stable conformations have been searched in the multidimensional conformational space using the logical selection of grid points approach [28]. The observed bond lengths and bond angles values in the crystal structure of tc^6Ade have been utilized [14]. Full geometry optimization calculations with variation of all the bond distances, bond angles along with the torsion angles, have been made using Molecular Mechanics Force Field (MMFF)[29], Parameterized Method (PM3) [30,31] and Hartree- Fock (HF)-Density Functional Theory (DFT) [32,33] methods for a few selected conformations. These methods are implemented in commercially available PC Spartan Pro software.

4.3 Results and Discussion:

A] Singly protonated tc^6Ade and ms^2tc^6Ade:

1] N(7) protonated tc^6Ade and ms^2tc^6Ade:

The predicted most stable conformation based on PCILO calculations for the N(7)-protonated ms^2tc^6Ade is depicted in Figure 2. Ignoring the 2-methylthio group, which is not present in tc^6Ade, in Figure 2, suffices to represent the most stable conformation for tc^6Ade as well. The preferred conformation is stabilized by hydrogen bonding between N(7)H and O(10). The preferred orientation of the N(6) substituent in the N(7)-protonated tc^6Ade , as well as in N(7) protonated ms^2tc^6Ade ,are alike and have been influenced by the N(7) protonation in a similar way. The preferred orientation of the N(6) substituent in N(7) protonated tc^6Ade and N(7)-protonated ms^2tc^6Ade is alike described by torsion angles α =180°, β=210°, γ=180°, δ=300°, ε=180°, θ=180°, ξ=330°, η=180°, ϕ=180° . However, as compared to the preferred N(6) substituent orientation in unprotonated tc^6Ade, m^6tc^6Ade,and ms^2tc^6Ade[17,18], the results for N(7) protonated tc^6Ade and ms^2tc^6Ade are significantly different. Instead of the indicated values in parentheses for the unprotonated form, the corresponding torsion angles for the N(7)-protonated tc^6Ade and ms^2tc^6Ade are the following α =180(0), β=210(0), γ=180(180), δ=300(0), ε=180(90), θ=180(180), ξ=330(60), η=180(60), ϕ=

180 (180). Thus the marked contrast is evident. Although, for N(7) protonated gc^6Ade, changes were restricted to torsion angles α and β and thus relative orientation of carboxyl group with respect to the carbonyl group in the uriedo (HN-CO-NH) linkage remained unaffected [24,28]. However, sharp changes are not limited to α and β torsion angles in tc^6Ade and ms^2tc^6Ade.

The predicted extended orientation of 2-methylthio group in N(7)-protonated ms^2tc^6Ade (torsion angles χ=180°, ψ=180°) is also substantially different than the eclipsed orientation, which is preferred for the unprotonated ms^2tc^6Ade (torsion angles χ=0°, ψ=180°) [18]. The eclipsed conformation is about 0.7kcal/mol higher in energy, and thus is also quite accessible for the N(7)-protonated ms^2tc^6Ade. The extended orientation of the 2-methylthio group in N(7)-protonated ms^2tc^6Ade may hinder close approach by uracil for canonical base pairing; however, canonical base pairing is realizable for N(7)-protonated ms^2tc^6Ade in view of the small 0.7kcal/mol energy difference for the alternative eclipsed (χ=0°) orientation of the 2-methylthio group.

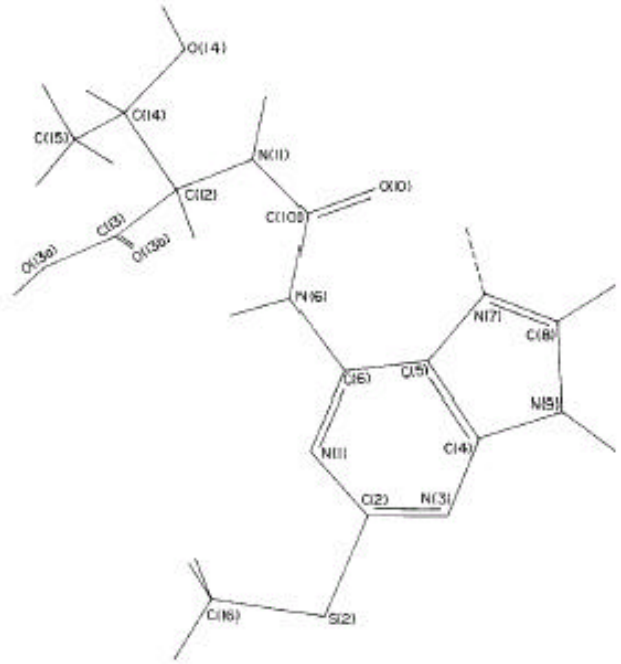

FIGURE 3. Predicted alternative stable structure for the N(7)-protonated mS^2tc^6Ade. The torsion angle values are $\alpha = 180°$, $\beta = 210°$, $\gamma = 0°$, $\delta = 300°$, $\varepsilon = 180°$, $\theta = 180°$, $\xi = 330°$, $\eta = 180°$, $\phi = 180°$, $\chi = 180°$, and $\psi = 180°$.

The alternative conformations, using PCILO energy calculation, for both N(7) protonated tc^6Ade and ms^2tc^6Ade are given in Table 1(a1). In the alternative conformation (Fig.3), the preferred trans arrangement of torsion angle γ (180°) is flipped to cis (γ=0°) orientation. This alternative structure is 1.3 kcal/mol higher than the preferred most stable conformation (fig.2) for both N(7) protonated tc^6Ade and ms^2tc^6Ade molecules. The intramolecular hydrogen bonding N(7)H...O(10) is retained, as well, in the alternative conformation. However, another intramolecular hydrogen bonding between N(6)H and O(13b) may be stronger in alternative structure. A weaker stabilizing interaction between N(11)H and O(14) may also be present in this conformation (see Table 4).

Table 1: Torsion angles in (°) obtained through PCILO energy calculations for all protonated tc^{6}Ade systems.

molecule information	α	β	γ	δ	ε	θ	ξ	η	φ	χ	ψ	Rel.energy	Structure
a] N(7)-tc^{6}Ade	180	210	180	300	180	180	330	180	180			0	most stable
a1]	180	210	0	300	180	180	330	180	180			1.3	alternative
b] N(7)-ms^{2}tc^{6}Ade	180	210	180	300	180	180	330	180	180	180	180	0	most stable
b1]	180	210	0	300	180	180	330	180	180	180	180	1.3	alternative
c] N(3)-tc^{6}Ade	0	180	180	300	180	180	330	180	180			0	most stable
c1]	0	180	0	300	180	180	330	180	180			0.2	alternative
d] N(3)-ms^{2}tc^{6}Ade	0	180	180	300	180	180	330	180	180	180	180	0	most stable
d1]	0	180	0	300	180	180	330	180	180	180	180	0.3	alternative
e] N(1)-tc^{6}Ade	0	180	180	300	180	180	330	180	180			0	most stable
e1]	0	180	0	300	180	180	330	180	180			0.04	alternative
f] N(1)-ms^{2}tc^{6}Ade	0	180	180	300	180	180	330	180	180	180	180	0	most stable
f1]	0	180	0	300	180	180	330	180	180	180	180	0.05	alternative
g] N(1)-N(7)	180	210	0	300	270	180	60	150	180			0	most stable
g1] tc^{6}Ade	180	210	180	330	150	180	60	150	180			2.9	alternative
h] N(1)-N(7)	180	210	0	300	270	180	60	150	180	180	180	0	most stable
h1]ms^{2}tc^{6}Ade	180	210	180	330	150	180	60	150	180	180	180	3.2	alternative
i] N(1)-N(3)	0	180	0	300	240	180	60	150	180			0	most stable
i1] tc^{6}Ade	0	180	180	300	240	180	60	150	180			6.0	alternative
j] N(1)-N(3)	0	180	0	300	270	180	60	150	180	180	180	0	most stable
j1]ms^{2}tc^{6}Ade	0	180	180	300	270	180	60	150	180	180	180	6.1	alternative
k] N(7)-N(3)	180	210	180	300	180	180	330	180	180			0	most stable
k1] tc^{6}Ade	180	180	0	300	180	180	330	180	180			0.3	alternative
l] N(7)-N(3)	180	210	180	300	180	180	330	180	180	180	180	0	most stable
l1] ms^{2}tc^{6}Ade	180	180	0	300	180	180	330	180	180	180	180	0.5	alternative

Table 2: Results for PM3 optimized PCILO most stable and alternative structures

molecule	α	β	γ	δ	ε	θ	ξ	η	ϕ	χ	ψ	Rel.energy	Starting
1] N(7)-tc^{6}Ade	171.6	-160.1	-171.8	-84.2	169.4	179.1	-22.7	-178.5	-177.3			0.7	Table1[a]
2]	-174.2	170.1	37.2	-83.5	-124.4	-179.0	-34.2	178.2	-179.0			0	Table1[a1]
3] N(7)-	168.7	-158.6	-171.5	-85.7	168.5	179.1	-22.6	-177.4	-177.3	-179.9	-179.7	2.3	Table1[b]
4] ms^{2}tc^{6}Ade	-172.8	169.4	34.3	-85.7	-107.6	179.4	-48.6	-86.9	177.0	-179.6	178.5	0	Table1[b1]
5] N(3)-tc^{6}Ade	8.0	-61.1	172.8	-82.7	143.8	178.9	-46.4	-78.2	176.6			0	Table1[c]
6]	-5.4	78.1	30.1	-121.0	-81.1	179.4	-57.4	-174.9	-179.1			8.4	Table1[c1]
7] N(3)-	11.4	-95.9	-177.9	-78.1	146.0	179.0	-44.7	-78.7	176.2	179.6	178.6	6.9	Table1[d]
8] ms^{2}tc^{6}Ade	1.4	-143.8	-27.2	-121.4	126.5	178.8	-64.4	-178.5	-179.4	177.1	-178.3	0	Table1[d1]
9] N(1)-tc^{6}Ade	-8.6	-165.5	-174.4	-86.7	167.8	179.8	-21.4	-176.3	-177.2			1.2	Table1[e]
10]	4.5	170.8	26.4	-97.3	-95.7	179.7	-55.4	-173.0	179.1			0	Table1[e1]
11] N(1)-	-9.2	-165.1	-173.2	-86.2	166.9	179.3	-21.6	-176.7	-176.9	-178.3	179.6	3.5	Table1[f]
12] ms^{2}tc^{6}Ade	-7.4	179.2	25.6	-153.4	122.2	179.6	-58.4	-172.0	-177.0	179.9	-179.9	0	Table1[f1]
13] N(1)-N(7)	-172.4	170.0	28.1	-73.6	-129.4	-178.9	51.2	173.9	-174.8			0	Table1[g]
14] tc^{6}Ade	-178.8	-144.3	158.9	-54.0	-171.8	178.6	55.9	177.1	-174.5			10.4	Table1[g1]
15] N(1)-N(7)	-170.8	167.5	32.6	-76.8	-128.9	-179.3	51.3	174.0	-174.5	-178.8	179.2	0	Table1[h]
16]ms^{2}tc^{6}Ade	-177.9	-145.5	158.9	-54.3	-172.1	178.4	56.3	176.7	-174.8	179.9	179.9	10.2	Table1[h1]
17] N(1)-N(3)	2.3	177.2	20.3	-66.3	-134.7	-178.8	52.3	173.3	-174.4			0	Table1[i]
18] tc^{6}Ade	-4.6	-169.0	153.4	-59.7	-175.3	178.6	54.2	177.3	-175.4			4.7	Table1[i1]
19] N(1)-N(3)	2.7	177.9	18.0	-66.1	-134.6	-178.9	52.1	173.6	-174.7	178.8	-179.2	0	Table1[j]
20]ms^{2}tc^{6}Ade	-4.4	-171.4	157.2	-61.3	-176.3	177.9	54.7	177.2	-175.2	-179.5	-179.7	2.7	Table1[j1]
21] N(7)-N(3)	179.1	-145.2	159.0	-51.3	-174.4	178.9	30.3	-167.1	-179.2			4.1	Table1[k]
22] tc^{6}Ade	-178.5	161.9	11.6	-73.1	-141.2	-178.9	-24.9	-176.9	-178.1			0	Table1[k1]
23] N(7)-N(3)	-179.8	-138.4	169.6	-62.1	-171.1	179.8	-8.4	-146.1	-177.0	-179.9	179.7	7.6	Table1[l]
24] ms^{2}tc^{6}Ade	-178.4	175.2	33.3	-77.7	-125.5	-178.2	-31.9	-179.1	178.8	-179.0	1 79.7	0	Table1[l1]

Table 3: HF(full optimized)-DFT(single pt.) results for PCILO most stable and alternative structures

molecule	α	β	γ	δ	ε	θ	ξ	η	ϕ	χ	ψ	Rel.energy	Starting
1] N(7)-tc^{6}Ade	-179.2	-178.9	177.0	-62.4	175.4	178.3	-27.8	-174.0	-176.5			0.1	Table1[a]
2]	179.0	-174.1	26.3	-77.5	-127.6	-179.0	-38.0	178.2	-178.6			0	Table1[a1]
3] N(7)-	-179.2	-179.1	177.0	-62.4	175.1	178.4	-28.0	-173.7	-176.5	179.6	-179.9	2.2	Table1[b]
4] ms^{2}tc^{6}Ade	179.4	-174.4	26.3	-78.1	-124.5	-179.5	-39.1	-178.0	-178.1	-179.7	179.3	0	Table1[b1]
5] N(3)-tc^{6}Ade	-9.8	165.1	172.6	-63.3	172.3	-179.7	-32.5	-171.9	-176.4			0.6	Table1[c]
6]	14.9	-157.3	27.0	-80.2	-142.3	-179.2	-34.0	-179.6	-178.4			0	Table1[c1]
7] N(3)-	-4.5	173.7	175.0	-62.5	170.1	179.4	-32.9	-173.1	-175.9	-178.2	126.4	0	Table1[d]
8] ms^{2}tc^{6}Ade	9.8	-162.2	28.3	-81.5	-137.9	-179.3	-35.6	-179.6	-178.3	177.5	-141.8	0.2	Table1[d1]
9] N(1)-tc^{6}Ade	-0.1	-179.0	176.0	-61.9	174.8	179.2	-27.7	-174.0	-176.0			3.1	Table1[e]
10]	-1.0	-170.8	21.9	-80.1	-141.2	-178.6	46.6	171.3	176.8			0	Table1[e1]
11] N(1)-	0.0	-179.0	176.0	-62.1	175.6	178.5	-27.3	-175.0	-176.3	-177.8	178.4	2.3	Table1[f]
12] ms^{2}tc^{6}Ade	-1.2	-174.0	26.0	-74.2	-133.5	-178.5	-36.1	-178.7	-178.1	-179.2	179.2	0	Table1[f1]
13] N(1)-N(7)	-177.3	-174.6	24.7	-76.2	-131.5	-178.8	42.1	170.8	176.9			0.3	Table1[g]
14] tc^{6}Ade	-154.8	-144.0	168.8	-65.9	-167.1	-179.1	48.5	174.2	176.4			0	Table1[g1]
15] N(1)-N(7)	-177.3	-174.8	24.8	-76.9	-130.3	-179.2	41.9	171.0	176.5	-179.5	179.7	0	Table1[h]
16]ms^{2}tc^{6}Ade	-154.9	-143.9	168.8	-66.0	-167.0	-179.1	48.9	174.4	177.1	-1.3	179.3	1.4	Table1[h1]
17] N(1)-N(3)	-0.6	-173.6	19.3	-73.3	-134.1	-178.3	40.8	171.6	177.2			0	Table1[i]
18] tc^{6}Ade	-1.8	-174.7	162.8	-68.8	-169.7	-179.8	43.9	171.5	174.8			6.3	Table1[i1]
19] N(1)-N(3)	-0.7	-173.4	19.3	-73.9	-135.0	-177.9	41.0	170.1	175.6	179.7	-179.9	0	Table1[j]
20]ms^{2}tc^{6}Ade	-1.1	-176.1	164.0	-70.6	-168.9	179.9	45.0	170.9	176.4	-179.2	-179.9	3.1	Table1[j1]
21] N(7)-N(3)	179.8	-175.2	173.0	-59.9	-177.8	178.3	-22.0	-170.7	-177.0			3.1	Table1[k]
22] tc^{6}Ade	-179.7	-174.4	22.9	-64.9	-140.2	-177.4	-32.1	-176.8	-178.3			0	Table1[k1]
23] N(7)-N(3)	-178.3	-172.4	175.0	-57.0	176.1	177.4	-25.4	-168.7	-176.4	-179.4	-178.9	5.0	Table1[l]
24] ms^{2}tc^{6}Ade	-179.2	-175.0	23.7	-67.0	-136.7	-177.9	-33.2	-177.1	-178.4	-179.9	178.8	0	Table1[l1]

Table 4:Hydrogen bonding geometrical parameters for all protonated tc[6]Ade systems

Atoms Involved (1-2-3)	Atom pair (1-2) A	Atom pair (2-3) A	Angle (1-2-3)	Reference
A] PCILO structures				
N(7)H...O(10)	1.000	1.618	120.4	Table1[a,b,a1,b1,k,l]
N(11)H...O(14)	1.010	2.141	104.0	Table1(a,b,a1,c,d,e,f,e1,f1,k,l,k1,l1)
N(6)H...O(13b)	1.010	2.037	127.9	Table1(a1,b1)
N(1)...N(6)H...O(13b)	2.480	2.037	144.3	Table1(a1,b1)
O(10)...N(11)H...O(14)	2.140	2.510	158.5	Table1(a1,b1)
N(1)H...O(10)	1.000	2.036	120.8	Table1(e,f,e1,f1)
N(7)H...O(10)	1.000	1.639	126.0	Table1(g,h,g1,h1)
N(6)H...O(13b)	1.010	1.690	167.8	Table1(g,h)
N(7)H...O(13b)	1.000	2.613	153.3	Table1(g1,h1)
N(1)H...O(10)	1.000	2.085	123.2	Table1(i,j,i1,j1)
N(6)H...O(13b)	1.010	1.769	120.5	Table1(i)
N(6)H...O(13b)	1.010	1.860	136.7	Table1(j)
B] PM3 structures				
N(7)H...O(10)	1.024	1.780	132.0	Table1(a,b,a1,b1,g,h,g1,h1,k, l ,k1,l1)
N(6)H...O(13b)	1.036	1.792	152.1	Table1(a1,b1,g,h,l1)
N(1)...N(6)H...O(13b)	2.430	1.790	134.4	Table1(a1,b1,l1)
O(10)..N(11)H...O(14)	2.420	1.910	143.7	Table1(a1)
O(10)...N(11)H...O(14)	2.400	2.401	133.2	Table1(b1)
N(11)H...N(1)	0.998	2.560	110.9	Table1(c)
C(16)H...O(13b)	1.097	2.570	124.7	Table1(d)
N(1)H...O(10)	1.020	1.808	128.3	Table1(e,e1,f,f1,i,j,i1,j1)
N(6)H...O(13b)	1.036	2.505	132.8	Table1(e)
N(11)H...O(14)	0.998	1.894	113.5	Table1(f,k,k1,l,l1)
N(6)H...O(13b)	1.036	1.734	142.0	Table1(i,j)
O(10)..N(11)H..O(14)	2.420	2.450	163.0	Table1(g,h)
N(7)H...O(13b)	1.024	2.583	118.3	Table1(g1,h1)
O(10)...N(11)H..O(14)	2.469	1.861	156.3	Table1(k1)
O(10)...N(11)H..O(14)	2.445	1.875	148.9	Table1(l1)

C] HF-DFT structures

N(7)H...O(10)	1.029	1.650	136.9	Table1(a,b,a1,b1)
N(11)H...O(14)	0.998	1.90	113.0	Table1(a,c,d,e,f,f1,j1,i1)
N(1)H...O(10)	1.021	1.747	132.6	Table1(e,f,e1,f1)
N(6)H...O(13b)	1.020	1.783	151.6	Table1(a1,b1,c1,d1)
N(6)H...O(13b)	1.020	1.828	145.4	Table1(e1)
N(6)H...O(13b)	1.020	1.735	150.0	Table1(f1)
N(7)...N(6)H...O(13b)	2.747	1.735	112.2	Table1(f1)
N(7)H...O(10)	1.029	1.686	133.3	Table1(g,h)
N(6)H...O(13b)	1.020	1.592	160.2	Table1(g,h)
N(7)H...O(13b)	1.029	1.621	170.9	Table1(g1,h1)
N(11)H...O(14)	0.99	1.999	110.0	Table1(g1,h1)
N(1)H...O(10)	1.021	1.555	138.7	Table1(i,j,i1,j1)
N(6)H...O(13b)	1.020	1.643	149.9	Table1(i,j)
N(6)H...O(13b)	1.020	1.672	149.2	Table1(j)
N(7)H...O(10)	1.029	1.584	137.3	Table1(k,l,k1,l1)
N(11)H...O(14)	0.99	1.789	117.2	Table1(k,l,l1)
N(6)H...O(13b)	1.020	1.621	154.1	Table1(k1,l1)
N(1)...N(6)H...O(13b)	2.380	1.621	133.9	Table1(k1,l1)
O(10)..N(11)H..O(14)	2.421	1.787	158.5	Table1(k1,l1)

Full geometry optimization for PCILO preferred most stable and PCILO alternative conformation has been made, using PM3 and HF-DFT methods. In case of HF-DFT full optimization by HF (basis set 3-21G*) method is followed by single point energy calculations using DFT (pBP*/DN*) method. The results obtained using these two optimization methods (PM3, HF-DFT) for both the N(7)-protonated tc^6Ade and ms^2tc^6Ade molecules show that optimized PCILO alternative structure turns out to be

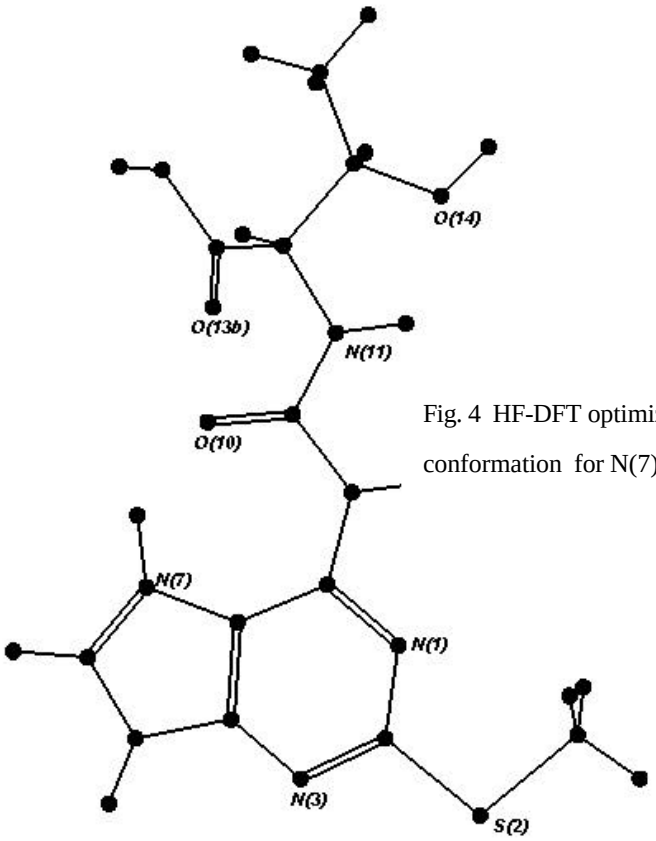

Fig. 4 HF-DFT optimized PCILO most stable conformation for N(7) - protonated ms^2tc^6Ade

more stable than the optimization of the PCILO preferred structure (see fig.4 and 5). However, for N(7)-tc^6Ade molecule, the energy difference between optimization of PCILO alternative and optimization of PCILO most stable structure using HF-DFT method is just 0.1kcal/mol and with PM3 method this difference is 0.7 kcal/mol (see Table 2 and 3). All optimized torsion angles of N(6) substituent in tc^6Ade and ms^2tc^6Ade are in good agreement with PCILO predicted stable structures (see Table 1, 2 and 3). The

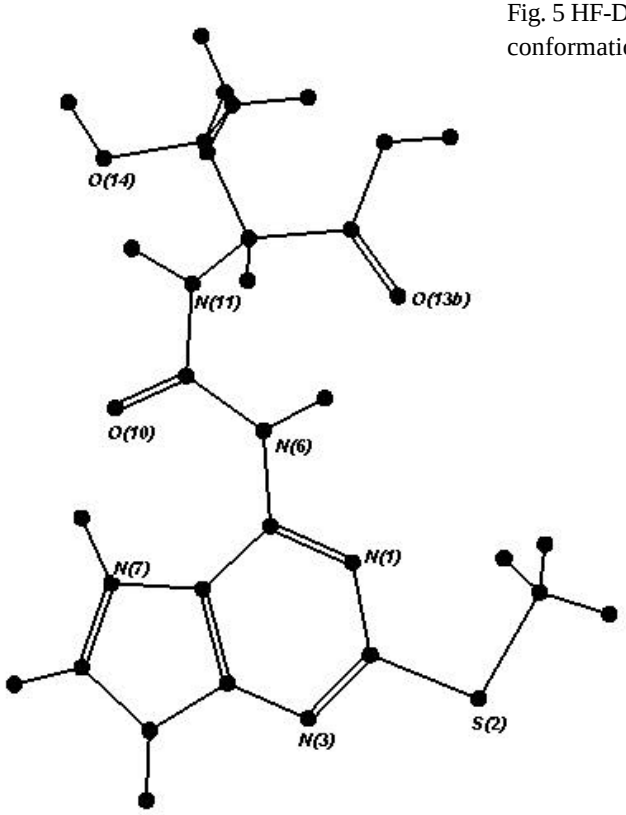

Fig. 5 HF-DFT optimized PCILO alternative stable conformation for N(7) protonated - ms^2tc^6Ade

improved geometrical parameters for hydrogen bonding indicate more stability to optimized PCILO alternative structures (Table 4). Slight change in preference of ε torsion angle value caused improved intramolecular hydrogen bonding between N(6)H and O(13b) (see Table 2, 3 and 4).

2] N(3) protonated tc^6Ade and ms^2tc^6Ade:

The preferred most stable conformation for N(3)-protonated ms^2tc^6Ade is depicted in Figure 6. The preferred orientation of the threonyl carbonyl substituent is alike in N(3) protonated ms^2tc^6Ade and tc^6Ade, thus the same figure is also representative of preferred most stable conformation for N(3)-protonated tc^6Ade ignoring the presence of the 2-methylthio group. The structure is stabilized by weak intramolecular hydrogen bonding between N(11)H and O(14). The N(6) substituent orientation takes distal ($\alpha=0^\circ$) conformation described by dihedral angles $\alpha=0^\circ$, $\beta=180^\circ$, $\gamma=180^\circ$, $\delta=300^\circ$, $\varepsilon=180^\circ$, $\theta=180^\circ$,$\xi=330^\circ$,$\eta=180^\circ$,$\phi=180^\circ$.

Fig.6 PCILO most stable structure for
N(3) protonated tc^6Ade and ms^2tc^6Ade

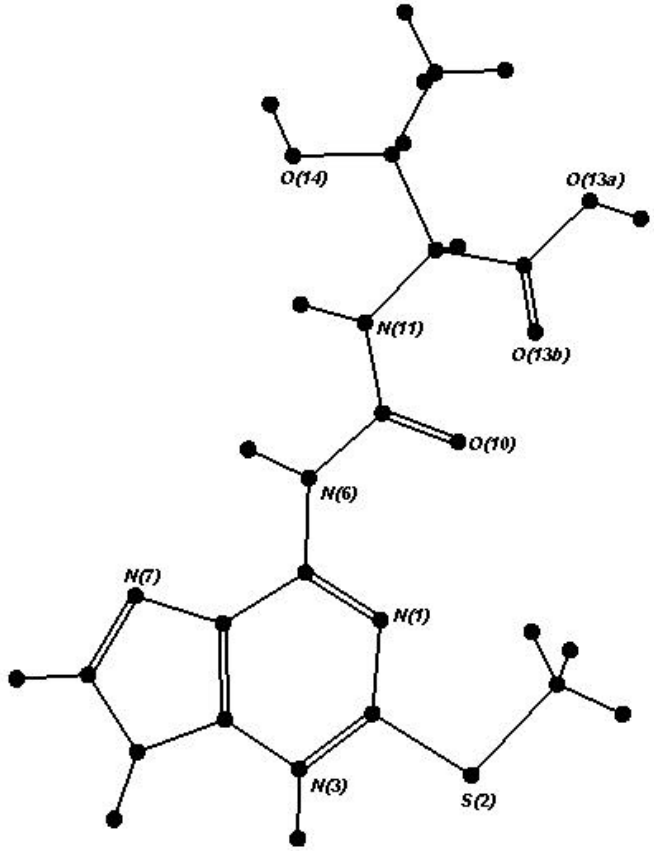

The orientation of N(6)substituent in N(3)-protonated tc^6Ade is significantly different than the favored orientation in unprotonated tc^6Ade [18]. Although N(3)-protonated gc^6Ade also prefers the distal ($\alpha=0^\circ$) conformation, significant differences are found in the preferred base substituent orientations between N(3)-protonated tc^6Ade and gc^6Ade [23]. The values for torsion angle γ, δ, ε, θ, ξ, η, ϕ, χ and ψ are alike for N(3) and N(7) protonated tc^6Ade and ms^2tc^6Ade.

The orientation of 2-methylthio group is extended in the preferred most stable conformation of N(3) - protonated ms^2tc^6Ade. This extended orientation of 2-methylthio group is different from the eclipsed orientation observed for unprotonated ms^2tc^6Ade [18]. The distal conformation of both N(3) protonated tc^6Ade and ms^2tc^6Ade blocks the access to N(1) for Watson-Crick base pairing.

The alternative stable structures for N(3)-protonated tc^6Ade and ms^2tc^6Ade are alike in torsion angles but energetically 0.2 kcal/mol higher and 0.3 kcal/mol higher than the respective preferred most stable structure of N(3)-protonated tc^6Ade and ms^2tc^6Ade. The torsion angle γ has been flipped from trans (γ=180°) conformation to cis (γ=0°) conformation, in the alternative structure. Same intramolecular hydrogen bonding

Fig. 7 HF-DFT optimized PCILO alternative stable conformation for N(3) protonated -ms^2tc^6Ade

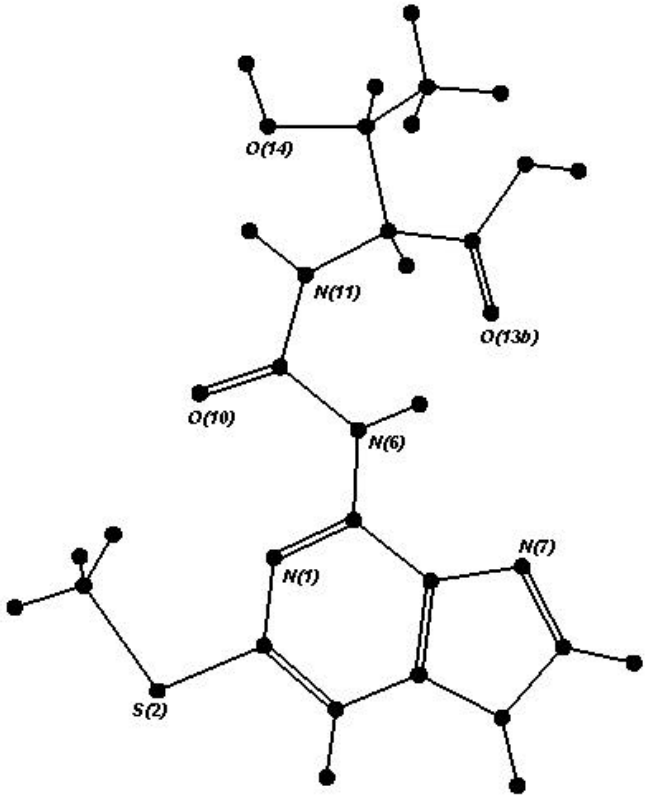

between N(11)H and O(14) is favoured in the alternative conformation (Table 4).

The automated full geometry optimization of PCILO most stable and alternative stable structures have been made using PM3 and HF-DFT methods. These two methods give different trends for stable structure, while PM3 method shows optimized PCILO most stable structure to be more stable than optimized PCILO alternative stable structure for N(3) protonated tc^6Ade ; for N(3) protonated ms^2tc^6Ade the opposite trend is shown (see Table 2). In case of HF-DFT method, optimized PCILO most stable structure

for N(3) protonated ms^2tc^6Ade is more stable than the optimized PCILO alternative structure (fig.7), but the reverse is true for optimized structures for N(3) protonated tc^6Ade. The energy difference between optimized PCILO most stable and optimized PCILO alternative structures is significantly less in HF-DFT results as compared to much higher energy differences shown by PM3 results (see Table 2 and 3) .

The torsion angles for HF-DFT optimized structures for both N(3)-protonated tc^6Ade and ms^2tc^6Ade are in close agreement with PCILO results. However, significant changes in torsion angles β, ε and η are seen for PM3 optimized structures. The HF-DFT optimization of PCILO most stable structure results in improved bond angle parameters (see Table 4) for hydrogen bonding of N(11)H and O(14). Also, the intramolecular hydrogen bonding between N(6)H and O(13b) is seen in optimized PCILO alternative structure. All these optimized N(3)-protonated tc^6Ade and ms^2tc^6Ade structures show restricted accessibility to N(1). This may disallow extended Watson-Crick base pairing with mRNA on anticodon 3'-adjacent side.

3] N(1)-protonated tc^6Ade and ms^2tc^6Ade :

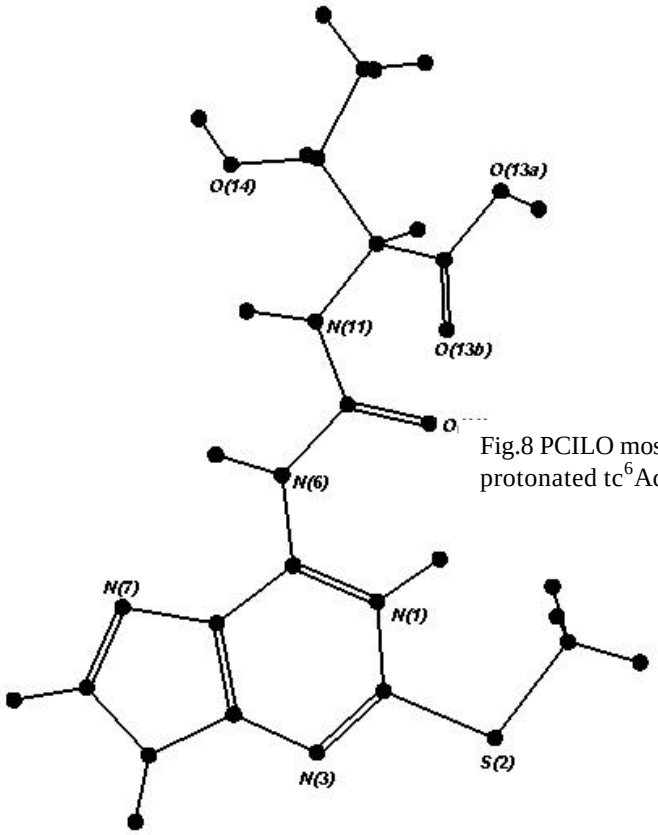

Fig.8 PCILO most stable conformation for N(1) protonated tc^6Ade and ms^2tc^6Ade

The PCILO most stable conformation for N(1) protonated tc^6Ade and ms^2tc^6Ade is alike, except for the presence of 2-methylthio group in ms^2tc^6Ade, and is shown in figure 8. The N(6) substituent orientation is distal (α=0°). The torsion angle values are α=0°, β=180°, γ=180°, δ=300°, ε=180°, θ=180°, ξ=330°, η=180°, ϕ=180°, χ=180°, ψ=180°. The effect of N(1) protonation on the N(6)substituent orientation is similar in N(1) protonated tc^6Ade and ms^2tc^6Ade. The preferred most stable conformation is stabilized by intramolecular hydrogen bonding between N(1)H and O(10). Hydrogen bonding between N(11)H and O(14) may also be a stabilizing factor for this preferred most stable conformation. The N(6) substituent orientation of N(1) protonated tc^6Ade and ms^2tc^6Ade is similar to that of N(6) substituent orientation in N(3) protonated tc^6Ade and ms^2tc^6Ade .

The higher energy alternatives to both N(1) protonated tc^6Ade and ms^2tc^6Ade are alike in torsion angles but somewhat different in relative energy. The higher energy PCILO alternative is just 0.04 kcal/mol higher and 0.05 kcal/mol higher to preferred PCILO most stable conformations for N(1) protonated tc^6Ade and ms^2tc^6Ade respectively. Similar hydrogen bonding is seen in alternative structures as that seen in the PCILO most stable conformations for N(1) protonated tc^6Ade and ms^2tc^6Ade. This alternative is very much comparable to the preferred PCILO most stable structure of N(1) protonated gc^6Ade [25]. The torsion angles α, β, γ, δ, θ of N(1) protonated tc^6Ade are same as that of N(1) protonated gc^6Ade. The preference for ε=270° in N(1) protonated gc^6Ade has given additional intramolecular hydrogen bonding between N(6)H and carboxyl O(13b). The distal conformation of N(1)-protonated tc^6Ade and ms^2tc^6Ade may be helpful in maintaining reading frame for codon - anticodon interactions.

PM3 as well as HF-DFT geometry optimization results prefer the optimized PCILO alternative structure to be more stable than the optimized PCILO most stable structure for both N(1)-protonated tc^6Ade and ms^2tc^6Ade .The intramolecular hydrogen bonding between N(1)H and carbonyl oxygen O(10) is well maintained in all PM3 and HF-DFT optimized structures. Another, intramolecular hydrogen bonding between N(6)H and carboxyl oxygen O(13b) is realized by slight adjustment of ε torsion angle in all optimized PCILO alternative structures. The energy differences between various optimized structures as well as the geometrical parameters for possible hydrogen bonding

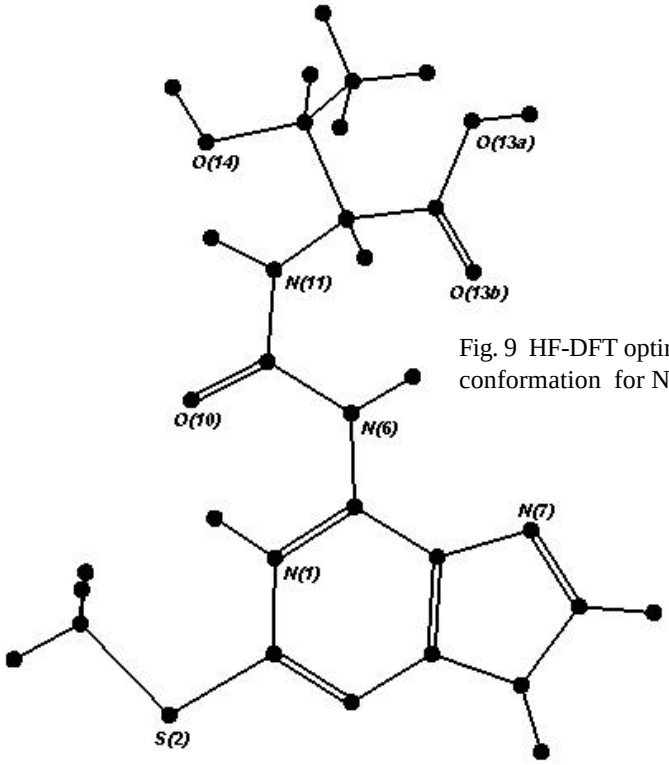

Fig. 9 HF-DFT optimized PCILO alternative stable conformation for N(1) protonated -ms^2tc^6Ade

interactions is given in Table (2,3,and 4). In HF-DFT optimized PCILO alternative structure for N(1)-protonated ms^2tc^6Ade, the intramolecular bifurcated hydrogen bonding is noticeable between N(7), N(6)H and carboxyl O(13b) sites (Table 4).

The effect of single protonation at each of N(7), N(1), and N(3) sites in tc^6Ade and ms^2tc^6Ade is alike. This clearly suggests that orientation of carbonyl oxygen O(10) is towards N(7) or N(1) site depending upon whichever of these sites is protonated. The effect of single protonation at N(3) site in both tc^6Ade and ms^2tc^6Ade orients the N(6) substituent in a manner similar to that in N(1) protonated tc^6Ade and ms^2tc^6Ade.

B] Diprotonated tc^6Ade and ms^2tc^6Ade:

1] (N(1), N(7)) diprotonated tc^6Ade and ms^2tc^6Ade:

The preferred most stable conformation for (N(1), N(7)) diprotonated tc^6Ade and ms^2tc^6Ade, based on PCILO energy calculations, is depicted in figure 10. The torsion angles for the preferred most stable conformation are α=180°, β=210°, γ=0°, δ=300°,

ε=270°, θ=180°, ξ=60°, η=150°, ϕ=180°, and the extended orientation (χ=180°, ψ=180°) is favoured for the methylthio substituent in ms^2tc^6Ade. The acceptor carbonyl oxygen O(10) is suitably placed, towards the donor N(7)H side instead of the donor N(1)H side for associating through the seven membered (O(10)C(10)N(6)C(6)C(5)N(7)H) hydrogen bond. Additionally, the carboxyl oxygen O(13b) is favorably placed for participating in the seven membered (O(13b)C(13)C(12)N(11)C(10)N(6)H) hydrogen bonding interaction with the N(6)H. This most stable conformation is closely comparable to

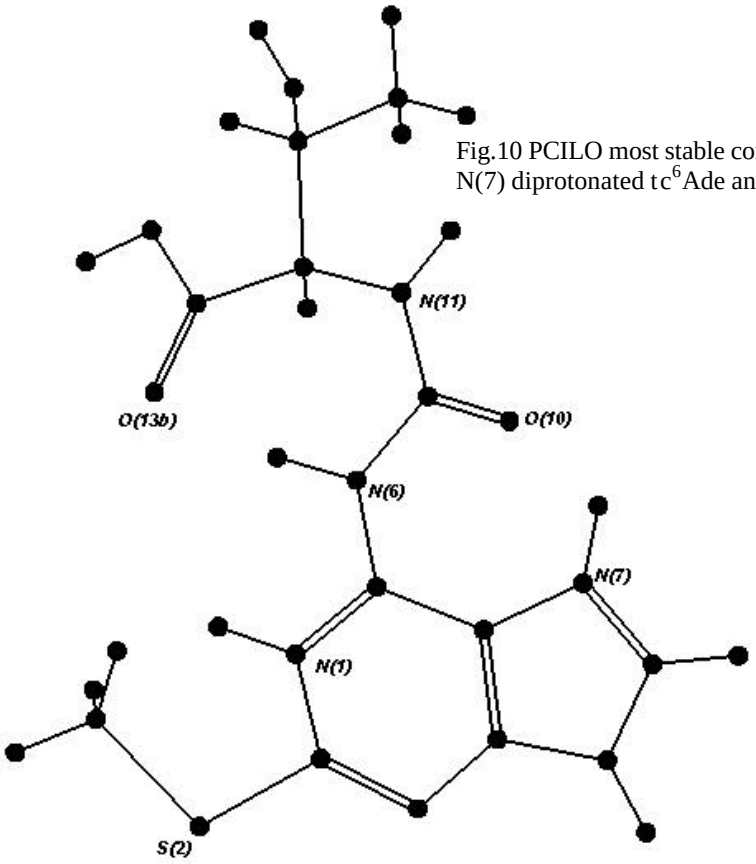

Fig.10 PCILO most stable conformation for N(1)-N(7) diprotonated tc^6Ade and ms^2tc^6Ade

PCILO alternatives of N(7) protonated tc^6Ade and ms^2tc^6Ade. The torsion angles ε, ξ of (N(1), N(7)) diprotonated tc^6Ade and ms^2tc^6Ade are changed to 270° and 60° respectively from 180° and 330° of N(7)-protonated tc^6Ade and ms^2tc^6Ade PCILO alternatives. The change in torsion angles ε, ξ improves the geometrical parameters for stronger hydrogen bonding between N(6)H and carboxyl oxygen O(13b).

The alternative conformation, based on PCILO energy calculations, for (N(1), N(7)) diprotonated tc^6Ade and ms^2tc^6Ade is unaffected by the presence of 2-methylthiolation and is given in Table 1. The torsion angle values for the PCILO alternative for both (N(1),N(7)) diprotonated tc^6Ade and ms^2tc^6Ade are α=180°, β=210°, γ=180°, δ=330°, ε=150°, θ=180°, ξ=60°, η=150°, ϕ=180°, and χ=180°, ψ=180° for the 2-methylthio substituent in ms^2tc^6Ade. Although, torsion angle preference is same in both alternatives of diprotonated (N(1), N(7)) tc^6Ade and ms^2tc^6Ade; the energy differences are not the same.(see Table 1). The intramolecular hydrogen bonding between N(7)H and O(10) is also present in these alternative conformations. Additionally, N(7)H site is also participating in intramolecular hydrogen bonding with carboxyl oxygen O(13b) (see Table 4).

PM3 optimized geometries arrived from PCILO most stable conformations of diprotonated (N(1), N(7)) tc^6Ade and ms^2tc^6Ade are found to be more stable than PM3 optimized geometries arrived from PCILO alternative conformations. Thus PM3 results have trend similar to PCILO results. The geometrical parameters for hydrogen bonding and energy differences for PM3 optimized diprotonated (N(1), N(7)) diprotonated tc^6Ade

Fig. 11 HF-DFT optimized PCILO alternative stable conformation for N(1)-N(7)-diprotonated ms^2tc^6Ade

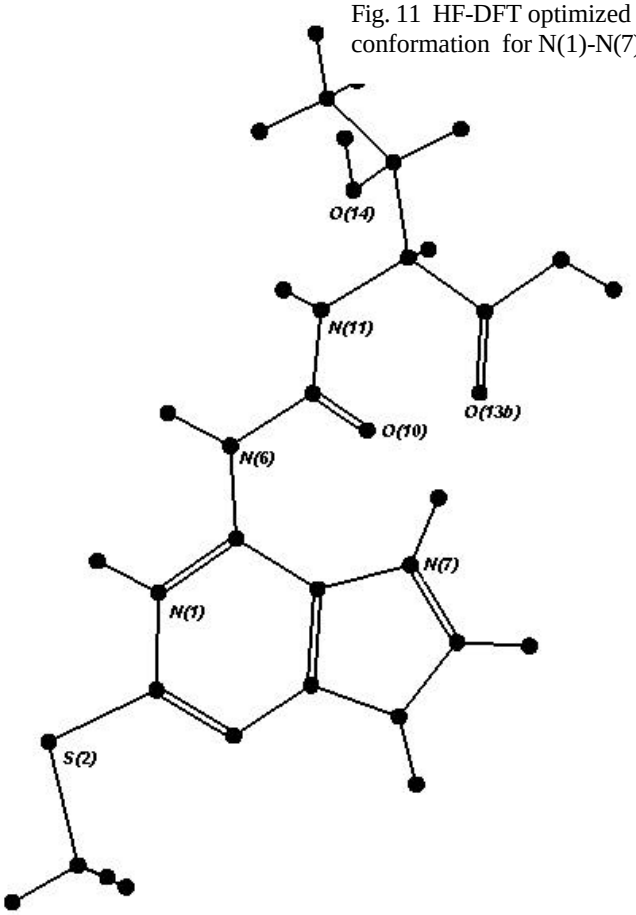

and ms^2tc^6Ade PCILO most stable and alternative structures are included in Table 4 and 2.

The HF-DFT optimization method has given same trend as that of PCILO results for the (N(1), N(7)) diprotonated ms^2tc^6Ade; but, optimized PCILO alternative is favoured over the optimized PCILO most stable structure in (N(1),N(7)) diprotonated tc^6Ade. The energy difference is however, just 0.3 kcal/mol between the optimized PCILO alternative structure and the optimized PCILO most stable structure of (N(1), N(7)) diprotonated tc^6Ade. The interesting feature is that eclipsed orientation is favoured by methyl thio substituent in the optimized PCILO alternative structure of (N(1), N(7)) diprotonated ms^2tc^6Ade. The intramolecular hydrogen bonding of N(7)H with carbonyl oxygen O(10) has become weaker but it becomes stronger and linear with carboxyl oxygen O(13b) in the optimized PCILO alternatives of both (N(1), N(7)) diprotonated tc^6Ade and ms^2tc^6Ade (see Table 4). The decisive role of N(7) protonation on the orientation of N(6) substituent is clear from these results.

2] (N(1), N(3)) diprotonated tc^6Ade and ms^2tc^6Ade :

Fig.12 PCILO most stable conformation for N(1)-N(3) diprotonated tc^6Ade

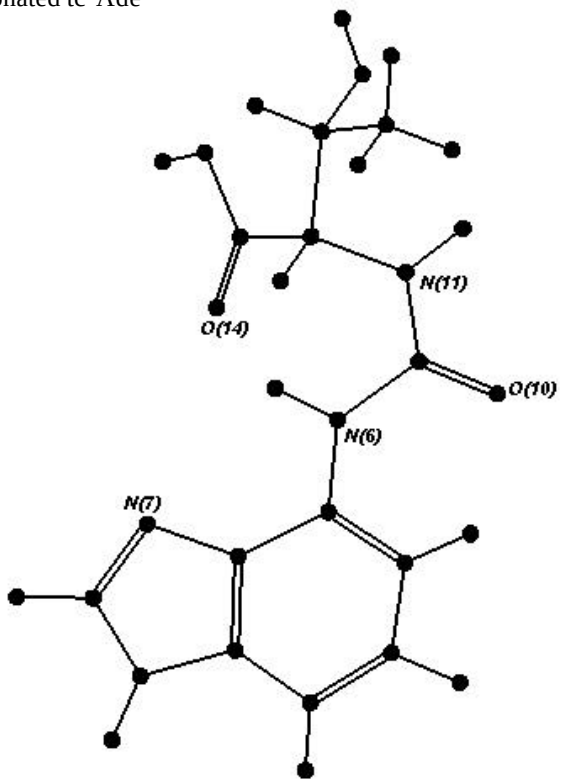

The most stable conformation for (N(1),N(3)) diprotonated tc^6Ade by PCILO is shown in figure 12. The torsion angle values are α=0°, β=180°, γ=0°, δ=300°, ε=240°, θ=180°, ξ=60°, η=150°, ϕ=180°. Except for ε, which is 270° for (N(1),N(3)) diprotonated ms^2tc^6Ade, all other above torsion angle values of the N(6) substituent also represent the preferred values for most stable conformation of (N(1),N(3)) diprotonated ms^2tc^6Ade. The extended orientation (χ=180°, ψ=180°) is preferred in the most stable conformation of (N(1),N(3)) diprotonated ms^2tc^6Ade. The acceptor carbonyl oxygen O(10) is placed on the same side of HN(1) and stabilizes the most stable structures through the six membered (O(10)C(10)N(6)C(6)N(1)H) hydrogen bonding. Additionally, the N(6)H donor site participates in hydrogen bonding with the carboxyl oxygen O(13b) through seven membered (O(13b)C(13)C(12)N(11)C(10)N(6)H) ring. The preference for ε=240° in (N(1),N(3)) diprotonated tc^6Ade shortens the distance between the N(6)H and O(13b) hydrogen bond donor-acceptor sites.

Alternative conformation for (N(1),N(3)) diprotonated tc^6Ade and ms^2tc^6Ade are nearly 6.0 kcal/mol higher than the preferred most stable conformation. The PCILO alternative is arrived by flipping of torsion angle γ from cis orientation to trans

Fig. 13 HF-DFT optimized PCILO alternative stable conformation for N(1)-N(3) diprotonated ms^2tc^6Ade

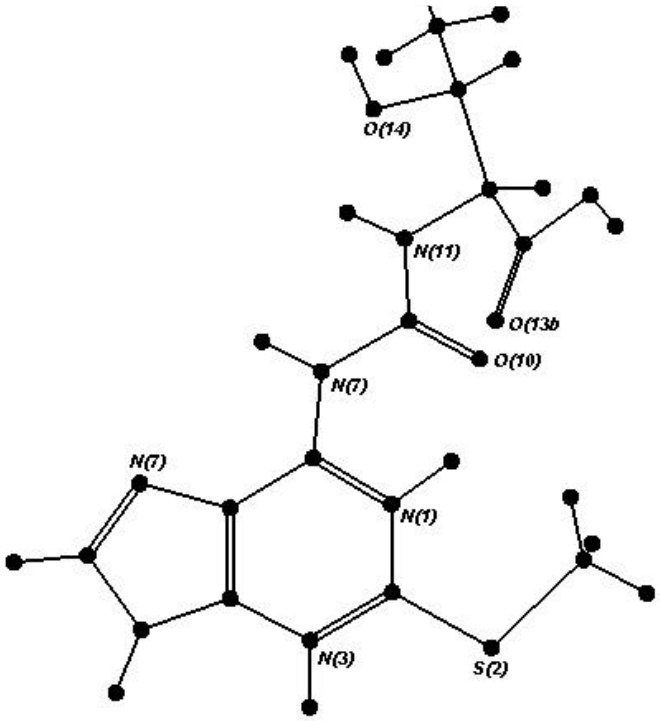

orientation in both (N(1),N(3)) diprotonated tc^6Ade and ms^2tc^6Ade (see Table 1). This alternative is stabilized by participation of donor N(1)H and acceptor O(10) sites in intramolecular hydrogen bonding.

The full geometry optimization results using PM3 and HF-DFT method, for (N(1),N(3)) diprotonated tc^6Ade and ms^2tc^6Ade, show that the optimized PCILO most stable conformation is more stable than optimized PCILO alternative structure (see Table 1). All the torsion angles are in good agreement with PCILO results. These optimized structures of (N(1),N(3)) diprotonated tc^6Ade and ms^2tc^6Ade retain intramolecular hydrogen bonding interactions similar to in PCILO most stable and alternative structures. Full geometry optimization improves the hydrogen bonding parameters for greater stabilization.

3] (N(3),N(7)) diprotonated tc^6Ade and ms^2tc^6Ade :

The preferred most stable conformation, based on PCILO energy calculations, for (N(3),N(7)) diprotonated tc^6Ade and ms^2tc^6Ade is shown in fig.14. The torsion angles describing orientation of N(6) substituent are α=180°, β=210°, γ=180°,

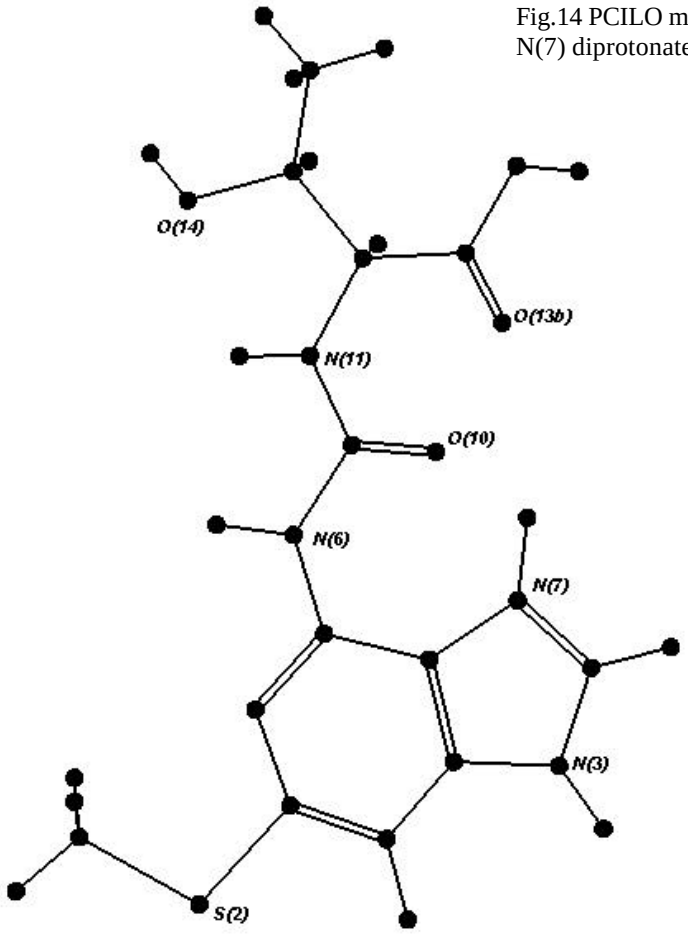

Fig.14 PCILO most stable conformation for N(3)-N(7) diprotonated tc^6Ade and ms^2tc^6Ade

δ=300°, ε=180°, θ=180°, ξ=330°, η=180°, ϕ=180° for both (N(3),N(7)) diprotonated tc^6Ade and ms^2tc^6Ade. The extended orientation (χ=180°, ψ=180°) is favoured for methyl thio substituent in ms^2tc^6Ade most stable conformation. The acceptor site O(10) participates with N(7)H donor site through seven membered (HN(7)C(5)C(6)N(6)C(10)O(10)) hydrogen bond. The weak intramolecular hydrogen bonding between donor N(11)H and acceptor hydroxyl oxygen O(14) stabilizes the preferred most stable conformation of (N(3),N(7)) diprotonated tc^6Ade and ms^2tc^6Ade. The PCILO preferred most stable conformations of both (N(3),N(7)) diprotonated tc^6Ade and ms^2tc^6Ade are exactly similar to that of PCILO preferred most stable conformations of both N(7)-protonated tc^6Ade and ms^2tc^6Ade. This clearly shows the predominant influence of N(7)-protonation on the orientation of N(6) substituent in tc^6Ade and ms^2tc^6Ade.

The alternative conformation, based on PCILO results, has been given in Table 1. The intramolecular hydrogen bonding N(7)H...O(10) is the common feature between PCILO alternative and most stable conformations of (N(3),N(7)) diprotonated tc^6Ade and ms^2tc^6Ade. The alternative conformation for (N(3),N(7)) diprotonated tc^6Ade and ms^2tc^6Ade are easily accessible since energy difference between them and the most stable structure is not much.

The full geometry optimization of PCILO most stable and PCILO alternative conformations for both (N(3),N(7)) diprotonated tc^6Ade and ms^2tc^6Ade, using PM3 and HF-DFT methods, shows trend similar to N(7)-protonated tc^6Ade and ms^2tc^6Ade . The optimized PCILO alternative structures (fig.15) are favoured in both diprotonated (N(3),N(7)) tc^6Ade and ms^2tc^6Ade because of much improved geometrical parameters for hydrogen bonding. The intramolecular bifurcated hydrogen bondings like N(1)...N(6)H...O(13b) and O(10)...N(11)H...O(14) (see Table 4) are additional factors for stabilizing the optimized PCILO alternative structures.

The PCILO conformational energy calculations for singly protonated molecules show clear preference (see Table 5A) for the tc^6Ade N(1) protonation. The PCILO alternative for N(1) protonated tc^6Ade is also equally accessible. However, PM3 optimization results gives preference for optimized PCILO alternative of N(7)-protonated tc^6Ade. The N(1) protonated tc^6Ade optimized PCILO most stable conformation is 4.2

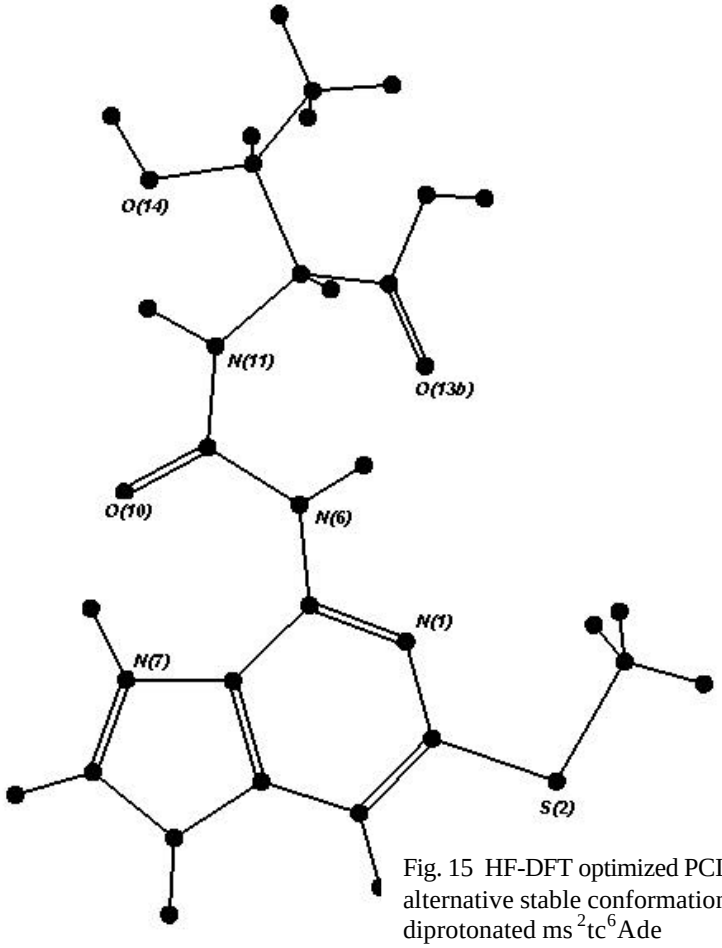

Fig. 15 HF-DFT optimized PCILO alternative stable conformation for N(3)-N(7) diprotonated ms^2tc^6Ade

kcal/mol higher in energy than the optimized PCILO alternative structure. The relative energies for N(1), N(3) and N(7) singly protonated tc^6Ade are summarized in Table 5A. The HF-DFT optimization of PCILO alternative structure for N(1) protonated tc^6Ade is most stable.

For the singly protonated ms^2tc^6Ade structures, the trend is similar to that of tc^6Ade in all PCILO, PM3 and HF-DFT methods. But HF-DFT optimization shows that PCILO alternative for N(7)-ms^2tc^6Ade is equally favoured to PCILO alternative of N(1)-ms^2tc^6Ade (see Table 5B).

The (N(1),N(7)) diprotonated tc^6Ade is preferred over other diprotonated tc^6Ade structures (Table 5C) using PCILO and PM3 methods. However HF-DFT optimization shows that, this diprotonated tc^6Ade is 0.8 kcal/mol higher in energy than (N(3),N(7)) diprotonated PCILO alternative, which is most preferred by HF-DFT method.

The diprotonated ms^2tc^6Ade structures follow the same trend for the most preferred structure as described for diprotonated tc^6Ade structure using PCILO and HF-DFT methods. However, PM3 optimization shows greater stability for PCILO alternative

of (N(3),N(7)) diprotonated ms^2tc^6Ade.

Table 5:Relative stability of various single and diprotonated tc^6Ade and ms^2tc^6Ade structures in Table 1 and on full geometry optimization using PM3 and HF-DFT.

A] Singly protonated tc^6Ade

Specifics probed	PCILO	PM3	HF-DFT	Reference
i) N(7)-tc^6Ade	19.9	0.7	5.5	Table1,2,and 3[a]
ii)	21.2	0	5.4	Table1,2,and 3[a1]
iii) N(3)-tc^6Ade	44.3	13.7	16.5	Table1,2,and 3[c]
iv)	44.5	22.2	15.9	Table1,2,and 3[c1]
v) N(1)-tc^6Ade	0	4.2	3.1	Table1,2,and 3[e]
vi)	0.04	2.6	0	Table1,2,and 3[e1]

B]Single site protonated ms^2tc^6ade

Specifics probed	PCILO	PM3	HF-DFT	Reference
i) N(7)-ms^2tc^6Ade	17.0	2.3	2.2	Table1,2,and 3[b]
ii)	18.3	0	0.0	Table1,2,and 3[b1]
iii) N(3)-ms^2tc^6Ade	25.8	20.3	13.0	Table1,2,and 3[d]
iv)	26.1	13.4	13.2	Table1,2,and 3[d1]
v) N(1)-ms^2tc^6Ade	0	8.3	2.3	Table1,2,and 3[f]
vi)	0.05	5.9	0.01	Table1,2,and 3[f1]

C] diprotonated tc^6Ade

Specifics probed	PCILO	PM3	HF-DFT	Reference
i) N(1), N(7)	0	0	0.8	Table1,2,and 3[g]
ii) -tc^6Ade	2.9	10.4	0.5	Table1,2,and 3[g1]
iii)N(1), N(3)	37.0	11.8	2.5	Table1,2,and 3[i]
iv) -tc^6Ade	43.0	16.2	6.8	Table1,2,and 3[i1]
v) N(3),N(7)	45.8	7.1	3.1	Table1,2,and 3[k]
vi) -tc^6Ade	46.1	3.0	0.0	Table1,2,and 3[k1]

D] diprotonated ms^2tc^6Ade

Specifics probed	PCILO	PM3	HF-DFT	Reference
i) N(1), N(7)	0	6.8	0.3	Table1,2,and 3[h]
ii) -ms^2tc^6Ade	3.2	17.0	1.9	Table1,2,and 3[h1]
iii)N(1), N(3)	12.6	13.6	7.5	Table1,2,and 3[j]
iv) -ms^2tc^6Ade	19.1	17.6	10.6	Table1,2,and 3[j1]
v) N(3),N(7)	20.6	7.6	5.0	Table1,2,and 3[l]
vi) -ms^2tc^6Ade	21.1	0	0	Table1,2,and 3[l1]

Although direct experimental evidence for comparision with the present inestigations is limited, nevertheless, crystal structures of tc^6Ade [14,15] provides valuable data on the possibilities of partial protonation or distribution of protonation at two sites as well as single or multiple site hydrogen bond donor-acceptor interactions.

The proximal conformation is preferred for (N(3),N(7)) diprotonated as well as for (N(1),N(7)) diprotonated tc^6Ade and ms^2tc^6Ade. Such protonation may thus allow participation of modified tc^6Ade in extended Watson-Crick base pairing with mRNA on anticodon 3'-adjacent side. This may alter the reading frame definition.

4.4 Conclusions: The comparison of the preferred and the alternative conformations of N(7)-protonated and (N(3),N(7)) , (N(1),N(7)) diprotonated tc^6Ade with the N(7)-protonated and (N(3),N(7)) , (N(1),N(7)) diprotonated ms^2tc^6Ade reveals, that, while the N(7))-protonated and diprotonated (N(3),N(7)) , (N(1),N(7)) tc^6Ade can easily participate in canonical WC base pairing , the reorientation of the 2-methylthio group to χ=0 alternative is required to enable WC base pairing for ms^2tc^6Ade also. The predicted preferred orientation of 2-methylthio group in unprotonated ms^2tc^6Ade indeed corresponds to χ=0 [18]. WC base pairing of anticodon 3'-adjacent base with mRNA may result in quadruplet (four nucleic acid bases) reading instead of the triplet genetic code for amino acids. Thus a possible alteration of the reading frame definition may result from the N(7)-singly and doubly protonated tc^6Ade. The 2-methylthio group orientation with χ=180 ,in N(7)-singly and doubly protonated ms^2tc^6Ade, however, obstructs the extended WC base pairing. Likewise methylation of the N(6) of tc^6Ade eliminates the hydrogen bond donor site involved in WC base pairing. Thus further modifications of tc^6Ade through 2-methylthiolation into ms^2tc^6Ade, as well as through N(6)-methylation into m^6tc^6Ade, serves to enhance the maintenance of the reading frame.

4.5 References:

1) Nishimura, S. Prog. Nucleic Acids Res. Mol. Biol. 1972, 12, 49-85

2) Bjork, G. R.; Ericson, J. U.; Gustafsson, C. E. D.; Hagervall, T. G.; Jonsson, Y. H.; Wikstrom, P. M. Ann. Rev. Biochem. 1987, 56, 263-287

3) Agris, P. F. Prog. Nucleic Acids Res. Mol. Biol 1996, 53, 79-129.

4) Sprinzl, M.; Horn, C.; Brown, M.; Ludovitch, A.; Steinberg, S. Nucleic Acid Res. 1998, 26, 148-153

5) Bjork, G. R. in Modification and Editing of RNA (eds. Grosjean, H.; Benne, R. 1998 Am. Soc. Microbiol., Washington, DC 20005) P.579-583

6) Motorin, Y.; Bec, G.; Tewari, R.; Grosjean, H. RNA 1997, 3, 721-733

7) Morin, A.; Auxilien, S.; Senger, B.; Tewari, R.; Grosjean, H. RNA 1998, 4, 24-37

8) Yarus, M. Science 1982, 218, 646-652

9)Tsang,, T.H.; Ames, B.N.; Buck, M.. Biochim Biophys Acta 1983, 741, 180-196

10) McMullan, R. K.; Sundaralingam, M. J. Am. Chem Soc. 1971, 93, 7050-7054

11) Bugg, C. E.; Thewalt, U. Biochem Biophys Res. Commun. 1972, 46, 779-784

12) Parthasararthy, R.; Ohrt, J. M.; Chheda, G. B. Acta Cryst. 1976, B32, 2648-2653.

13) Adamiak, D. A.; Blundell, T. L.; Tickle, I. J.; Kosturkiewicz, Z. Acta Cryst. 1975, B31, 1242-1246

14) Parthasararthy, R.; Ohrt, J. M.; Chheda, G. B. Biochemistry 1977, 16, 4999-5008

15a) Parthasararthy, R.; Soriano-Garcia, M.; Chheda, G. B. Nature 1976, 260, 807-808

15b) Parthasarthy, R.; Ohrt, J.M.; Chheda, G.B. J. Am. Chem. Soc. 1974, 96, 8087-8094

16) R. Tewari Int. J. Quantum. Chem. 1988, 34, 133-142

17) R.Tewari Ind. J. Biochem Biophys 1987, 24, 170-176

18) Tewari, R. J. Biomol. Struct. Dyn. 1990, 8, 675-686

19) Watts, M. T.; Tinoco, I. Biochemistry 1978, 17, 2455-2463

20) Grosjean, H; geHenau, S; Crothers, D.M. Proc. Natl. Acad. Sci. (USA) 1978, 75, 610-614

21) Davis, D. R. in Modification and Editing of RNA (eds. Grosjean, H.; Benne, R. Am. Soc. Microbiol., Washington, DC 20005) 1998, 85-102

22) Lawley, P. D; Brooks, P. Biochem. J. 1964, 92, 19C-20C

23) Tewari, R. Int. J. Quantum Chem. 1994, 51, 105-112

24) Tewari, R. Chem. Phys. Lett. 1995, 238, 365-370

25) Tewari, R. Int. J. Quantum Chem. 1997, 62, 551-556

26) Sonawane, K. D; Sonavane, U. B.;Tewari, R. Int. J. Quantum Chem. 2000, 78, 398-405

27) Malrieu, J. P. in Semiempirical Methods of Electronic Structure Calculations, Part A, Techniques, Segal, G A.; Ed.; Plenum, New York, 1977, 69 - 103

28) Tewari, R. Int. J. Quantum Chem. 1987, 31, 611-624

29) Halgren, T. A. J. Comp. Chem. 1996, 17, 490-519

30) Dewar, M. J. S.; Thiel, W. J. Am. Chem. Soc. 1977, 99, 4899-4907

31) Stewart, J. J. P. J. Comp. Chem. 1991, 1, 320-341

32) Becke, A. D. Phys. Rev. A 1988,38, 3098-3100

33) Perdew, J. P. Phys. Rev. B. 1986, 33, 8822-8824

Chapter 5: Structural consequences of anticodon loop having modified nucleosides

5.1 Introduction: Structural investigations of individual modified nucleosides present at strategic positions (34^{th}, 37^{th}) of anticodon loop have been described in earlier chapters. The simultaneous presence of modified nucleosides at 34^{th} (wobble) and 37^{th} (anticodon 3'adjacent) positions, in anticodon loop of tRNAs may lead to very interesting structural consequences. The anticodon stem loop (ASL) of human $tRNA^{Lys}$ having modifications (mcm^5s^2U34 and ms^2tc^6A37) and $tRNA^{Asn}$ (Q_{34} and tc^6A_{37}) are investigated using semi-empirical PCILO, Monte Carlo conformational search (molecular mechanics level) and Molecular Dynamics methods.

Human $tRNA^{Lys}$ acts as a primer for HIV replication; with its 3' end eighteen residues (nucleotides) being complementary to the primer binding site (PBS) on the viral RNA. Additionally, UUU anticodon of $tRNA^{Lys}$ has been found to interact with 'A' rich region 10 residues upstream of PBS of viral RNA [1-3]. The modified U34 (mcm^5s^2U) has been recognized to be a stabilizing factor for these interactions [3-4]. Probable interactions between another hypermodified nucleoside $ms^2tc^6A_{37}$ and modified uridine (mcm^5s^2U) at 34^{th} position may result in an unusual $tRNA^{Lys3}$ anticodon structure [5,8]. The tendency of frameshifting in bacterial and mammalian $tRNA^{Lys}$ besides HIV primer activity may conceivably be the consequences of some unusual anticodon loop structure. However, usual canonical anticodon loop structure has recently been observed in the crystal structure investigation [6]. Based on NMR investigations of Ecoli-tRNA lysine, similar open anticodon loop framework for human $tRNA^{Lys}$ [7] is also suggested. Present structural investigations have been made to understand anticodon loop conformations besides probing the role of modified nucleosides present in it.

The asparaginyl tRNA is found in Rat liver, Ecoli, Bovine liver and human liver [9,10,11]. The anticodon loop sequence is similar to human $tRNA^{Lys}$, but Q occurs at 34^{th} nucleoside position and tc^6A occurs instead at 37^{th} position of anticodon loop. The preferred orientation of N(6) substituent in tc^6Ade is probed when modified base (Q_{34}) is

also present at 34^{th} position in the anticodon loop.

5.2 Nomenclature, Convention, and Procedure:

For PCILO energy calculations and preferred conformation search also made at the level of molecular mechanics using Monte Carlo technique, anticodon loops having sequences C_{32}-U_{33}-$mcm^5s^2U_{34}$-U_{35}-U_{36}-$ms^2tc^6A_{37}$-A_{38} and C_{32}-U_{33}-Q_{34}-U_{35}-U_{36}-tc^6A_{37}-A_{38} were terminated with methyl phosphate groups at both (5' and 3') ends. The Holbrook data [12] for ribose -phosphate backbone, has been utilized to build both the anticodon loops. The crystallographic data has been utilized for tc^6Ade, ms^2tc^6Ade and Q as described in earlier chapters. However, trans orientation of C(5) substituent of $mcm^5s^2U_{34}$ is preferred (see chapter III(A)). The results of multidimensional conformational search for the preferred orientations of substituents in 34^{th} and 37^{th} bases have been obtained using PCILO and logical selection of grid points approach as described in earlier chapters. The crystal structure model for the anticodon loop ribose-phosphate backbone is retained throughout.

Another technique Monte Carlo simulation using molecular mechanics approach has been utilized for conformational search on these crystal structure model based anticodon loops. This, conformational search follows two steps 1) Monte Carlo conformational search on the substituent of 34^{th} and 37^{th} bases of anticodon loop with frozen backbone. 2) Minimization by molecular mechanics for selected structures from step1, with unfrozen backbone but retaining distance constraint between 32^{nd} and 38^{th} ribose C1' atoms. The procedure may be repeated for obtaining lower energy (more stable) conformations.

To study dynamics of anticodon stem loop with respect to time, the third technique, Molecular Dynamics (MD) has been used. The procedure adopted for MD is as follows. The coordinates for anticodon stem loop (ASL) for $tRNA^{Lys}$ and $tRNA^{Asn}$ have been taken from protein data bank molecule no. (1FIR) [6]. The sequence of $tRNA^{Asn}$ [10] is built using SYBYL biopolymer module, keeping ribose-phosphate backbone as that of 1FIR. Adding hydrogen atom to phosphate group of each residue neutralizes the molecule. In ASL of $tRNA^{Asn}$, positively charged Q resulted in overall +1 charge on the molecule. Distance constraint is applied between 27-43 and 28-42 residues

to keep the stem rigid. The calculations were performed on Silicon Graphics Indy Workstation (R5000) with 64 MB RAM. The commercial software 'Sybyl6.5' from Tripos Inc.(st.Louis,MO) is utilized for the purpose.

The trajectories of Molecular Dynamics simulation are obtained for partially solvated (600 water molecules) ASL of $tRNA^{Lys}$ for the time length of 250ps and of $tRNA^{Asn}$ ASL for 109ps duration. The constant temperature (canonical ensemble) simulation has been done with 8A° non-bonded cutoff, keeping dielectric function 'constant' and considering dielectric constant to be 1 with minimal periodic boundary condition (cube of length 41.4 A°). The water density of the system is 0.39. Kollman All atom Force Field (1986) with Gaeiger-Marsilli charges has been used with TIP3P water type for MD simulation.

The equilibration protocol consists of 2000 cycles of steepest descent minimization applied to the whole system in order to relax steric clashes. This was followed by temperature ramp for structure from 50°K to 300°K using 50°K, 1ps temperature step up to 200°K and 25°K, 1ps temperature step up to 300°K. This was followed by 240ps time length MD for $tRNA^{Lys}$ and 100ps time length MD for $tRNA^{Asn}$ at constant temp of 300°K. The data were recorded at 250fs interval during initial temperature ramp and subsequently at 1000fs till completion of MD simulation. Various other conditions used for MD simulation are, 1fs time step, initial-Boltzmann velocilty distribution, 10fs non-bonded update with scaled velocities, 5fs temperature coupling time and SHAKE algorithm for anticodon stem hydrogens.

The definitions of torsion angles for ribose-phosphate backbone as well as substituents sidechains of modified bases (at 34^{th} ,37^{th} positions) are as described in earlier chapters. The torsion angles of N(6) substituent in ms^2tc^6Ade and tc^6Ade are subscriped by 't', however, in Q_{34}, it is subscripted by 'q' and in $mcm^5s^2U_{34}$ subscripted by 'u'.

5.3 Results and Discussions:

A] PCILO results:

i) $tRNA^{Lys}$: The most stable conformation obtained from PCILO energy calculations for anticodon loop of $tRNA^{Lys}$ is given in Fig.1[a,b]. The preferred orientation of N(6)

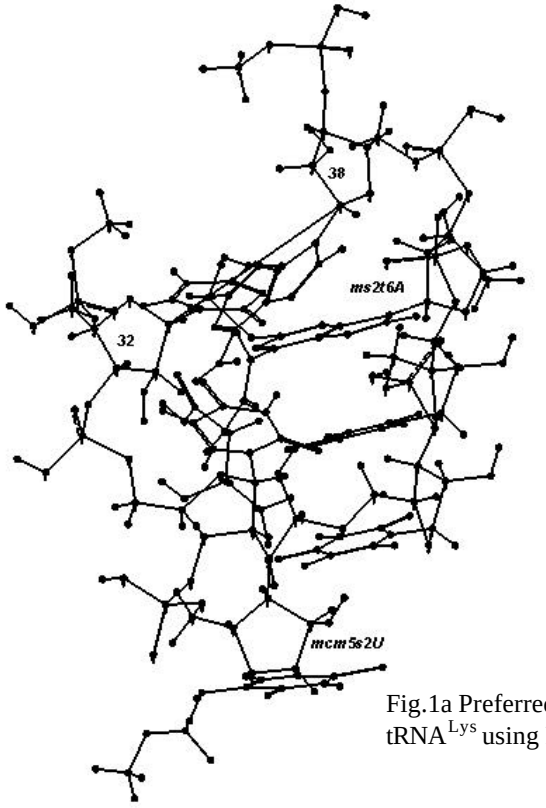

Fig.1a Preferred conformation for anticodon loop of $tRNA^{Lys}$ using PCILO energy calculations

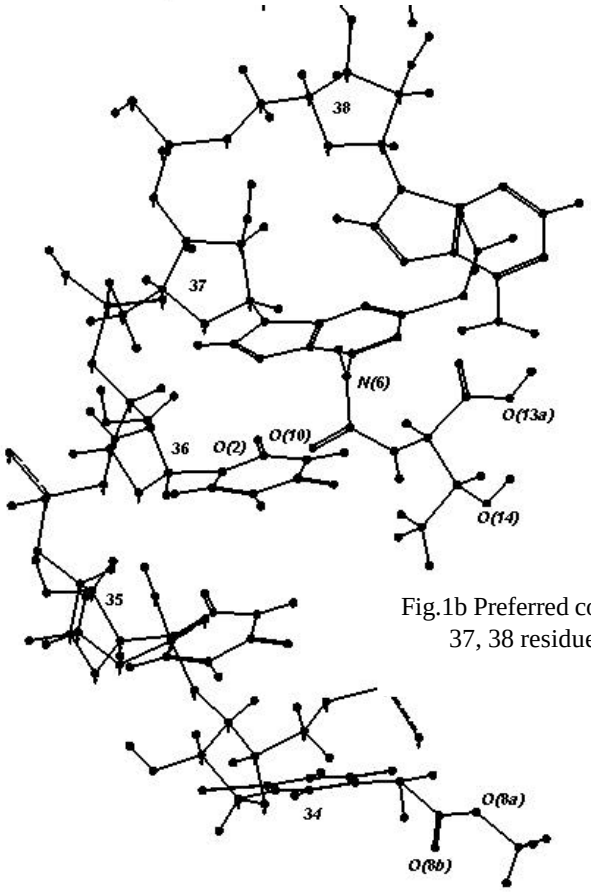

Fig.1b Preferred conformation with only 34, 35, 36, 37, 38 residues of anticodon loop of $tRNA^{Lys}$

substituent of $ms^2tc^6Ade_{37}$ is described by torsion angles α_t=90°, β_t=300°, γ_t=30°,

δ_t=270°, ε_t=210°, θ_t=180°, ξ_t=60°, η_t=60°, ϕ_t=300° [Table1(b)]. Although the substituent orientation is not exactly distal (α_t=0°), but keeps N(6)H_{37} site away from participation in Watson-Crick base pairing. Interresidue hydrogen bondings, like N(6)H_{37}...O(2)$_{32}$; N(11)H_{37}...O1'$_{33}$ and N(1)$_{32}$...N(6)H_{37} stabilize this conformation (see Table 2). The 2-methylthio group of ms^2tc^6Ade (χ_t=240°, ψ_t=180°) orients not in the eclipsed conformation but the methyl group is tilted from the plane of adenine.

The C(5)-position substituent of $mcm^5s^2U_{34}$ orients with non-planar value of torsion angle α_u=240° and planar values for β_u=180°,γ_u=180°, δ_u=180°. Geometrical parameters indicate weak (see Table 2) intramolecular hydrogen bonding interactions between C(7)$H^1{}_{34}$...O2P_{34} and C(7)$H^2{}_{34}$...O2P_{34}. The C(5) - substituent in $mcm^5s^2U_{34}$ does not interact with any other residue, including the 37th modified base. Both modified bases at 34th and 37th sites do not show any unusual feature.

Table 1: Torsion angles in ms^2tc^6Ade and mcm^5s^2U of $tRNA^{Lys}$

	α_t	β_t	γ_t	δ_t	ε_t	θ_t	ξ_t	η_t	ϕ_t	χ_t	ψ_t	α_u	β_u	γ_u	δ_u	Ref.
a]	60	0	180	300	330	180	60	180	180	180	180	180	180	180	180	PCILO Starting
b]	90	300	30	270	210	180	60	60	300	60	30	240	180	180	180	PCILO most stable
c]	-8.9	81.4	-15.2	-107.3	148.8	-171.1	39.3	155.5	177.2	-133.9	-178.9	-101.9	-177.1	-171.2	172.0	MMFF optimized

The MMFF minimized PCILO most stable conformation is included in Table 1(c)[fig.2a,b]. The structure is relaxed through optimization of all the internal coordinates. The distal (α_t = -8.9°) conformation is preferred for N(6) substituent of $ms^2tc^6Ade_{37}$ in MMFF minimized PCILO most stable structure. However, similar conformation is retained by C(5) substituent of $mcm^5s^2U_{34}$. The discontinuity of stacking is present in 36th and 37th bases. Various hydrogen bondings (Table 2) help in stabilizing

the anticodon loop which shows usual U-turning at 34th residue.

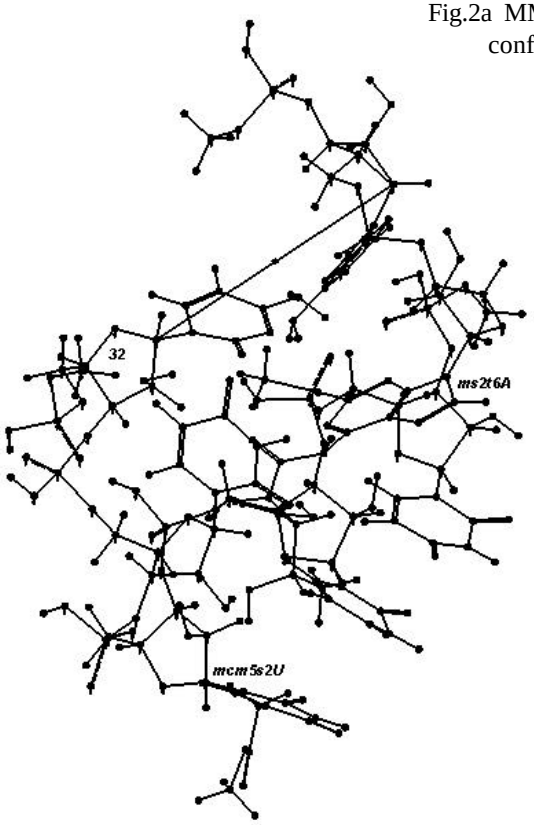

Fig.2a MMFF optimized PCILO most stable conformation of anticodon loop of $tRNA^{Lys}$

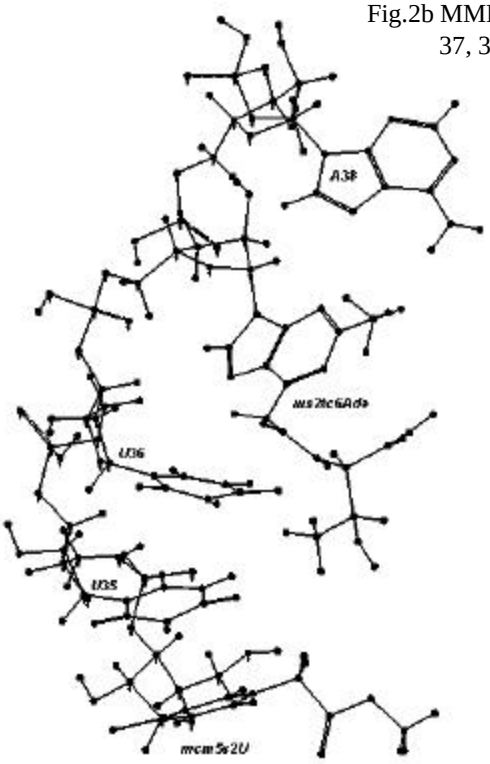

Fig.2b MMFF optimized structure with only 34, 35, 36, 37, 38 residues of anticodon loop of $tRNA^{Lys}$

The $N(11)H_{37}...O1'_{33}$ interresidue hydrogen bonding is retained in minimized PCILO most stable structure. The interresidue interaction $N(6)H_{38}...S(2)_{37}$ may explain the tilted 37^{th} base adenine ring.

Table 2: Geometrical Parameters for hydrogen bonding in the preferred PCILO as well as MMFF optimized conformations of $tRNA^{Lys}$

Atoms Involved (1-2-3)	Atom pair (1-2) A	Atom pair (2-3) A	Angle (1-2-3)	Reference
$N(11)H_{37}...O1'_{33}$	1.091	1.448	129.3	Table 1[b]
$N(6)H_{37}...N(1)_{32}$	1.091	1.950	146.5	Table 1[b]
$N(6)H_{37}...O(2)_{32}$	1.091	0.907	95.8	Table 1[b]
$C(7)H_{34}...O2P_{34}$	1.097	1.602	88.7	Table 1[b]
$C(7)H_{34}...O2P_{34}$	1.097	1.564	90.6	Table 1[b]
$C(7)H_{34}...O2'_{33}$	1.098	2.378	128.9	Table 1[c]
$C(6)H_{34}...O5'p_{34}$	1.098	2.648	156.9	Table 1[c]
$O2'H_{33}...O(14)_{37}$	0.980	1.750	170.9	Table 1[c]
$N(11)H_{37}...O1'_{33}$	1.090	1.967	133.0	Table 1[c]
$N(6)H_{38}...S(2)_{37}$	1.090	2.543	152.4	Table 1[c]
$N(3)H_{33}...O5'p_{36}$	1.090	1.644	152.1	Table 1[c]
$N(4)H_{32}...O2P_{37}$	1.090	1.852	145.2	Table 1[c]

ii) $tRNA^{Asn}$ (Q_{34} and tc^6A_{37}) : The preferred PCILO conformation for N(6) substituent in tc^6Ade is given (Fig.3[a,b], Table 3[b]) . The N(6) substituent orientation is similar to preferred orientation of ms^2tc^6Ade in $tRNA^{Lys}$. The N(6) substituent of tc^6Ade is interacting with 32^{nd} and 33^{rd} residues. The stabilization of the preferred orientation of N(6) substituent of tc^6Ade may occur through interresidue hydrogen bonding interactions like $N(6)H_{37}...N(1)_{32}$, $N(11)H_{37}...O1'_{33}$ and $N(6)H_{37}...O(2)_{32}$ as given in Table 4.

The proximal (towards the six membered ring) orientation is preferred by C(7)-substituent of Q_{34}. The hydrogen bonding $N^+H2_{(34)}...O(10)_{34}$ observed in crystal structure has been disrupted; instead, the imino group $N^+H2_{(34)}$ participates in hydrogen bonding interaction with hydroxyl ($O2'H_{33}$) group of 33^{rd} ribose. The imino group also

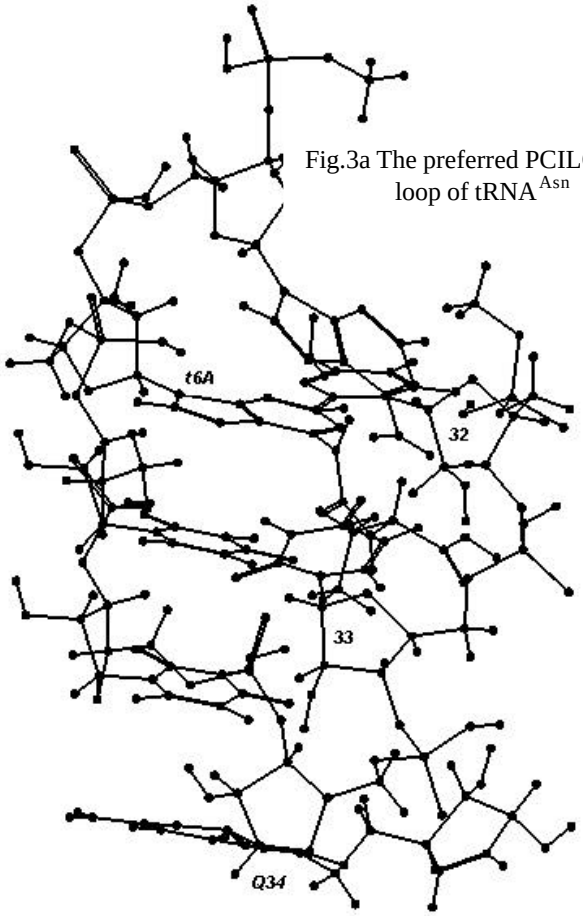

Fig.3a The preferred PCILO conformation of anticodon loop of $tRNA^{Asn}$

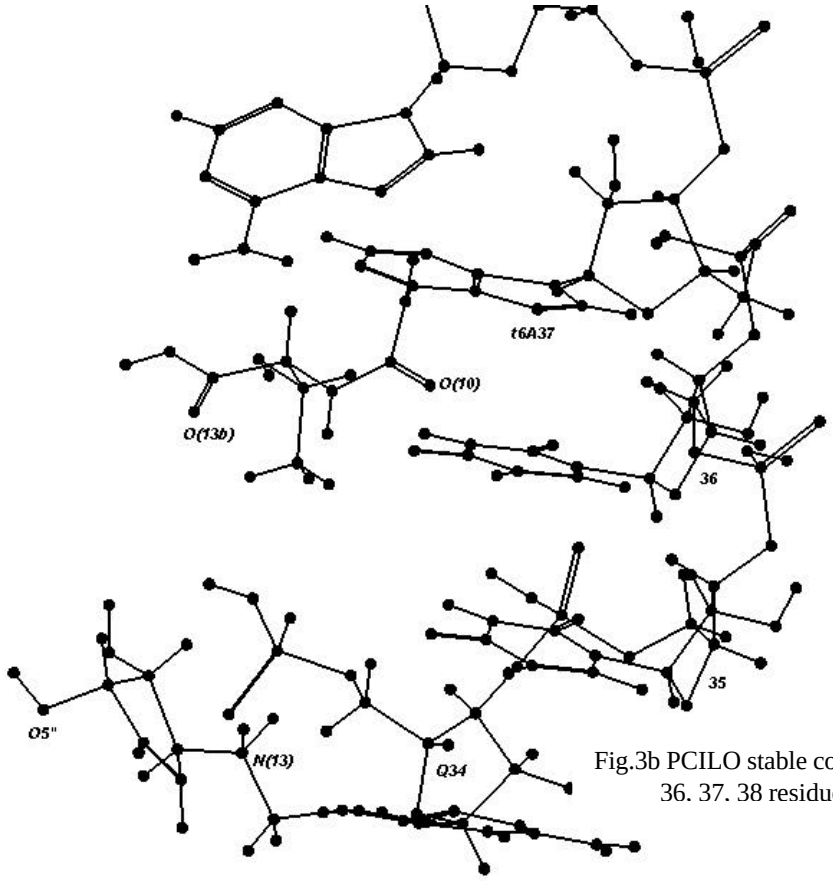

Fig.3b PCILO stable conformation with only 34, 35, 36. 37. 38 residues.

interacts with phophate oxygen of 34th residue(Table 4). Torsion angles and geometrical parameters for likely H-bonding interactions are included in Table 3 and 4. The preferred orientation of C(7)-substituent of Q_{34} does not interact with the N(6)-substituent of tc^{6}Ade.

Table 3: Torsion angles in tc^{6}Ade$_{37}$ and in Q_{34} of tRNA^{Asn}

	α_t	β_t	γ_t	δ_t	ε_t	θ_t	ξ_t	η_t	ϕ_t	α_q	β_q	γ_q	δ_q	ε_q	Ref
a]	60	0	180	300	330	180	60	180	180	121	174	167	90	270	PCILO Starting
b]	90	300	0	210	180	180	180	180	180	90	234	47	90	270	PCILO most stable
c]	57.6	-57.7	-9.8	-122.7	149.8	-174.6	172.4	50.8	-176.5	38.5	-121.2	87.0	70.9	-41.6	MMFF optimized

Table 4: Geometrical Parameters for hydrogen bonding in the preferred PCILO as well as MMFF optimized conformations

Atoms Involved (1-2-3)	Atom pair (1-2) A	Atom pair (2-3) A	Angle (1-2-3)	Reference
N(11)H$_{37}$...O1'$_{33}$	1.091	1.339	142.8	Table 3[b]
N(6)H$_{37}$...N(1)$_{32}$	1.091	1.950	146.5	Table 3[b]
N(6)H$_{37}$...O(2)$_{32}$	1.091	0.907	95.8	Table 3[b]
HN$^+$H$_{34}$...O2'$_{33}$	1.091	2.984	143.7	Table 3[b]
HN$^+$H$_{34}$...O3'p$_{33}$	1.096	2.549	149.2	Table 3[b]
C4''H$_{34}$...O3'p$_{33}$	1.098	2.289	154.8	Table 3[b]
HN$^+$H$_{34}$...O2'$_{33}$	1.012	1.755	151.6	Table 3[c]
C(15)H$_{37}$...O4''$_{34}$	1.097	2.571	118.5	Table 3[c]
N(11)H$_{37}$...O1'$_{33}$	1.091	2.154	165.9	Table 3[c]
C(14)H$_{34}$...N(1)$_{37}$	1.097	2.346	117.3	Table 3[c]
O2'H$_{32}$...O(13b)$_{37}$	0.98	2.245	133.2	Table 3[c]
N(6)H$_{38}$...O(2)$_{32}$	1.013	1.712	164.6	Table 3[c]
N(3)H$_{33}$...O3'p$_{36}$	1.013	1.665	154.6	Table 3[c]

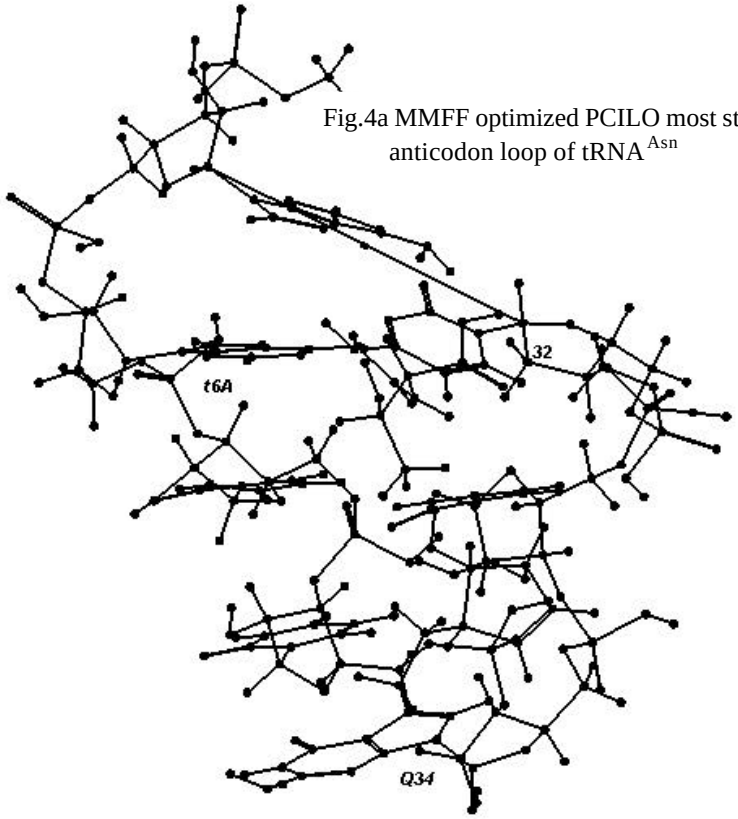

Fig.4a MMFF optimized PCILO most stable conformation for anticodon loop of tRNA^{Asn}

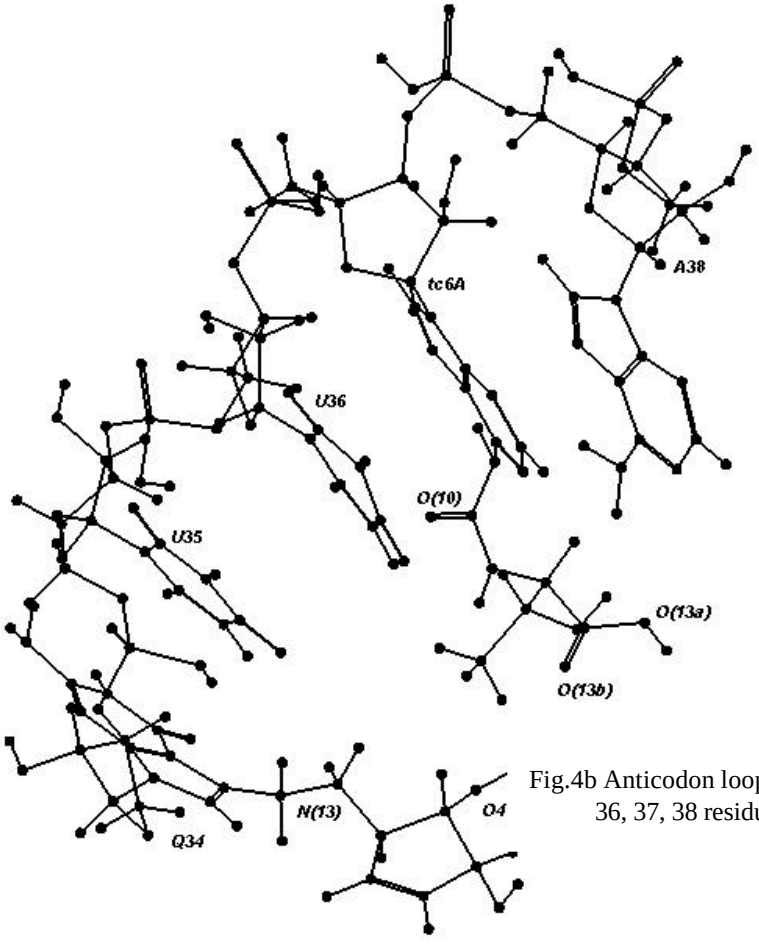

Fig.4b Anticodon loop of tRNA^{Asn} with 34, 35, 36, 37, 38 residues.

The MMFF optimized PCILO most stable conformation (Table3(c), fig.4[a,b]) retains distal conformation for the N(6) substituent in tc^6Ade. However, orientation of the C(7)-substituent in Q_{34} takes it away from the six membered ring. The interresidue hydrogen bondings, $N(11)H_{37}...O1'_{33}$, $N^+H2_{(34)}...O2'_{33}$ and $N(6)H_{38}...O(2)_{32}$ are retained with improved geometrical parameters (Table 4). The interresidue interaction between $C(15)H_{37}...O''_{34}$ is noticeable and occurs without disrupting base stacking or altering anticodon loop conformation. The hydrogen bonding parameters are given in Table 4.

B] Monte Carlo conformational search :

i) $tRNA^{Lys}$:

The torsion angle values and relative energy differences for the selected conformers from Monte Carlo conformational search are included in Table(5a). The lower energy conformation (Table 5a[I], Fig.5[a,b]) shows proximal orientation for N(6)-substituent in ms^2tc^6Ade. The 37^{th} base has come out of stacking to interact with the 34^{th} modified base (fig.3). The 34^{th}, 35^{th} and 36^{th} bases are partially stacked; but 36^{th} nucleotide prefers syn conformation (the glycosydic angle for 36^{th} is -146.7°) for hydrogen bonding interaction with N(7) site of the 37^{th} adenine. Strong interresidue hydrogen bonding $O(13a)H_{37}...O(2)_{34}$ is indicated in this conformation. Usual U-turning is realized through interresidue interaction $N(3)H_{33}...O5'P_{36}$. The 37^{th} modified base participates in hydrogen bonding interaction with 33^{rd}, 34^{th}, 36^{th} and 38^{th} residues. The geometrical parameters for hydrogen bonding are given in Table (5b). The O(8b) of C(5)-substituent in $mcm^5s^2U_{34}$ is placed above the plane of uridine base and interacts with the hydroxyl group of 33^{rd} ribose. The interresidue hydrogen bonding $N(3)H_{33}...O5'p_{36}$ is present for usual U-turning in the anticodon loop. The interesting feature of this conformation is that, modified bases at 34^{th} and 37^{th} locations participate in hydrogen bonding interactions without disturbing the entire anticodon loop conformation; only stacking of the 37^{th} base is affected. With its extended orientation of N(6)-substituent $ms^2tc^6Ade_{37}$ reaches to 34^{th} residue ($O(2)_{34}$ site) for hydrogen bonding interactions.

The alternative stable conformation obtained (fig.6[a,b] ,Table 5a[II]) is 3.8kcal/mol higher than the previously described structure (fig.5). The orientation of N(6)-substituent in ms^2tc^6Ade of this alternative structure resembles with

crystallographic as well as the preferred

Fig.5a Lowest energy conformation obtained through Monte Carlo conformational search for $tRNA^{Lys}$

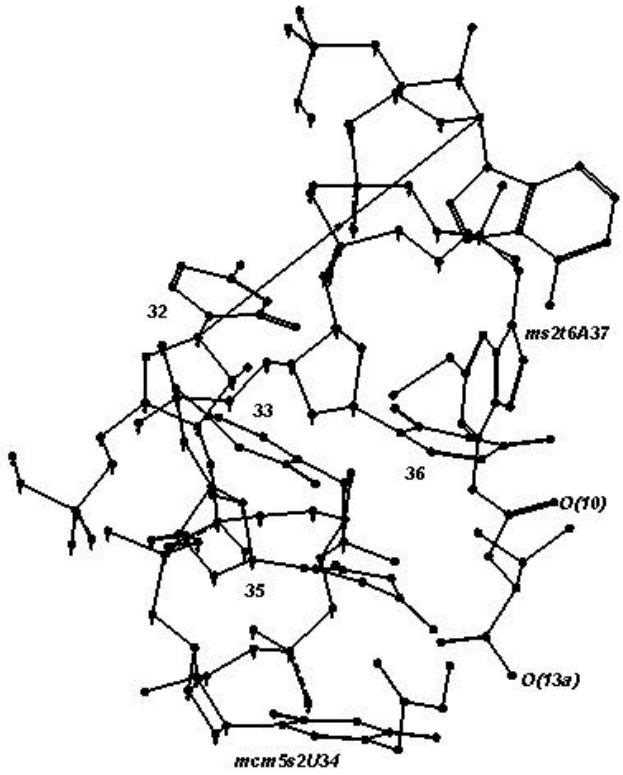

Fig.5b Anticodon loop of $tRNA^{Lys}$ with 34, 35, 36, 37 residues

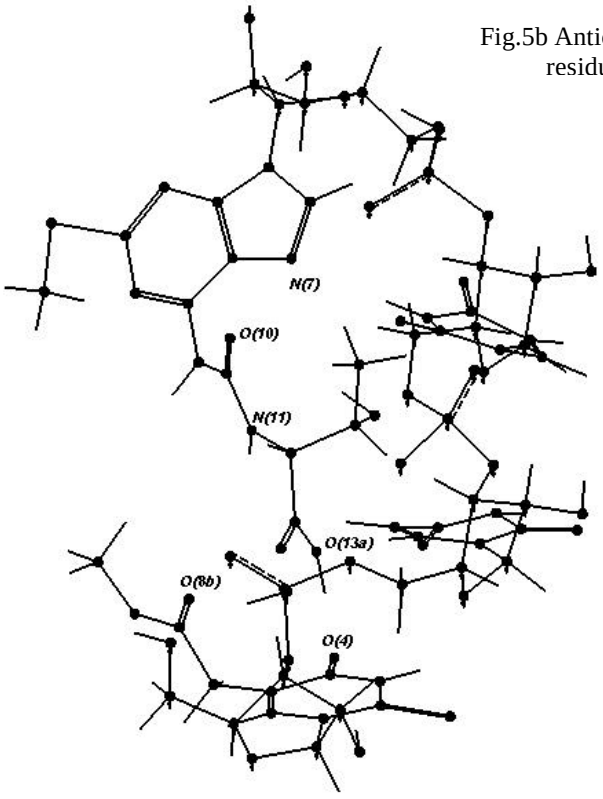

Table 5a: Structures obtained through Monte Carlo conformational search for $tRNA^{Lys}$

	α_t	β_t	γ_t	δ_t	ε_t	θ_t	ξ_t	η_t	ϕ_t	χ_t	ψ_t	α_u	β_u	γ_u	δ_u	Rel. Energy
I]	142.6	157.7	-172.9	-165.5	164.2	168.7	35.2	-52.4	-158.5	-139.2	167.4	77.6	167.1	177.1	171.9	0
II]	0.1	9.1	163.2	-107.7	-22.4	175.1	59.5	47.8	-179.7	-178.6	173.8	75.1	-172.8	168.3	-141.1	3.8

Table 5b: Geometrical parameters for H-bonding

Atoms Involved (1-2-3)	Atom pair (1-2) A	Atom pair (2-3) A	Angle (1-2-3)	Reference
$O2'H_{33}...O(8b)_{34}$	0.980	1.703	173.2	Table 5a[I]
$O(13a)H_{37}...O(2)_{34}$	0.97	1.610	168.9	Table 5a[I]
$N(11)H_{37}...O2'_{33}$	1.011	1.870	144.8	Table 5a[I]
$N(6)H_{37}...O2'_{33}$	1.011	2.040	127.9	Table 5a[I]
$N(3)H_{36}...N(7)_{37}$	1.013	2.260	174.0	Table 5a[I]
$N(3)H_{33}...O5'p_{36}$	1.090	1.650	134.6	Table 5a[I]
$N(6)H_{38}...S(2)_{37}$	1.090	2.400	159.8	Table 5a[I]
$O2'H_{33}...O(8b)_{34}$	0.980	1.820	155.7	Table 5a[II]
$O(13a)H_{37}...O(4)_{35}$	0.97	1.920	155.7	Table 5a[II]
$C(10)H_{34}...O(13b)_{37}$	1.098	2.390	158.8	Table 5a[II]
$C(5)H_{36}...O(13b)_{37}$	1.098	2.320	128.1	Table 5a[II]
$N(11)H_{37}...N(1)_{37}$	1.013	1.910	131.0	Table 5a[II]
$N(1)_{37...}N(11)H_{37...}O(13a)H_{37}$	1.910	2.380	127.9	Table 5a[II]
O(14)H37...O(13a)37	0.97	2.590	127.2	Table 5a[II]
$N(6)H_{37}...O(2)_{32}$	1.011	1.770	166.8	Table 5a[II]
$O2'H_{37}...O(10)_{37}$	0.980	1.690	163.6	Table 5a[II]
$O2'H_{37}...O1'_{38}$	0.980	1.920	146.3	Table 5a[II]

theoretical results [13,14]. The bifurcated intramolecular hydrogen bonding $N(1)_{37}...N(11)H_{37}...O(13a)_{37}$ stabilizes the distal orientation of the N(6)-substituent. This well stacked anticodon loop also shows interaction between 34^{th} and 37^{th} modified bases ($C(10)H_{34}...O(13b)_{37}$). The C(5)-substituent in $mcm^5s^2U_{34}$ interacts with 33^{rd} and 37^{th}

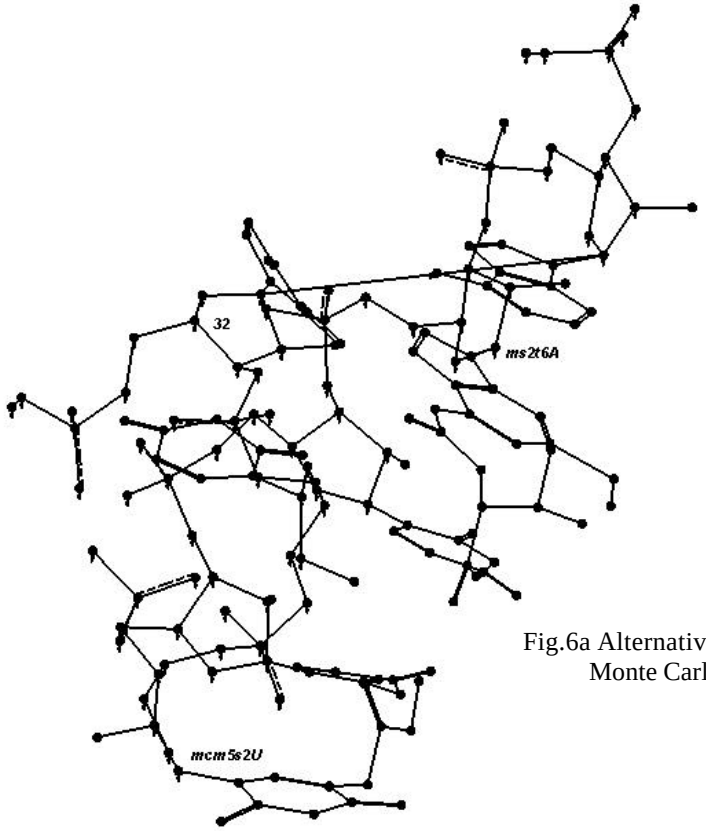

Fig.6a Alternative structure obtained through Monte Carlo conformational search for $tRNA^{Lys}$

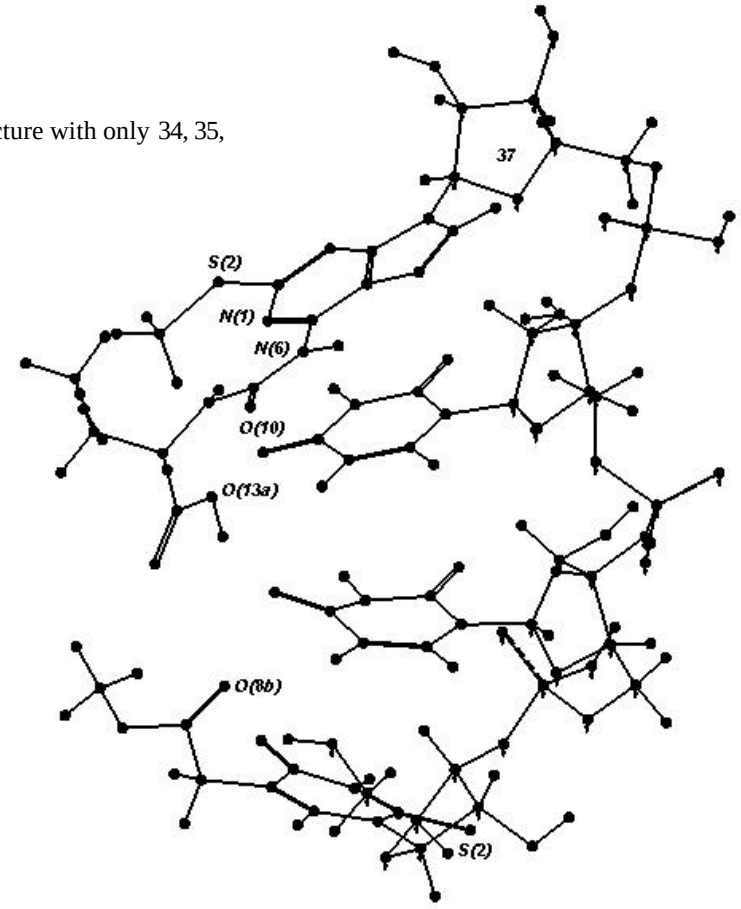

Fig.6b Alternative structure with only 34, 35, 36, 37 residues

nucleosides. The interaction between 34^{th} and 37^{th} residues occurs without disturbing base stacking or anticodon loop conformation. These none too strong interactions may not persist for long time in molecular dynamics simulations. However, this type of conformational search shows possible arrangements of modified bases for their interactions in the anticodon loop. The hydrogen bonding parameters are included in Table 5b.

ii) $tRNA^{Asn}$:

The conformation obtained through Monte Carlo conformational search is depicted in Fig.7[a,b] (Table 6a[I]). The anticodon loop bases are well stacked; however, discontinuity of base stacking is seen between 37^{th} and 38^{th} residues. Interesting feature of this conformation is that, N(6)-substituent is oriented proximal and interacts with adenine ring through intramolecular hydrogen bonding of $O(14)H_{37}...N(7)_{37}$ (see Table 6b). The N(6) substituent in tc^6Ade_{37} interacts with various H-bond donor-acceptor sites in nucleosides 32^{nd}, 34^{th} and 38^{th} for interresidue hydroden bonding. The proximal orientation of N(6)-substituent may also play a role in codon - anticodon interactions as discussed in chapter (IV).

Table 6a: Torsion angles and relative energy of selected conformations of $tRNA^{Asn}$ (tc^6Ade_{37} and Q_{34}) from Monte Carlo comformational search.

	α_t	β_t	γ_t	δ_t	ε_t	θ_t	ξ_t	η_t	ϕ_t	α_q	β_q	γ_q	δ_q	ε_q	Rel. Energy
I]	139.0	64.8	-178.9	-69.0	-13.3	-8.7	-32.7	14.0	-176.0	92.3	-174.1	77.5	46.5	-161.4	0
II]	4.5	-1.2	-162.0	87.1	-111.1	8.3	73.9	-72.9	178.0	94.1	-175.0	71.8	55.3	-53.0	62.0

The C(7)-substituent in queuosine has preferred trans (spreads away from the six membered ring) conformation and participates in interresidue hydrogen bondings like $N^+H2_{34}...O(4)_{35}$, $N^+H2_{34}...O2'_{33}$ and $O4''H_{34}...O(4)_{36}$. Also, strong (based on geometrical

parameters) interaction $O5''H_{34}...O(10)_{37}$ (see table 6b) is present between both hypermodified bases. The conformation of queuosine however does not influence accessibility of sites for codon - anticodon base pairing. The observed hydrogen bonding ,$N^{+}H2_{34}...O(10)_{34}$ in queuosine crystal [15] is not found in the anticodon loop.

Table 6b: Geometrical parameters for H-bonding

Atoms Involved (1-2-3)	Atom pair (1-2) A	Atom pair (2-3) A	Angle (1-2-3)	Reference
$HN^{+}H_{34}...O(4)_{35}$	1.011	1.669	157.3	Table 6a[I]
$HN^{+}H_{34}...O2'_{33}$	1.013	1.821	161.0	Table 6a[I]
O4''H34...O(4)36	0.980	2.292	120.2	Table 6a[I]
O5''H34...O(10)37	0.980	1.663	153.1	Table 6a[I]
$N(14)H_{37}...N(7)_{37}$	1.013	1.744	155.2	Table 6a[I]
$O(13a)H_{37}...N(7)_{38}$	0.980	2.003	136.7	Table 6a[I]
O2'H32...O(13b)37	0.970	1.823	149.4	Table 6a[I]
$N(3)H_{33}...O5'p_{36}$	1.013	1.778	135.9	Table 6a[I]
$N(6)H_{38}...O(13a)_{37}$	1.012	1.809	146.9	Table 6a[I]
$HN^{+}H_{34}...O(4)_{35}$	1.012	1.633	157.6	Table 6a[II]
$HN^{+}H_{34}...O2'_{33}$	1.013	1.792	160.1	Table 6a[II]
O4''H34...O(4)36	0.980	1.941	135.5	Table 6a[II]
O5''H34... O(4)36	0.970	1.728	150.8	Table 6a[II]
C(15)H37...O5''34	1.097	2.583	125.6	Table 6a[II]
N(11)H37...N(1)37	1.013	1.832	137.0	Table 6a[II]
O(14)H37...O(10)37	0.970	1.633	143.7	Table 6a[II]
O2'H32...O(10)37	0.970	2.414	137.8	Table 6a[II]
O(13a)H37...O(14)37	0.980	1.693	145.8	Table 6a[II]
N(3)H33...O5'p36	1.012	1.744	144.5	Table 6a[II]
O2'H32...O(2)32	0.970	1.782	137.8	Table 6a[II]

The second conformation from Table 6a[II] (fig.8[a,b]) is 62 kcal/mol higher than the first conformation. The anticodon loop has expected base stacking and distal orientation is preferred for base substituent in tc^{6}Ade. The intramolecular interaction $N(1)_{37}...N(11)H_{37}$ stabilizes the distal conformation. The queuosine substituent orientation is similar to that of the previously discussed conformation. However, weak

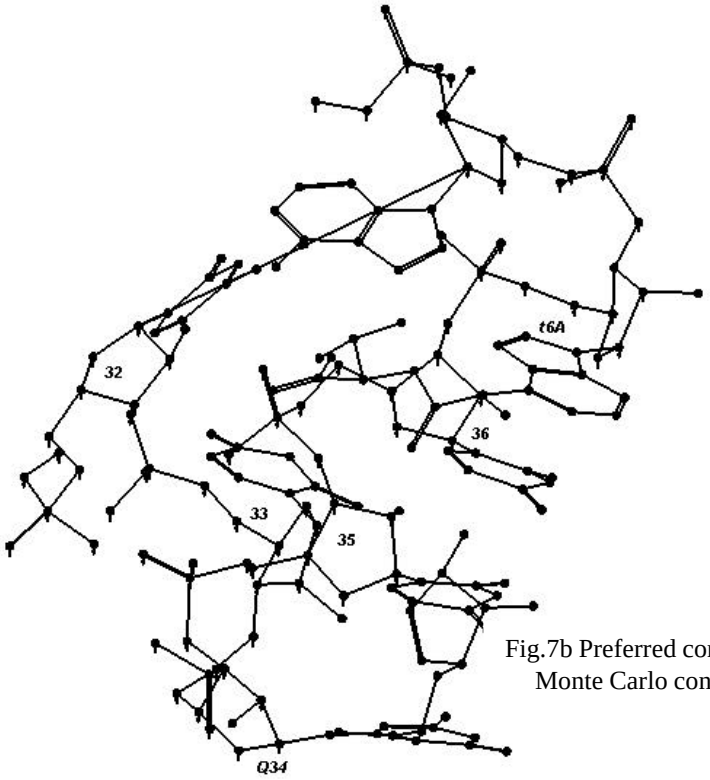

Fig.7b Preferred conformation obtained through Monte Carlo conformational search for $tRNA^{Asn}$

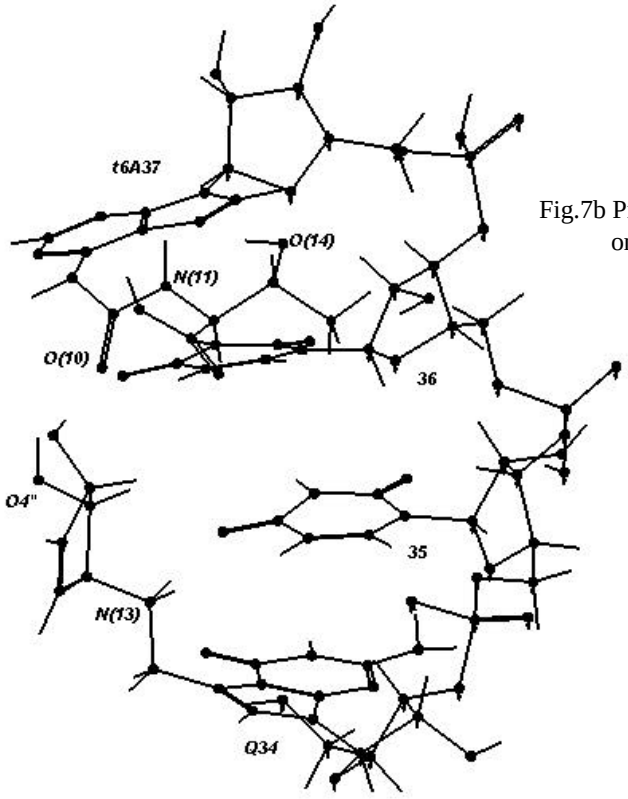

Fig.7b Preferred conformation with only 34, 35, 36, 37 residues

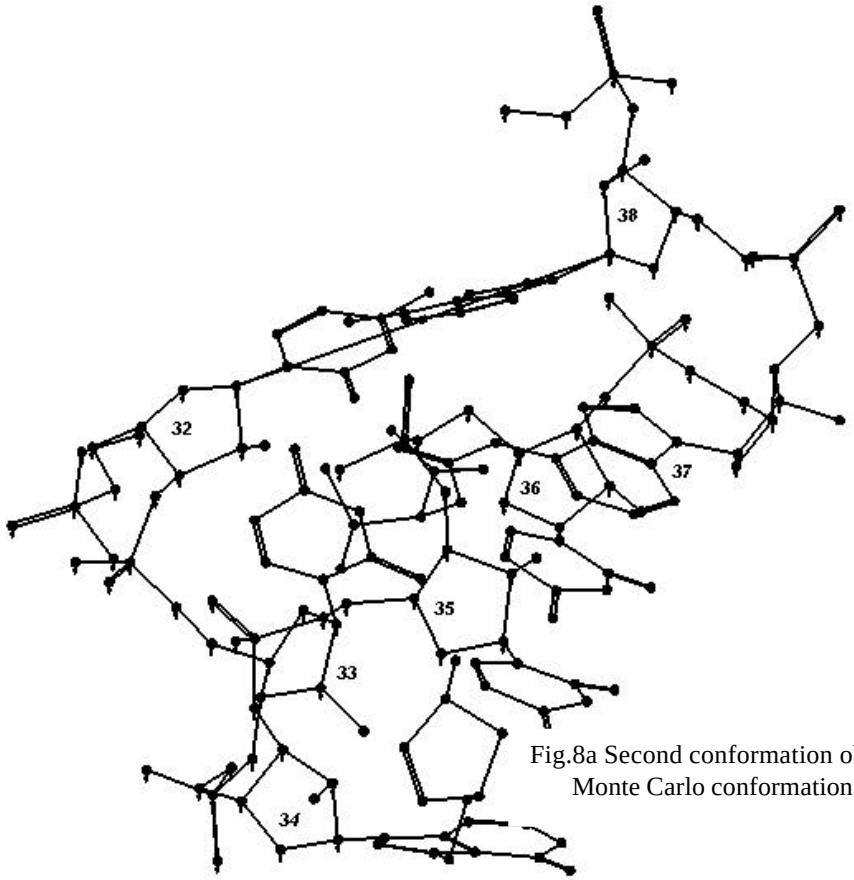

Fig.8a Second conformation obtained through Monte Carlo conformation search for tRNA ^{Asn}

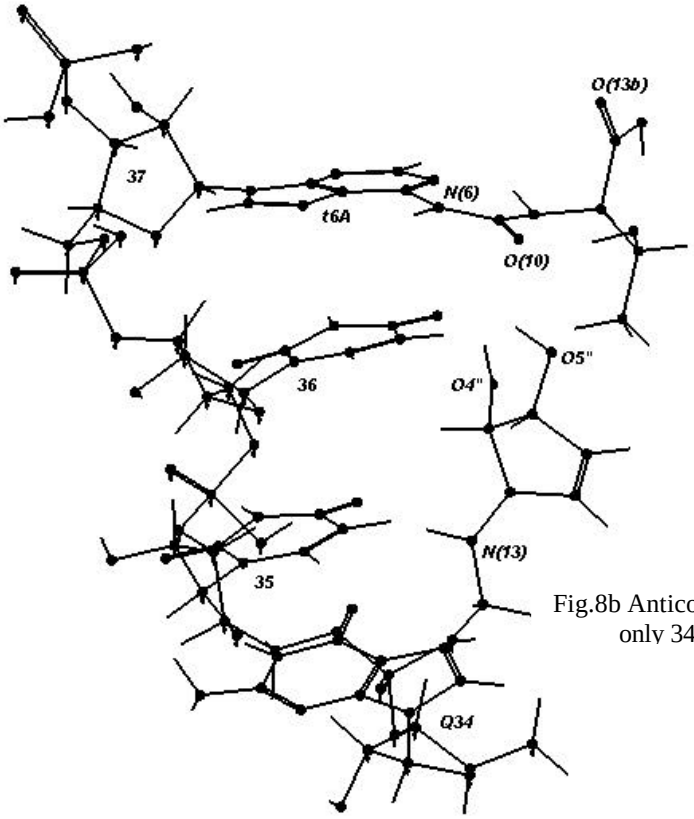

Fig.8b Anticodon loop of tRNA ^{Asn} with only 34, 35, 36, 37 residues

$C(15)H_{37}...O5''_{34}$, is present between two hypermodified bases at 34^{th} and 37^{th} sites. The geometrical parameters for hydrogen bonding are included in Table 6b.

Scarce experimental data on these systems restricts direct comparison, Nevertheless plausible intramolecular interactions are brought out by the present investigations which may have structural - functional significance for tRNA.

C] Molecular Dynamics Simulation :

The Molecular Dynamics (MD) method, is used to explore time dependent behaviour of anticodon loop conformations. The first anticodon stem loop (ASL) studied is human $tRNA^{Lys}$ with the presence of extensive modifications $ms^2tc^6Ade_{37}$ and $mcm^5s^2U_{34}$ in the anticodon loop.

i) $tRNA^{Lys}$:

Figure 9 represents a) starting structure at 0ps and b) snap shot at 66ps. Another, average picture is presented in fig.10. The anticodon loop has proper base stacking as 35^{th}, 36^{th} and 37^{th} bases are stacked over the 34^{th} base. Also, 32^{nd} base stacks over 34^{th} base. But, 33^{rd} base is inclined to the plane of 34^{th} base. The A-helix character is maintained, showing anti conformation of nucleosides and C3'-endo character for all riboses except 33^{rd}, which prefers C2'-endo puckering. The helix shows slight bend or appears to condense, over the length of the MD simulation run.

The all heavy atom root mean square (RMS) deviation from the starting crystal structure is shown in Fig.11a. The 125ps to 175ps region shows lower rms (around 5A°) as compared to other time zones. The trajectory shows stabilization of system away from the reference crystallographic structure. However, equilibration of system is evident, as internal temperature of solute closely matches with internal or local temperature of solvent. This criteria of equilibration is discussed in sybyl force field manual [16]. Fig.11b shows local temperature plot for solute and solvent with time. The system seems to be well equilibrated for time span of 125ps to 155ps and rms is as well lower in this part. The improvement in the quality of MD trajectory can be achieved through improved treatment for long-range interactions [17].

The N(6) substituent orientation in ms^2tc^6Ade is distal ($\alpha_t = 0°$) as shown in

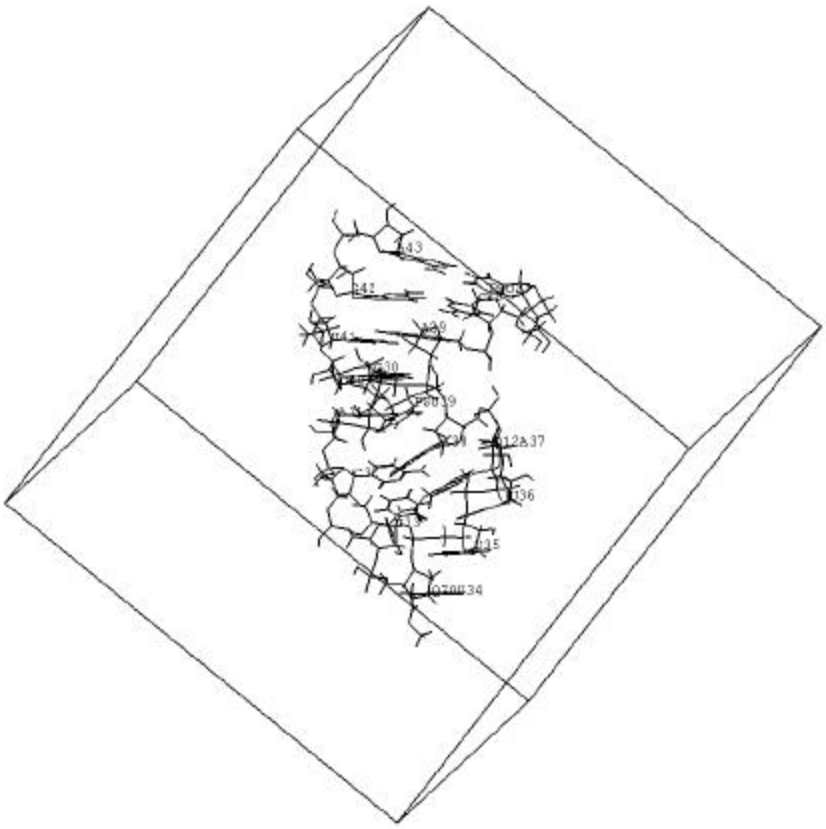

Fig.9a Human tRNA ^{lys} at 0ps

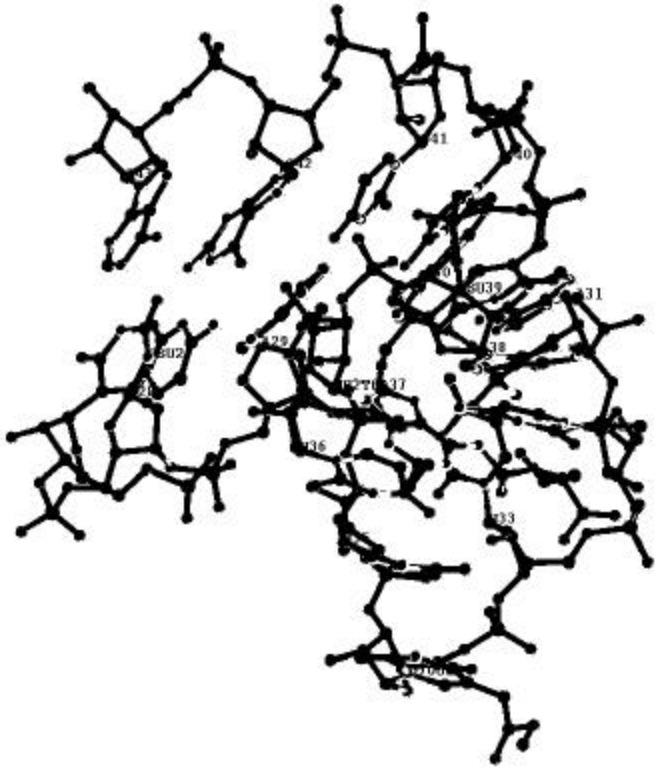

Fig. 9b snapshot at 66ps

Fig.10a Anticodon loop of human $tRNA^{Lys}$ (average structure between 155 to 175ps)

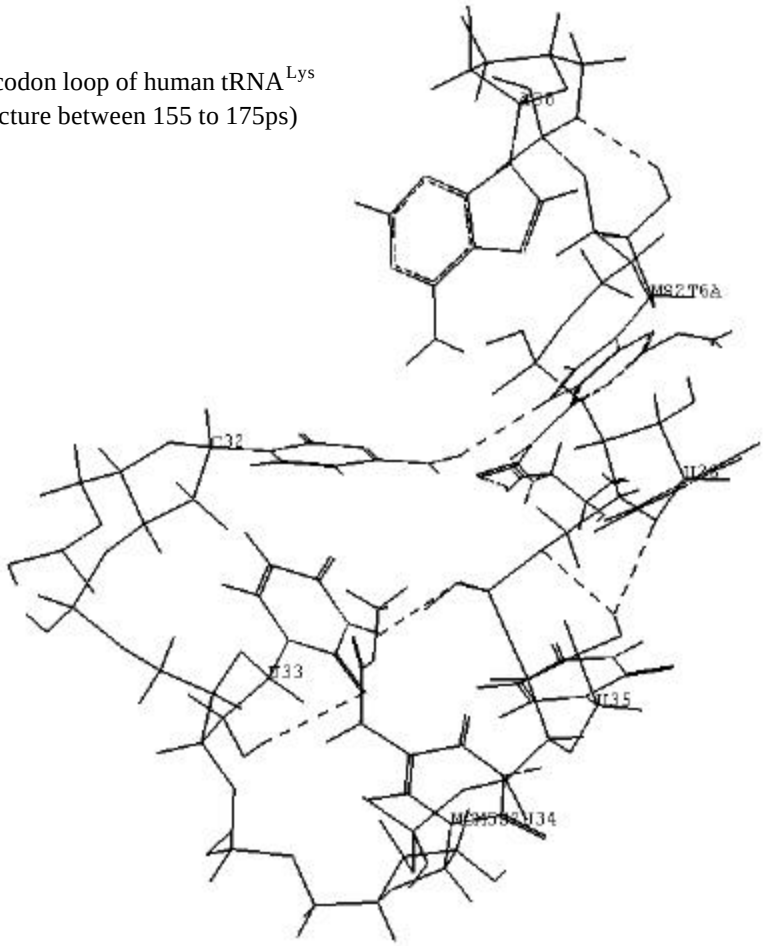

Fig.10b 34^{th} and 37^{th} residues of $tRNA^{Lys}$

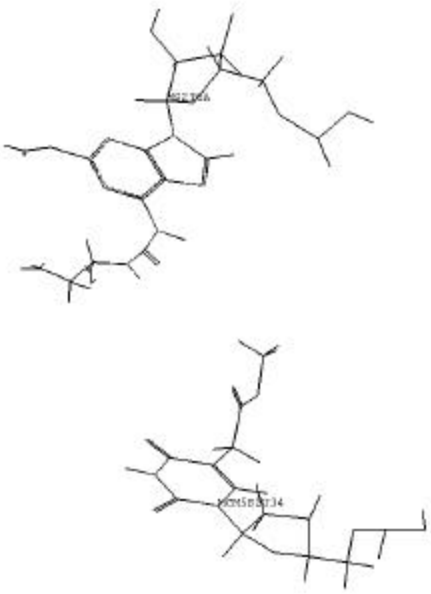

Fig.10c Average Structure between 155 to 175ps

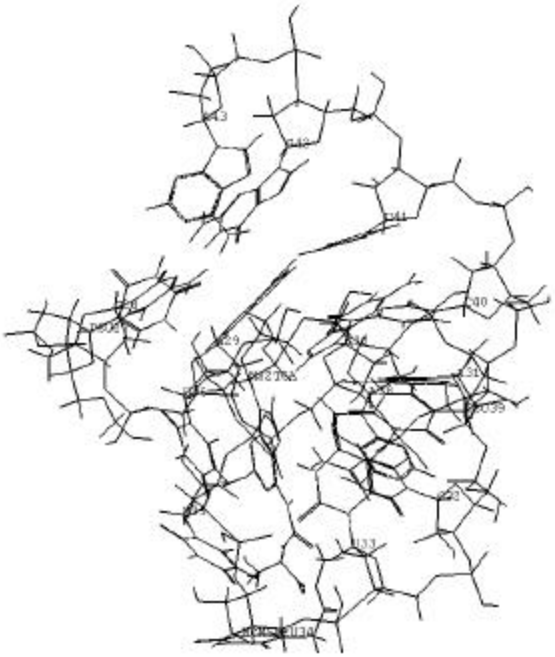

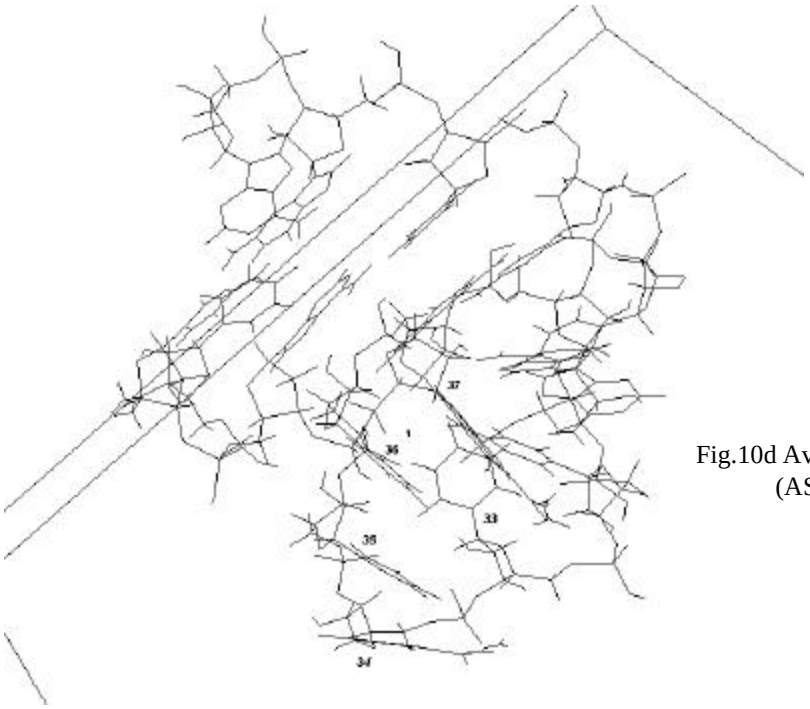

Fig.10d Average picture of hyman $tRNA^{Lys}$ (ASL) between 50ps to 250ps

fig.12. The other time dependent plots of torsion angles β_t, γ_t, δ_t, ε_t, θ_t, ξ_t, η_t are shown in fig.12. The time behavior of all torsion angles indicates mainly three features a) transitions to +g(60°), -g(-60°) and t(180°) domains. b) slow variation to near domain and c)high amplitude of fluctuations. Only torsion angle α_t, and ξ_t show low amplitude of fluctuation as compared to others. The torsion angles β_t, θ_t, ξ_t prefer two regions of torsion angle values through transitions (see fig.12). The metylthio group orientation is also highly changeable and dynamic.

The C(5)-substituent of $mcm^5s^2U_{34}$ also has changeable - dynamic orientation (fig.12). The α_u torsion angle exhibits high amplitude of fluctuation and transition to alternative orientation as well. The two zones of torsion angle α_u [-100, 100] clearly keep C(5)-substituent positioned below or above the plane of uridine base.

In the time course of MD simulation, N(6) substituent of ms^2tc^6Ade does not uniformly maintain interresidue hydrogen bonding with C(5)-substituent of $mcm^5s^2U_{34}$. However, Watson- Crick edge of 32^{nd} base participates in hydrogen bonding with Hoogsteen edge of 37^{th} adenine. The U-turn featured hydrogen bonding N $(3)H_{33}...O2P_{36}$ persists after 130ps; but may be weakened due to competing interaction of N $(3)H_{33}$ site with phosphate group of 30^{th} nucleotide. The intraresidue hydrogen bonding $O(13a)H_{37}...O(10)_{37}$ is maintained just for 30ps (see fig.13).

Fig. 11a

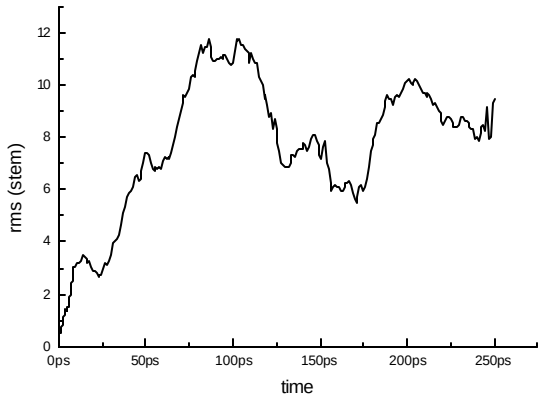

Fig. 11b

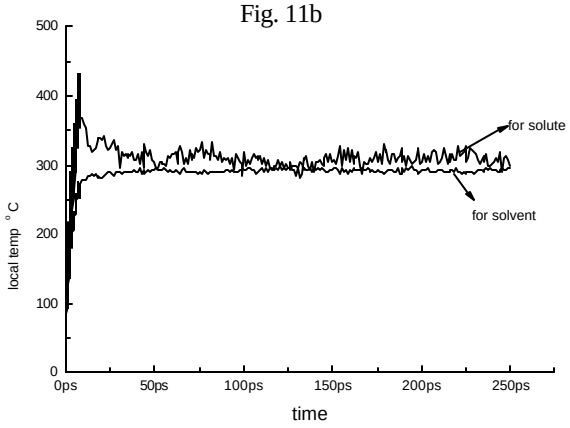

Fig. 12

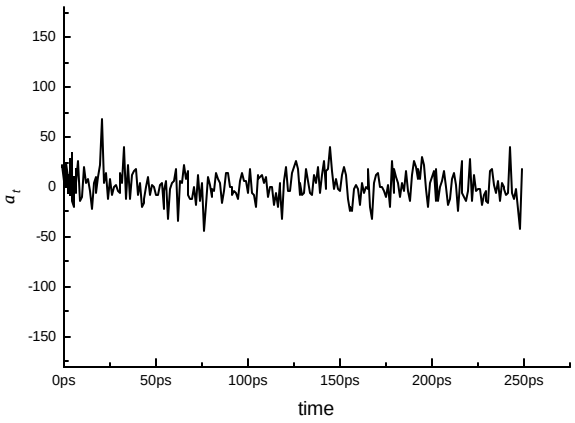

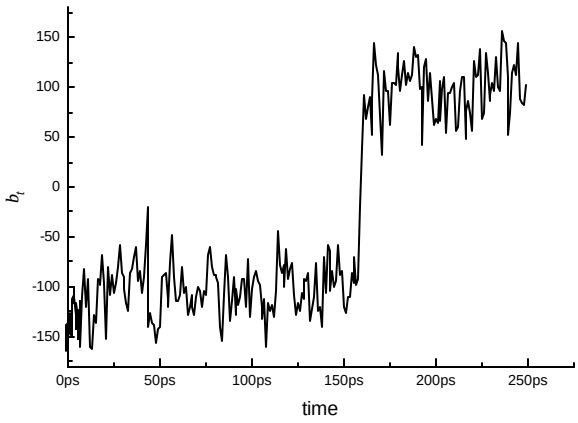

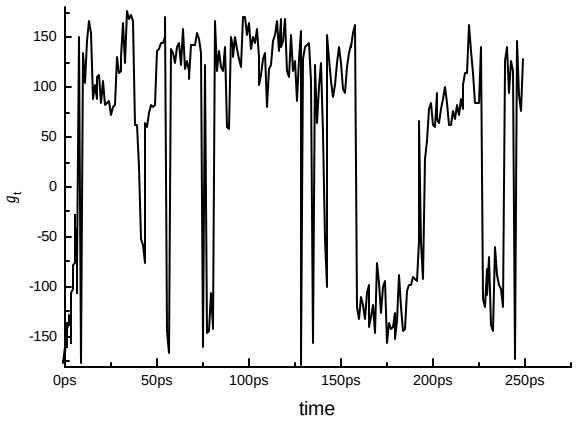

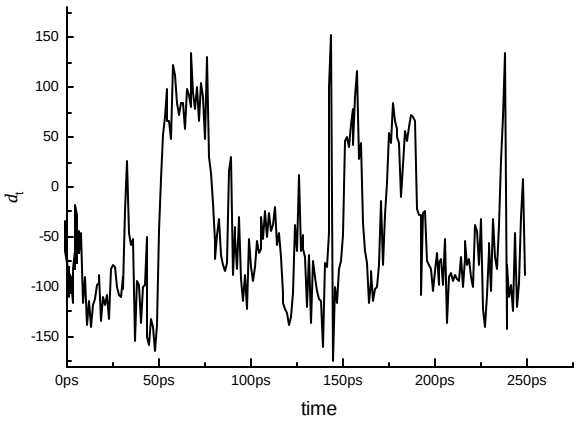

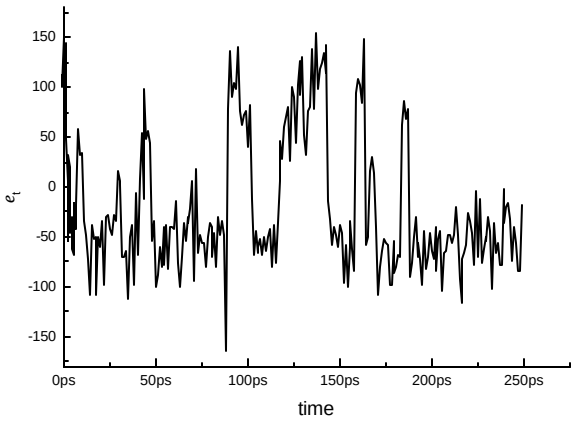

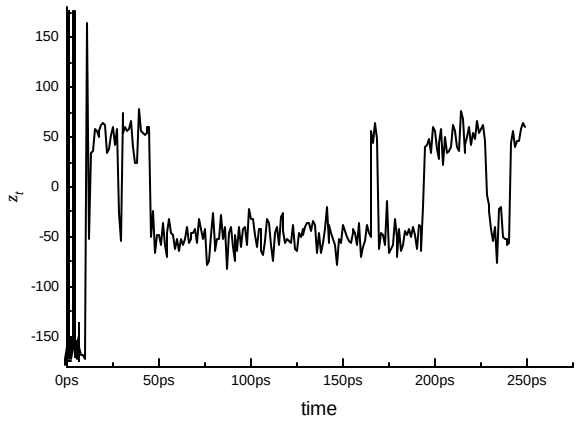

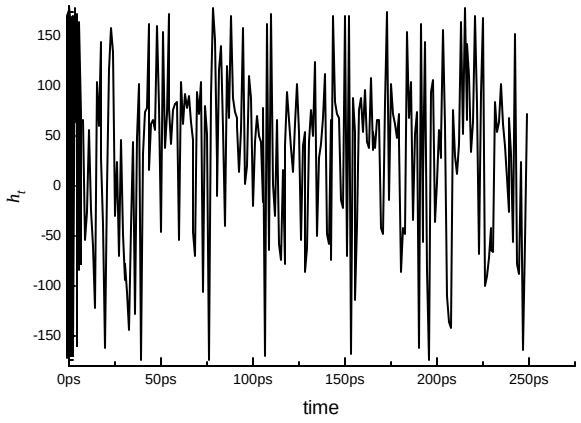

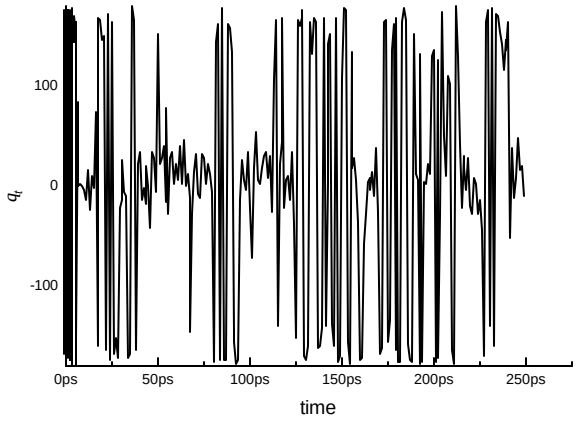

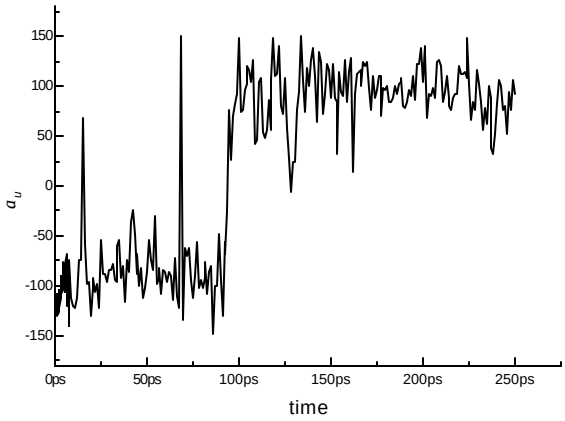

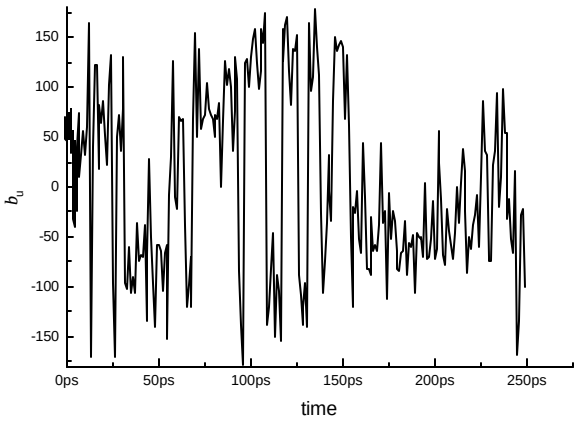

Fig. 12

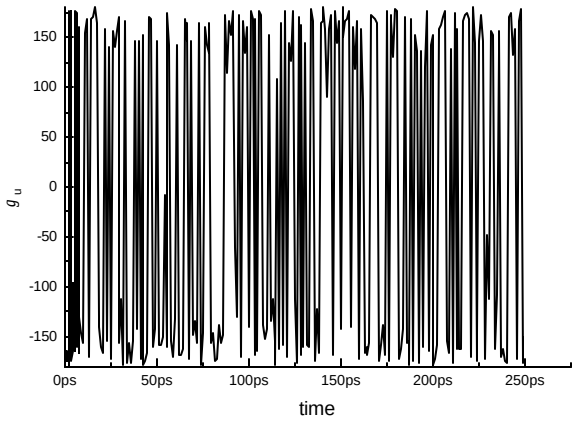

Fig. 13

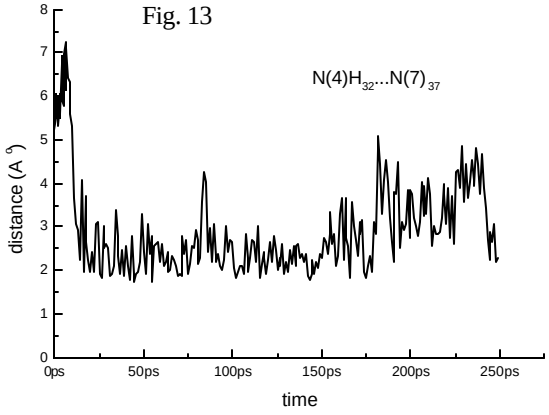

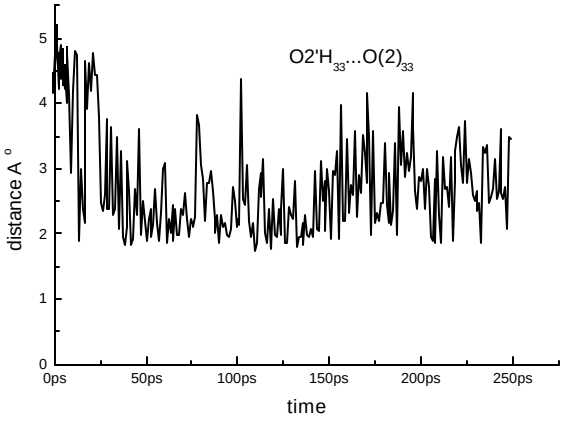

Fig. 13

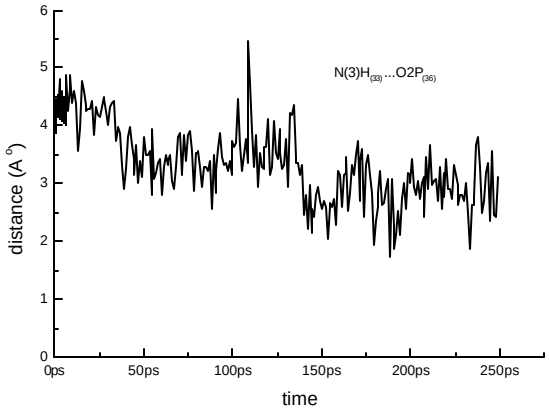

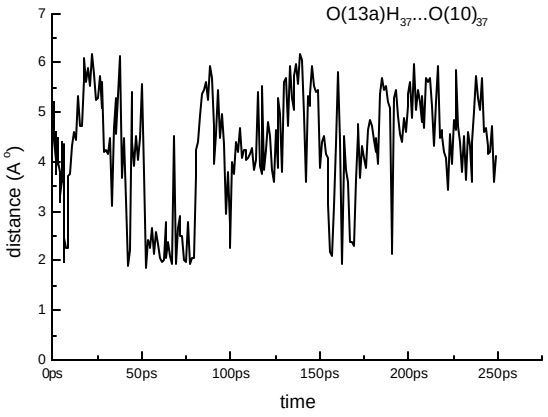

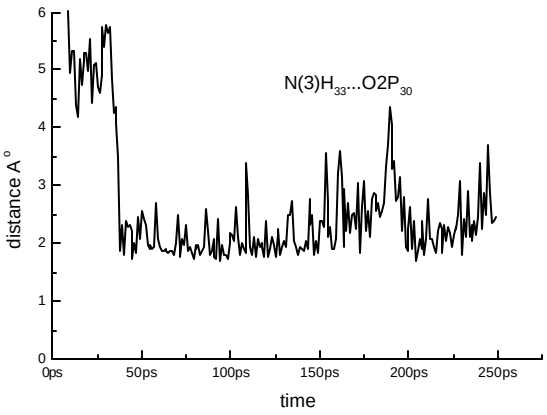

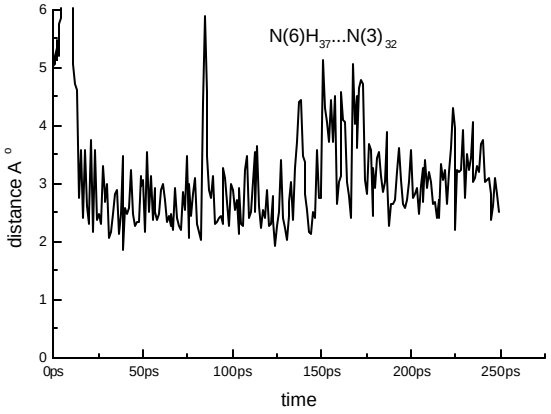

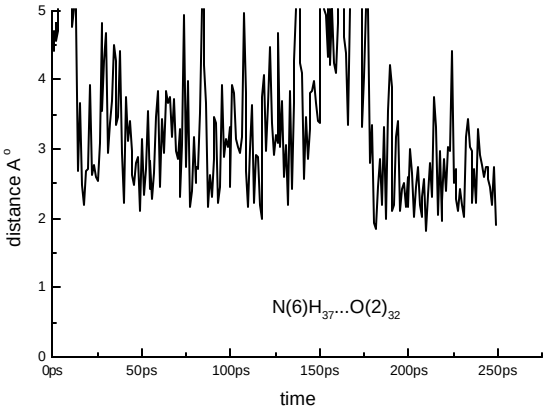

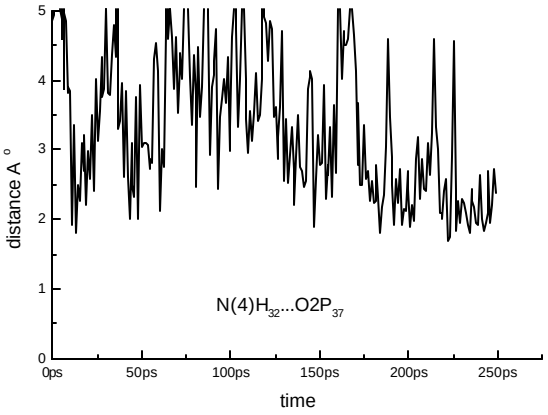

These results are helpful in explaining the general conclusions about the presence of U-turn feature, A-RNA character and orientation of modified bases.

ii) $tRNA^{Asn}$:

The all heavy atom root mean square (rms) deviation is given in fig.14[a,b], along with local temperature graph for solute and solvent. The rms is stable around 4.5 to 5A° for nearly 30 to 70ps time span and thereafter increases progressively. Fig.14b clearly shows equilibration of system in the time zone of 30ps to 70ps. For the equilibrated system, rms is found to be stable.

The molecule overall shows A-type helix character for anticodon stem loop, since C3'-endo puckering and glycosyl anti conformation of nucleotides are preferred. U turn feature for the anticodon loop is disrupted by different stacking arrangement. (see fig.16 and Fig.19). The 32^{nd}, 33^{rd} bases are stacked on 34^{th} phosphate group and partial stacking of 34^{th} , 35^{th} and 36th bases is found to be somewhat disturbed. However, after 75ps, 35^{th} base comes slowly out of stacking and stacking is noticed between 37^{th} ,36^{th} and 34^{th} bases. The 32^{nd} and 38^{th} bases are stacked with stem part. Helix bending is observed. The preference for different stacking arrangements of anticodon loop has provided occasional interresidue interaction between modified bases Q_{34} and tc^6Ade_{37}. However, distal ($\alpha_t = 0°$) arrangement of N(6) substituent in tc^6Ade has not been affected by interresidue interactions with 34^{th} modified nucleoside. Similarly, orientation of C(7)-substituent in Q_{34} is not much altered due to interaction with 37^{th} base (see fig.17)

The N(6) substituent orientation in tc^6Ade retains unique stable torsion angles α_t,and ξ_t values in the course of time variation. All other torsion angles prefer transitions, high amplitude of fluctuations and slow variation with respect to time. The C(7)-substituent in Q_{34} base exhibits highly dynamic orientation (see fig. 15). The intraresidue hydrogen bonding interaction $N^+H2_{34}...O(10)_{34}$ (observed in crystal structure) is well maintained up to 60ps and weakly maintained between 80ps to 95ps; occasionally it is disturbed. Interresidue hydrogen bonding interaction of diol group of Q_{34} with carbonyl group of ureido linkage from tc^6Ade is well maintained after 50ps (see fig.18). The Hoogsteen edge of 37^{th} adenine base participates in hydrogen bonding with Watson-Crick edge of 33^{rd} base. These other interactions besides interaction between 34^{th} and 37^{th} residue lead to an unusual anticodon loop conformation.

The unconventional structure for anticodon loop, anticipated for human $tRNA^{Lys}$ by Agris and co-workers [5] is not found in our MD results. The results of

Fig. 14a

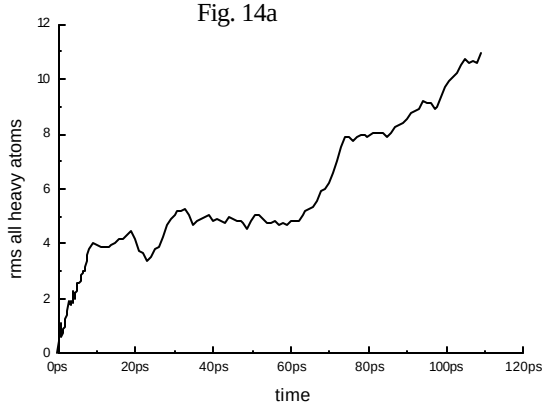

Fig. 14b

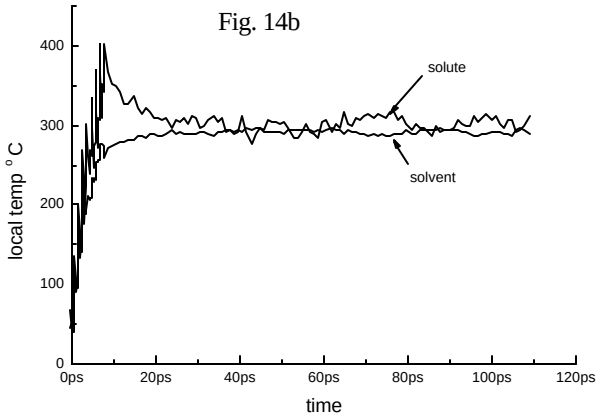

Fig. 15

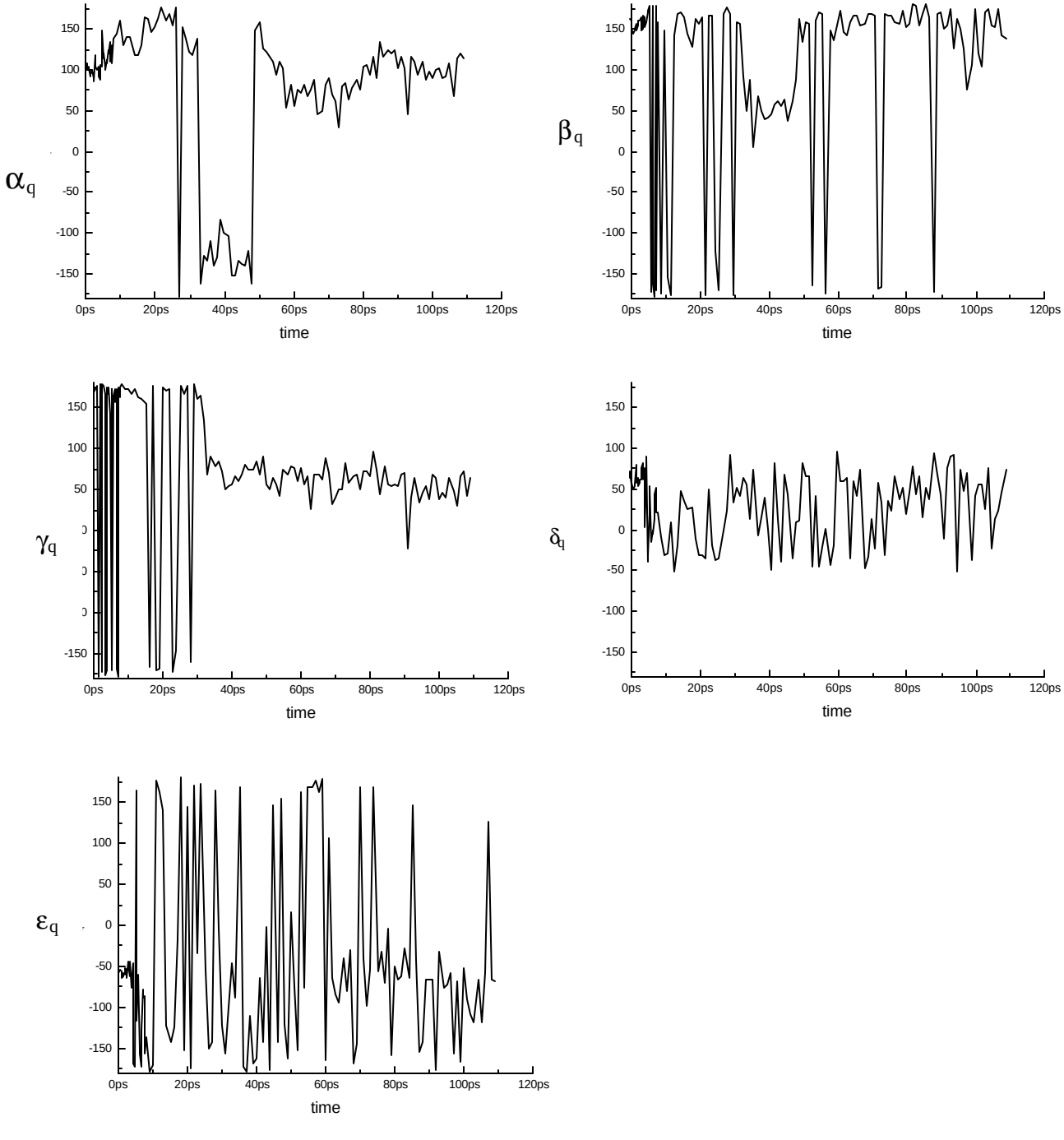

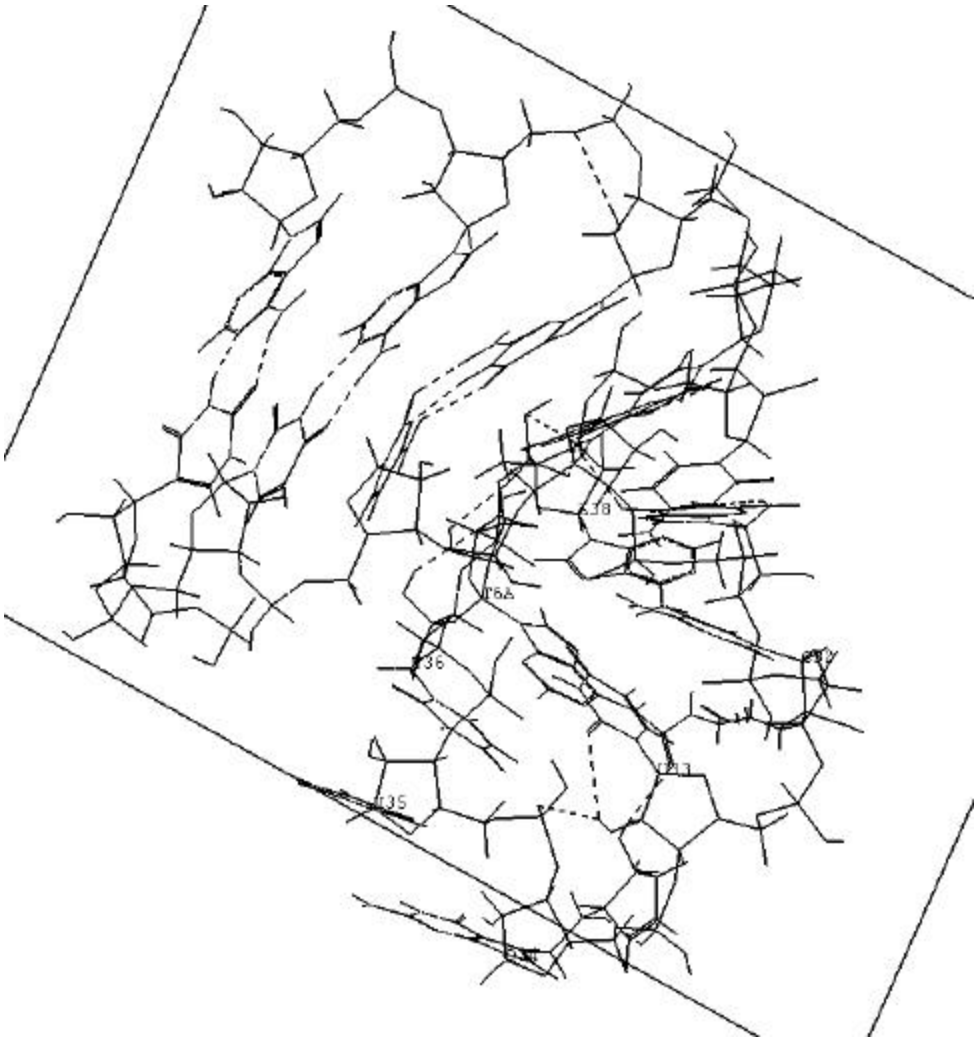

Fig.16a Average between 50 to 70ps for asperaginyl tRNA

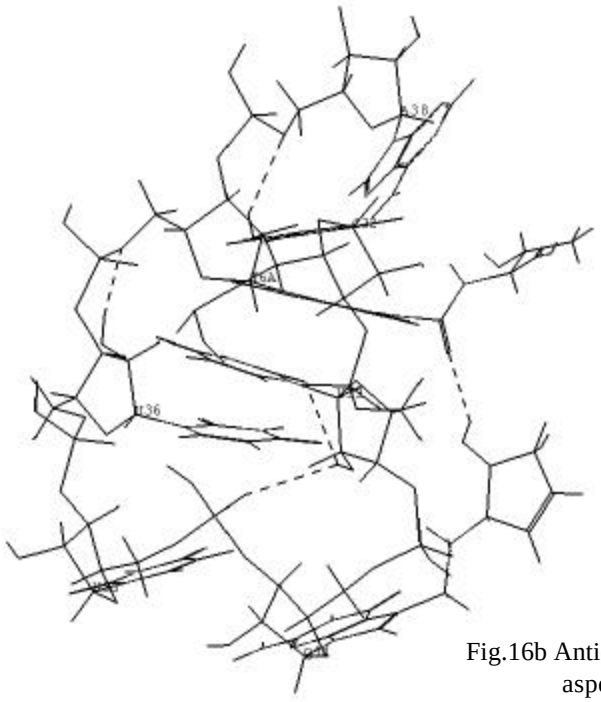

Fig.16b Anticodon in tRNA asperaginyl

Fig. 17

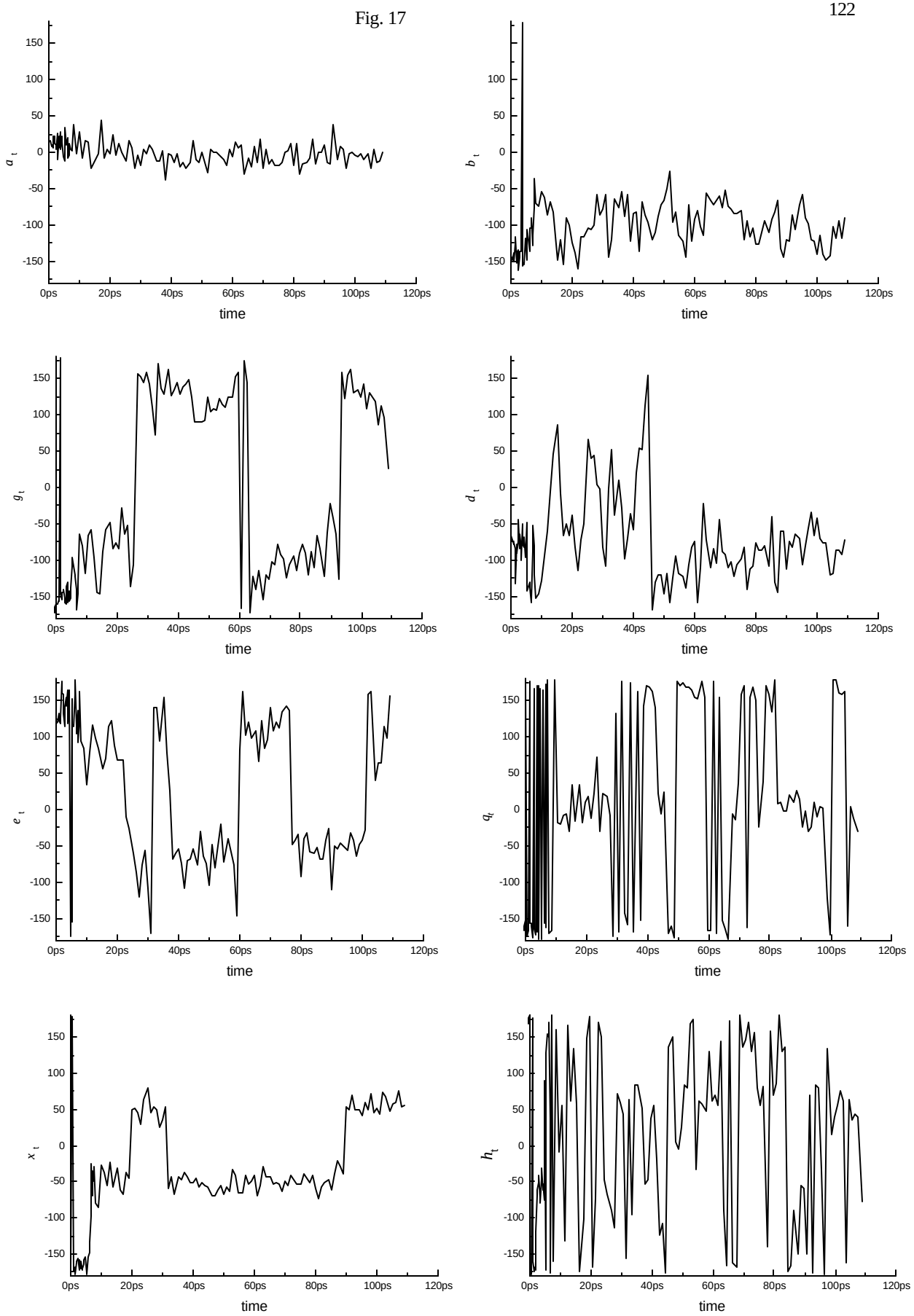
a_t
b_t
g_t
d_t
e_t
q_t
x_t
h_t
150
100
50
0
-50
-100
-150
0ps
20ps
40ps
60ps
80ps
100ps
120ps
time

Fig.18

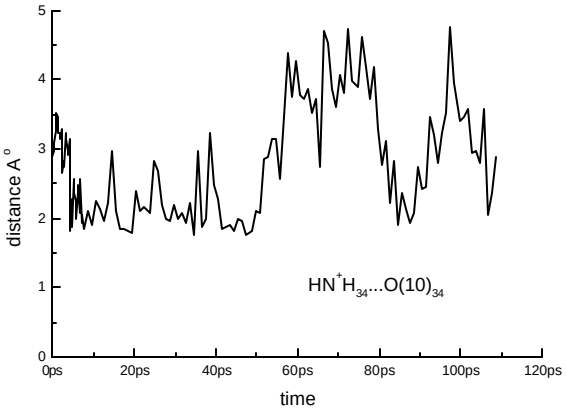
distance A°
HN+H34...O(10)34
time
0ps 20ps 40ps 60ps 80ps 100ps 120ps
0 1 2 3 4 5

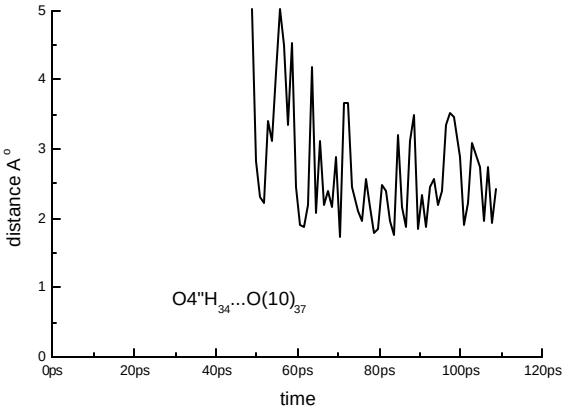
distance A°
O4"H34...O(10)37
time
0ps 20ps 40ps 60ps 80ps 100ps 120ps
0 1 2 3 4 5

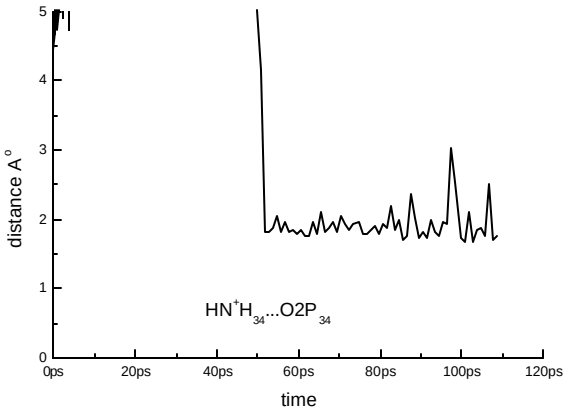
distance A°
HN+H34...O2P34
time
0ps 20ps 40ps 60ps 80ps 100ps 120ps
0 1 2 3 4 5

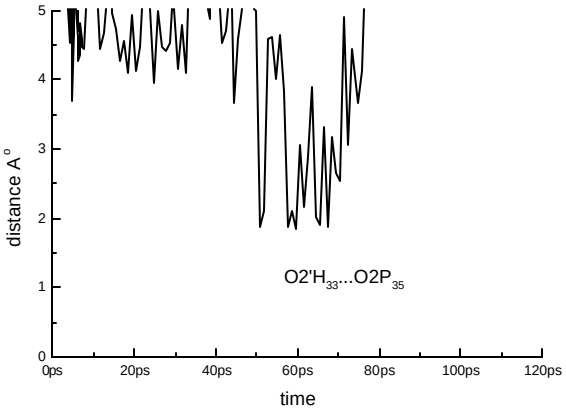
distance A°
O2'H33...O2P35
time
0ps 20ps 40ps 60ps 80ps 100ps 120ps
0 1 2 3 4 5

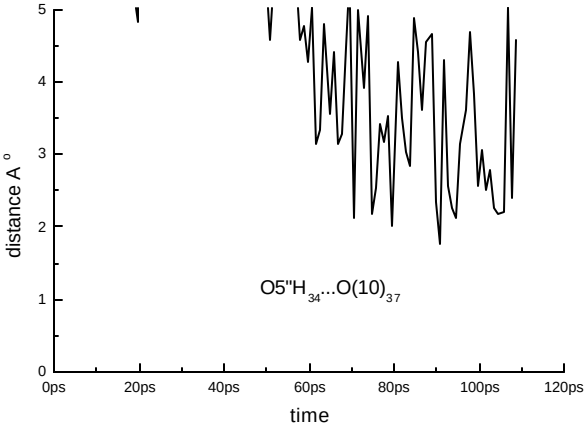
distance A°
O5"H34...O(10)37
time
0ps 20ps 40ps 60ps 80ps 100ps 120ps
0 1 2 3 4 5

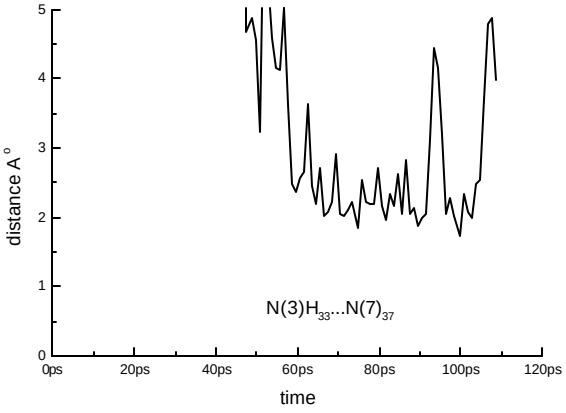
distance A°
N(3)H33...N(7)37
time
0ps 20ps 40ps 60ps 80ps 100ps 120ps
0 1 2 3 4 5

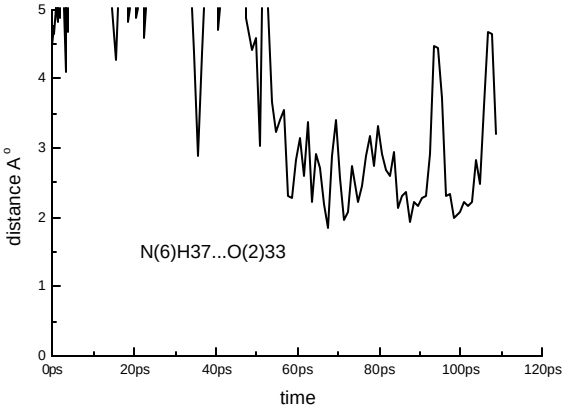
distance A°
N(6)H37...O(2)33
time
0ps 20ps 40ps 60ps 80ps 100ps 120ps
0 1 2 3 4 5

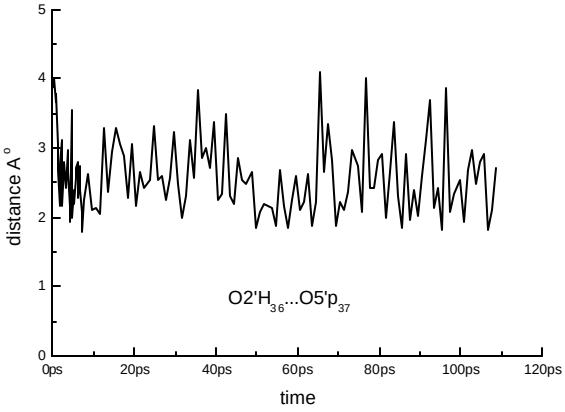
distance A°
O2'H36...O5'p37
time
0ps 20ps 40ps 60ps 80ps 100ps 120ps
0 1 2 3 4 5

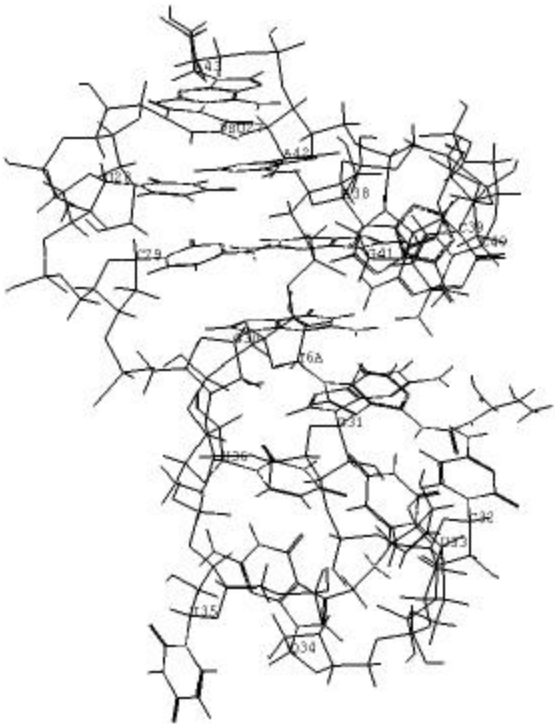

Fig.19 [a,b] Average for last 15ps

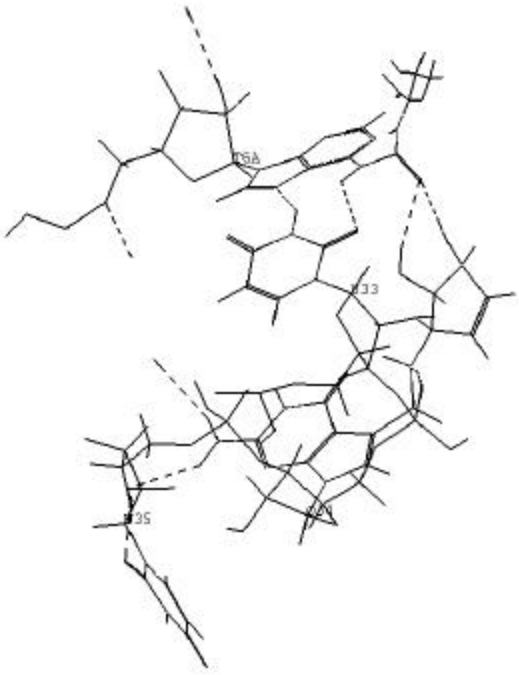

Fig.19b Interaction of Q_{34} and tc^6Ade_{37}

present study, however, agree with NMR study on E-coli tRNA lysine [7] with modification ($mnm^5s^2U_{34}$ and tc^6Ade_{37}) which shows an open conventional anticodon loop and also suggests similar results for human $tRNA^{Lys}$ with ($mcm^5s^2U_{34}$ and $ms^2tc^6Ade_{37}$). Nevertheless, the present results show an unconventional feature for $tRNA^{Asn}$ due to interactions between hypermodified bases Q_{34} and tc^6Ade_{37}.

5.4 Conclusions:

The preference for an open conventional anticodon loop is consistently indicated. This is also required for accuracy and efficiency of protein biosynthesis. Unconventional structure of anticodon loop may confer specificity. The role of modified nucleosides in the anticodon loop may result in distinct structural features for specific tRNA molecules, that may also be functionally useful, specially so since tRNA is a multifunctional molecule involved in many other cellular processes besides translation.

5.5 References:

1) Ratner, L.; Haseltine W.; Patarca ,B.; Livak K. J.; Starcich, B.; Joseph, S. F.; Doran, E. R.; Rafalski, J. A.; Whitehorn, E. A.; Baumeister, K.; Ivanoff, L.; Petteway, S. R. J.; Pearson, M. L.; Lautenberger J. A.; Papas, T. S.; Ghrayeb, J.; Chang, N. T.; Gallo, R. C.; Wong-Staal, F. Nature 1985, 313, 277-284.

2) Isel, C.; Ehresmann, C.; Keith, G.; Ehresmann, B.; Marquet, R. J. Mol. Biol .1995, 247, 236-250

3) Isel, C.; Marquet, R.; Keith, G.; Ehresmann, C.; ,Ehresmann, B. J. Biol. Chem 1993, 268, 25269-25272

4) Isel, C.; Lanchy, J. M.; LeGrice, S. F.; Ehresmann, C.; Ehresmann, B.; Marquet, R. EMBO J. 1996, 15, 917-924

5) Agris, P. F.; Guenther, R.; Ingram, P. C.; Basti, M. M.; Stuart, J. W.; Sochacka, E.; Malkiewicz, A. RNA ,1997, 3, 420-428

6) Benas, P.; Bec, G.; Keith, G.; Marquet, R.; Ehresmann, C.; Ehresmann, B. and Dumas, P. RNA ,2000, 6, 1347-1355

7) Sundaram, M.; Durant, P. C.; Davis, D. R. Biochemistry 2000, 39(41), 12575-12584

8) Yarian, C.; Marszalek, M.; Sochacka, E.; Malkiewicz, A.; Guenther, R.; Miskiewicz, A.; Agris, P. F. Biochemistry, 2000, 39(44), 13390-13395 ; Stuart, J. W.; Gdaniec, Z.; Guenther, R.; Marszalek, M.; Sochacka, E.; Malkiewicz, A.; Agris, P.F. Biochemistry, 2000, 39(44), 13396-13404.

9) Ohashi,K.; Harada, F.; Ohashi, Z.; Nishimura, S.; Stewart, T. S.; Vogeli, G.; McCutchan, T. and Soll, D. Nucleic Acid Res.1976, 3, 3369 - 3376

10) Chen, E.Y.; Roe, B. A. Biochem, Biophys Res. Comm 1978, 82, 235-246

11) Chen, E.Y.; Roe, B. A. Biochim Biophysica Acta 1980, 610, 272-284

12) Holbrook, S. R.; Sussman, J. L.; Warrant, R. W.; Kim, S. H. J. Mol. Biol. 1978, 123, 631-660

13) Parthasararthy, R.; Soriano-Garcia, M; Chheda, G. B Nature 1976, 260, 807-808

14) Tewari, R. J. Biomol. Struct. Dyn. 1990, 8, 675-686

15) Yokoyama, S.; Miyazawa, T.; Itaya, Y.; Yamaizumi, Z.; Kasai, H.; Nishimura, S. Nature 1979, 282, 107-109

16) SYBYL Force Field Mannual version 6.4, Tripos Inc, St. Louis, USA

17) Auffinger, P.; Louise-May, S.; Westhof, E. J. Am. Chem. Soc. 1995, 117, 6720-6726

List of Publications :

1. N(7)-protonation induced conformational flipping in hypermodified nucleic acid bases N6 - (N-threonyl carbonyl) adenine and its 2-methylthio- or N(6)-methyl- derivatives.
   U.B. Sonavane, K.D. Sonawane, Annie Morin, Henri Grosjean and R. Tewari
   Int. J. Quantum Chem. 75 (3), 223-229 (1999).
2. Conformation of hypermodified nucleoside threonylcarbamoyladenosine t6A in model anticodon loop segments
   U. B. Sonavane, A. Morin, H. Grosjean and R. Tewari
   J. Biosciences 24/s1, 98 (1999)
3. Conformational flipping of the N(6) substituent in diprotonated N6 - (N- glycyl carbonyl) adenines: the role of N(6) H in purine ring protonated ureido adenines.
   K. D. Sonawane, U. B. Sonavane and R. Tewari
   Int. J. Quantum Chem. 78, 398-405 (2000).
4. Conformational Preferences of Anticodon 3'-adjacent Hypermodified Nucleic Acid Base *cis*-or *trans*-Zeatin and its 2-methylthio Derivative, *cis*-or *trans*-ms^{2}Zeatin.
   K. D. Sonawane, U. B. Sonavane and R. Tewari
   J. Biomol. Struct. Dynamics, 19 (4), 637-648, (2002).
5. Conformational preferences of the base substituent in hypermodified nucleotide Queuosine 5`-monophosphate 'pQ' and protonated variant `pQH+'
   U.B. Sonavane, K.D. Sonawane and R. Tewari
   (Communicated)